

β -CATENIN IN RENAL DYSPLASIA

β -CATENIN OVEREXPRESSION WITHIN THE METANEPHRIC MESENCHYME
CAUSES RENAL DYSPLASIA VIA UPREGULATION OF THE GDNF SIGNALLING AXIS

By SANJAY SARIN, H.B.Sc

A Thesis Submitted to the School of Graduate Studies in Partial Fulfillment of the Requirements
for the Degree Master of Science

TITLE: β -catenin overexpression within the metanephric mesenchyme causes renal dysplasia via upregulation of the Gdnf signalling axis

AUTHOR: Sanjay Sarin, H.B.Sc (McMaster University)

SUPERVISOR: Dr. Darren Bridgewater

NUMBER OF PAGES: xvi, 98

ABSTRACT

Renal dysplasia, a developmental disorder characterized by defective nephrogenesis and branching morphogenesis, ranks as one of the major causes of renal failure among the pediatric population. The molecular mechanisms underlying the pathogenesis of renal dysplasia are not well understood; however, changes in gene expression are a major contributing factor. In this study, we demonstrate that the levels of activated β -catenin, a transcriptional co-regulator, are elevated in the nuclei of ureteric, stromal, and mesenchymal cells within dysplastic human kidney tissue. To determine the mechanisms by which mesenchymal β -catenin over-expression leads to renal dysplasia, we generated a conditional mouse model in which β -catenin was stabilized exclusively in the metanephric mesenchyme. Kidneys from these mutant mice are remarkably similar to dysplastic human kidneys. In addition, these mutant mice also demonstrate the formation of 4 to 6 ectopic kidneys. While nephrogenesis appeared normal, investigation of ureteric branch pattern revealed ectopic ureteric budding off the Wolffian duct, ectopic branching off the initial ureteric bud stalk and a disorganization of branch patterning. In-situ hybridization of mutant kidneys revealed increased expression of *Gdnf*, *Cret*, and *Wnt11*, key factors that regulate ureteric branch patterning. We further demonstrate that β -catenin directly binds to TCF consensus binding sites within the *Gdnf* promoter region located 4.9kb, 2.25kb and 2.1kb upstream of the *Gdnf* transcriptional start site. Molecular cloning of the 4.9kb fragment upstream of a luciferase gene revealed that β -catenin regulates gene transcription from the 4.9kb consensus site. Consistent with these findings, genetic deletion of β -catenin from the metanephric mesenchyme cell lineage lead to decreased *Gdnf* expression and a reduction in ureteric branching morphogenesis resulting in renal hypoplasia. Taken together, our findings establish that β -catenin is an essential regulator of *Gdnf* expression within the metanephric mesenchyme. Furthermore, we have identified a novel disrupted signalling pathway that

contributes to the pathogenesis of renal dysplasia. In this pathway, an over-expression of β -catenin directly leads to an over-expression of *Gdnf*, causing ectopic and disorganized branching morphogenesis and, consequently, renal dysplasia.

ACKNOWLEDGEMENTS

Like many students I have left the acknowledgements section for last, which was a terrible idea. There is no doubt that this will be poorly written and overlook many individuals who have helped me throughout these last two years. Well, with that being said, I like to start off with thanking my parents and sister. Even though not one of you knew what I was doing, your love and support towards anything and everything I do is what keeps me going.

To my labmates, I would like to thank all of you for making the day to day grind a little bit easier and making my lab experience something that I will never forget. To Donna, Sam, Irena and Dhuha, even though our time in the lab was limited, all of you made the last stretch much more fun and exciting. A special thank you to Matthew Krause for putting up with all my questions, complaints and late night phone calls. Your assistance and guidance with the microscopes, immunohistochemistry, pretty much everything got me to where I am today, 4:00am and still writing. To Karin Trajcevski, all of your suggestions never fell on deaf ears, thanks for all your help, especially with Elements. To Aliyah Nissar, I can honestly say I won't miss those late night writing sessions. I will however miss all those coffee breaks, scope-room breaks, and music-breaks. You're an awesome scientist and I know you will do great out in Toronto. It's funny that not one of the people I mentioned above was part of my lab, yet they felt like labmates. I have you to thank for that Dr. Hawke. Thanks for bringing a lonely single grad student under your wing (pun intended) and into your lab space. Thanks for giving me access to all of your lab equipment and reagents. I've written out a ton of I.O.U's and you will one day see them returned. Even though I was never part of your lab, thanks for making me feel like I was.

To Felix Boivine, the second graduate student. Your arrival to the lab was no doubt a blessing, you brought with you a ton of scientific expertise and know how. Good luck with the

rest of your time at McMaster, I know you'll be quite the successful researcher. To Auiha Li, our brilliant lab technician, you were essential to this project and your work is greatly appreciated.

I would also like to thank my committee members, Dr. Joan Krepinsky and Dr. Peter Margetts for their friendly guidance, thought provoking suggestions, edits and for giving me an opportunity to present my research at nephrology rounds.

Finally, to my supervisor Dr. Darren Bridgewater, I don't really know what to say that you don't already know. You took a chance on a student with limited lab experience and gave him a home and a goal for 2 years. Your patience and positive outlook are two of the many great qualities you possess. I deeply appreciate everything you have done for me inside and outside of the lab. I will definitely miss our lab meetings and friendly chats about the Cowboys and obviously kidney development. I am truly fortunate to have had the opportunity to work alongside with you. When I look back at my experiences during my masters, just know that you were the one who made it all possible. So with all that out of the way, thank you for being an amazing supervisor, mentor, dictator, boss, commander, chief, colleague and friend.

TABLE OF CONTENTS

DESCRIPTIVE NOTES	ii
ABSTRACT	iii
ACKNOWLEDGEMENTS	v
TABLE OF CONTENTS	vii
LIST OF SUPPLEMENTARY FIGURES	x
LIST OF FIGURES	xi
LIST OF ABBREVIATIONS	xiii
DECLARATION OF ACADEMIC ACHIEVEMENT	xvi
1.0 BACKGROUND INFORMATION	1
1.1 Kidney anatomy and function	1
1.1.1 Gross anatomy of the mammalian kidney	1
1.1.2 Kidney function and the nephron	5
1.2 Kidney development	7
1.2.1 Pre-metanephric (kidney) development	7
1.2.2 Mammalian metanephric kidney development	9
1.3 Gdnf/Ret signalling	12
1.3.1 Gdnf/Ret signalling in ureteric bud formation	12
1.3.2 Gdnf/Ret signalling in branching morphogenesis	13
1.4 Wnts/Wnt signalling	16
1.4.1 General overview of Wnt signalling	16
1.4.2 Canonical Wnt/ β -catenin signalling	17
1.4.3 β -catenin	19

1.5 Canonical/ β -catenin signalling in kidney development	19
1.5.1 Wnt/ β -catenin signalling in the ureteric epithelium	20
1.5.2 Wnt/ β -catenin signalling in the cap mesenchyme	22
1.6 Renal Dysplasia	25
1.6.1 Human renal dysplasia	25
1.6.2 Characteristics of human renal dysplasia	26
1.6.3 β -catenin in renal dysplasia	28
2.0 HYPOTHESIS AND OBJECTIVES	30
2.1 Overall hypothesis	30
2.2 Study objectives	30
3.0 MATERIALS AND METHODS	31
4.0 RESULTS	40
4.1 β -catenin is over-expressed in human renal dysplasia	40
4.2 Generation of mesenchyme specific β -catenin gain-of-function mutants	42
4.3 β -cat ^{GOF-MM} mutants demonstrate renal dysplasia	46
4.4 Nephrogenesis is maintained in β -cat ^{GOF-MM} mutants	50
4.5 β -cat ^{GOF-MM} mutants display sporadic zones of disorganized nephrogenic structures and ectopic kidney formation	53
4.6 Abnormal branching morphogenesis in β -cat ^{GOF-MM} mutants	57
4.7 Increased <i>Gdnf</i> expression in β -cat ^{GOF-MM} mutants	61
4.8 Generation of mesenchyme specific β -catenin Loss-of-function mutants	64
4.9 β -cat ^{LOF-MM} demonstrate renal hypoplasia	66

4.10	β -cat ^{LOF-MM} demonstrate delayed and reduced branching morphogenesis	69
4.11	Decreased <i>Gdnf</i> expression in β -cat ^{LOF-MM} mutants	71
4.12	β -catenin binds TCF/LEF consensus sequences in the <i>Gdnf</i> promoter and regulates transcription	73
4.13	Undifferentiated mesenchyme in dysplastic human renal tissue demonstrates both increased β -catenin and <i>Gdnf</i> levels	77
5.0	DISCUSSION	79
5.1	Overall findings	79
5.2	Maintenance of nephrogenesis in β -cat ^{GOF-MM} mutants	80
5.3	Transcriptional regulation of <i>Gdnf</i>	82
5.4	Wnt proteins controlling <i>Gdnf</i> expression	83
5.5	Ectopic and disorganized branching morphogenesis in β -cat ^{GOF-MM} mutants	84
5.6	Ectopic kidney formation in β -cat ^{GOF-MM} mutants	85
5.7	Conclusion	88
6.0	REFERENCES	89

LIST OF SUPPLEMENTARY FIGURES

Supplementary 1.	Gross anatomy of mouse kidneys	2
Supplementary 2.	Basic structure of the kidney	4
Supplementary 3.	Basic structure of the nephron	5
Supplementary 4.	Establishment of the Wolffian duct and nephrogenic cord	8
Supplementary 5.	Morphology of the branching ureteric bud/epithelium	10
Supplementary 6.	Morphology of nephrogenesis	11
Supplementary 7.	Gdnf/Ret signalling and branching morphogenesis	15
Supplementary 8.	Canonical Wnt/ β -catenin signalling	18
Supplementary 9.	Wnt/ β -catenin signalling in the ureteric epithelium	21
Supplementary 10.	Wnt/ β -catenin signalling in nephrogenesis	24
Supplementary 11.	Human renal dysplasia	27

LIST OF FIGURES

Figure 1.	β -catenin levels are elevated in Human Renal Dysplasia	41
Figure 2.	Generation of mesenchyme specific β -catenin gain of function mutants	43
Figure 3.	Levels of transcriptionally active β -catenin are increased in β -cat ^{GOF-MM} mutants	45
Figure 4.	Kidneys from new born β -cat ^{GOF-MM} mutants are severely abnormal	48
Figure 5.	β -cat ^{GOF-MM} mutants demonstrate Renal Dysplasia	49
Figure 6.	Nephrogenesis progresses normally in β -cat ^{GOF-MM} mutant Kidneys	52
Figure 7.	β -cat ^{GOF-MM} mutants display sporadic zones of disorganized nephrogenic structures	55
Figure 8.	β -cat ^{GOF-MM} mutants display ectopic kidney formation	56
Figure 9.	Abnormal branching morphogenesis in TCF/LacZ; β -cat ^{GOF-MM} mutants	58
Figure 10.	Abnormal branching morphogenesis in β -cat ^{GOF-MM}	60
Figure 11.	Increased <i>Gdnf</i> Expression in β -cat ^{GOF-MM} mutants	63
Figure 12.	Generation of mesenchyme specific loss of function β -catenin mutants	64
Figure 13.	β -cat ^{LOF-MM} mutants demonstrate renal hypoplasia	67

Figure 14.	β -cat ^{LOF-MM} mutants demonstrate renal hypoplasia during kidney development	68
Figure 15.	β -cat ^{LOF-MM} demonstrate delayed and reduced branching Morphogenesis	70
Figure 16.	Decreased <i>Gdnf</i> expression in β -cat ^{LOF-MM} mutants	72
Figure 17.	β -catenin binds TCF/LEF consensus sequences in the <i>Gdnf</i> promoter	75
Figure 18.	The 4.9kb <i>Gdnf</i> promoter fragment activates gene Transcription	77
Figure 19.	Dysplastic kidney tissue demonstrates elevated levels of β -catenin and <i>Gdnf</i>	78

LIST OF ABBREVIATIONS

IM	Intermediate mesoderm
WD	Wolffian duct
NC	Nephrogenic cord
UB	Ureteric bud
MM	Metanephric mesenchyme
CAKUT	Congenital anomalies of the kidney and urinary tract
P0	Postnatal day 0
E15.5	Embryonic day 15.5
MET	Mesenchymal to epithelial transition
PTA	Pre-tubular aggregate
RV	Renal vesicle
CS	Comma-shaped body
SB	S-shaped body
Gdnf	Glial derived neurotrophic factor
c-Ret	Receptor tyrosine kinase Ret
GFR α 1	Gdnf family co-receptor alpha-1
Wnt11	Wingless type 11
Wnt	Wingless type
Fz	Frizzled receptor
LRP5/6	Lipoprotein receptor-related protein
TCF/LEF	T-cell factor/Lymphoid enhancer factor
GSK3	Glycogen synthase kinase 3

Dsh	Dishevelled
APC	Adenomatosis polyposis coli
CK1 α	casein kinase alpha-1
LiCl	Lithium chloride
Wnt9b	Wingless type 9b
Wnt4	Wingless type 4
Gata3	Trans-acting T-cell-specific transcription factor 3
Emx2	Empty spiracles-like protein 2
Lim1/Lhx1	Lim/homeobox protein Lhx1
Fgf8	Fibroblast growth factor 8
Pax8	Paired box gene 8
Pax2	Paired box gene 2
Tgf β 2	Transforming growth factor beta-2
Dkk1	Dkkopf 1 homolog
Six2	Sine oculis homeobox 2
WT-1	Wilms-tumour 1
RAR β 2	Retinoic acid receptor beta 2
PCR	Polymerase chain reaction
PBS	Phosphate buffered saline
PFA	Paraformaldehyde
DAPI	4',6-diamidino-2-phenylindole
DBA	3, 3'-diaminobenzidine
H+E	Hematoxylin and eosin

GS	Goat serum
BSA	Bovine serum albumin
LacZ	β -galactosidase reporter
H ₂ O ₂	Hydrogen Peroxide
MABT	Maelic acid buffer containing tween-20
ChIP	Chromatin Immunoprecipitation
FBS	Fetal bovine serum
HEK293	Human embryonic kidney stem cells 293
DMEM	Dulbecco's modified eagle medium

DECLARATION OF ACADEMIC ACHIEVEMENT

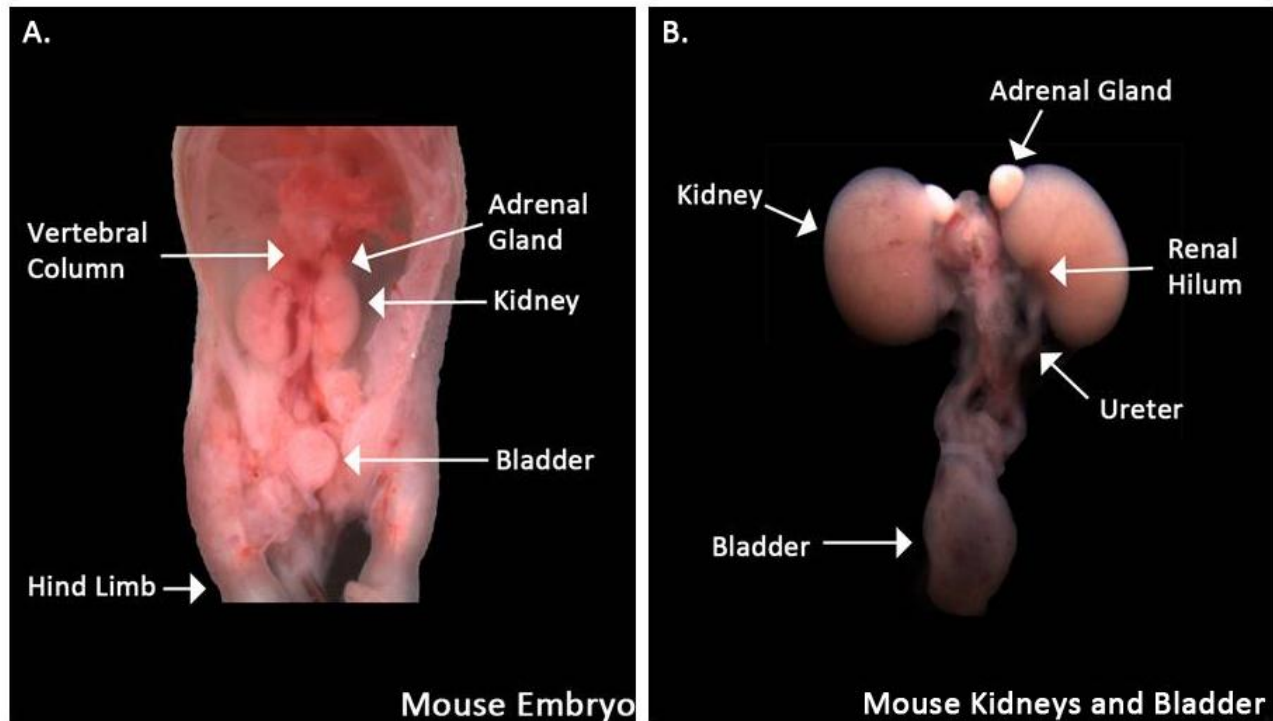
I personally accomplished all the research and necessary tasks for Figure 1 through Figure 19. Figure 17 and Figure 18, I worked alongside and shadowed Auiha Li, our lab technician.

1.0 BACKGROUND INFORMATION

1.1 Kidney Anatomy and Function

1.1.1: Gross Anatomy of the Mammalian Kidney

The kidneys are a pair of reddish ‘bean-shaped’ organs that are located in the posterior abdominal cavity, sitting on either side of the vertebral column. Due to the asymmetry within the abdominal cavity caused by the liver, the right kidney rests slightly lower than the left (Supplementary 1A). The medial portion of the kidney contains the renal hilum, where the renal artery enters the organ and the renal vein and ureter exit. Blood that is to be filtered by the kidney enters via the renal artery and exits through the renal vein. The filtered plasma (urine) then exits the kidney through the ureter, which extends downwards and joins with the urinary bladder (Supplementary 1B).

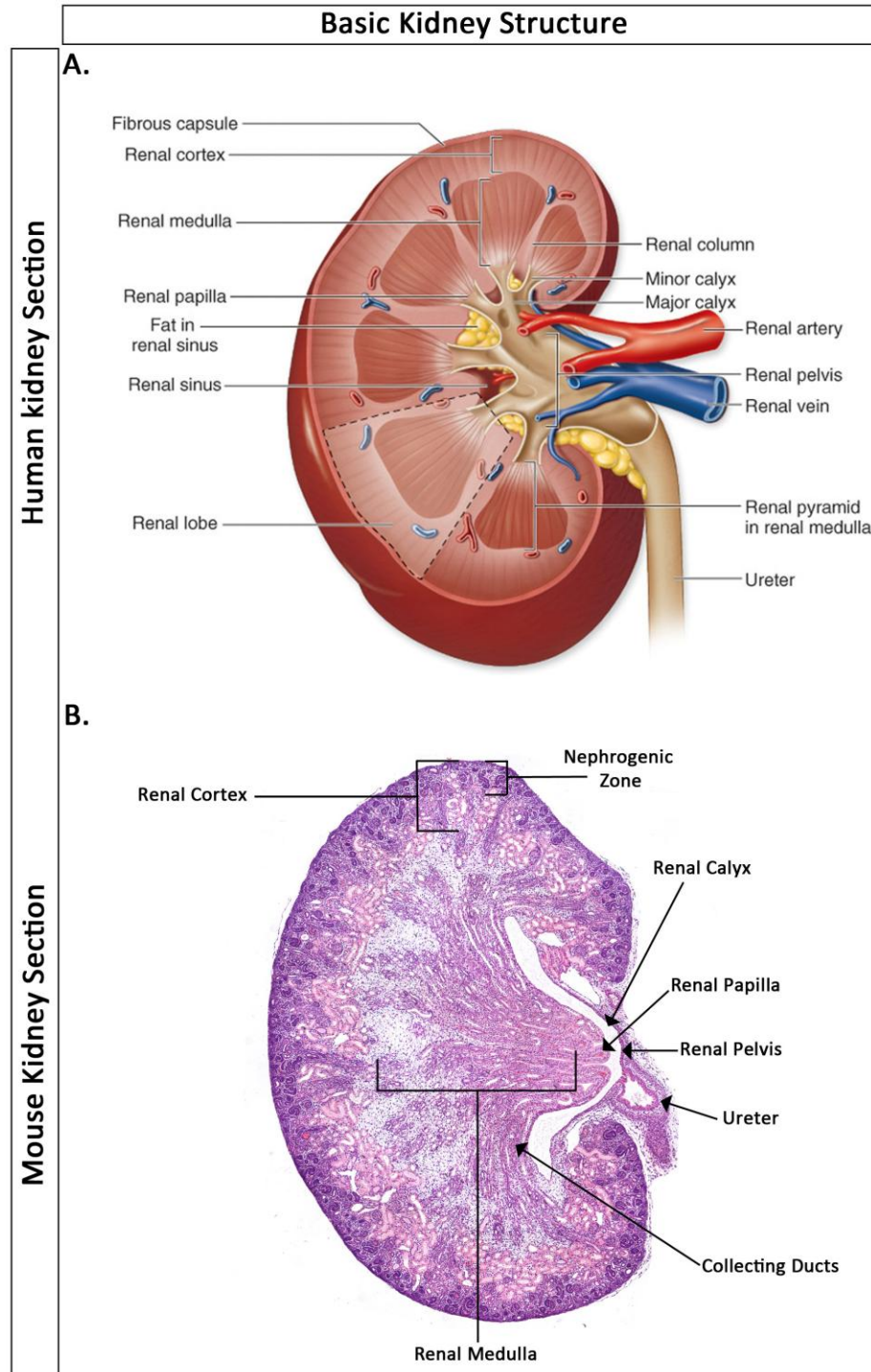
Supplementary 1: Gross anatomy of mouse kidneys

Gross Anatomy of Mouse Kidneys: (A) A Snapshot of embryonic day 15.5 mouse displaying the location of kidneys with respect to the vertebral column, adrenal gland, bladder and hind limb. (B) Gross anatomy of a resected embryonic day 15.5 mouse kidneys with the ureter and bladder intact.

A coronal section of the kidney reveals a number of distinct regions (Supplementary 2A). The outermost region of the kidney is the renal capsule, a smooth transparent sheet of dense connective tissue that runs continuous with the outer coat of the ureter. The renal capsule serves as a barrier against trauma and helps maintain the shape of the kidney [1]. The parenchyma of the kidney is divided into two major regions: the outer renal cortex and deeper renal medulla. The renal medulla is subdivided into a number of sections called renal pyramids. At the tips of the renal pyramids, tubules called collecting ducts drain into common passageways called minor calyces. This region is known as the renal papilla. Several minor calyces converge to form larger

passageways called major calyces, which drain into the renal pelvis, a funnel-shaped structure that connects to the ureter. There are some obvious distinctions between the anatomy of human kidneys, and those of mice. For instance, the mouse kidney does not have distinct renal pyramids as seen in human kidneys. Furthermore, mice contain only a single calyx which receives the urine from all the collecting ducts (Supplementary 2B). Aside from these minor differences, both contain nephrons with similar appearances.

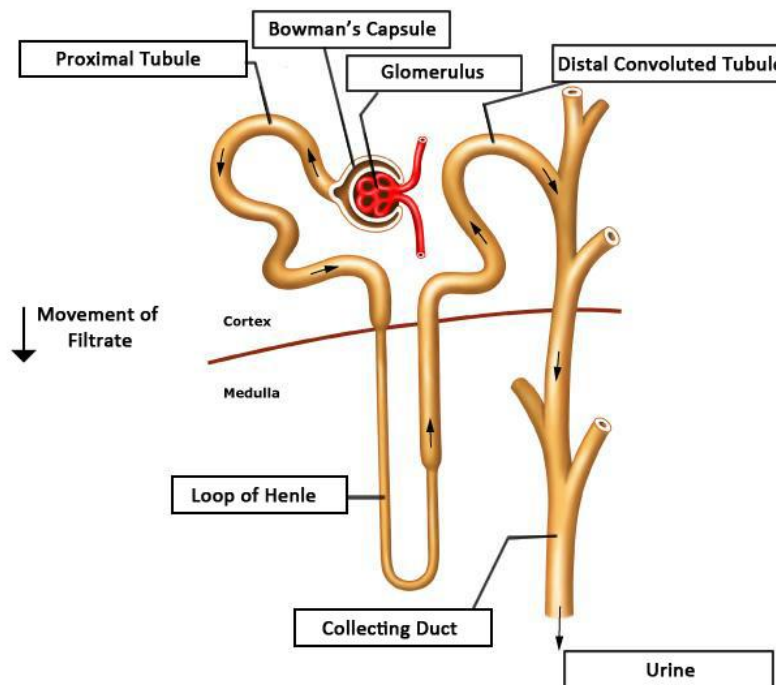
Supplementary 2: Basic structure of the kidney



Basic Structure of the Kidney: (A) Coronal section of a cartoon adult human kidney outlining various regions, Image adapted [2]. (B) Sagittal section of a P0 mouse kidney marking various regions.

Within the renal pyramids of the kidney, microscopic subunits called nephrons, the functional units of the kidney, work to filter the blood and form urine. Each nephron consists of two parts: 1) a renal corpuscle located in the cortex, and 2) a renal tubule that passes from the cortex deep into the medulla. The renal corpuscle is made up of a glomerular tuft, a capillary network enveloped by podocytes that is enclosed by a Bowman's capsule. The lumen of the Bowman's capsule is continuous with the renal tubule. The renal tubule is divided into three distinct regions: the proximal convoluted tubule, the loop of Henle, and the distal convoluted tubule. During the process of urine formation, fluid travels through the renal tubules, where its composition is modified. Fluid from individual nephrons then drains into common passageways called collecting ducts. The fluid that exits the collecting duct is called urine (Supplementary 3).

Supplementary 3: Basic structure of the nephron



Basic structure of the Nephron: Diagram outlining all the basic regions of the mammalian nephron. Black arrow indicates the movement of filtrate as it passes through the nephron and exits out the collecting duct as urine.

1.1.2: Kidney Function and the Nephron

The kidney plays an essential role in the filtration of blood and excretion of waste in the form of urine. In doing so, the kidney functions as a regulator of whole-body homeostasis. As mentioned previously, the functional unit of the mammalian kidney is the nephron. These units are responsible for blood filtration, re-absorption of solutes and ions including glucose and salt, and excretion of harmful toxins into the urine[2].

The process of urine formation begins as blood enters the glomerular capillaries via the afferent arteriole. The glomerular capillaries perform the first step in filtering the blood. The endothelial cells of the glomerular capillaries are fenestrated and permeable to plasma water and dissolved solutes; however, before the fluid in blood plasma can enter the interior of the Bowman's capsule it must be filtered through three layers that act as a selective barrier. The first layer of the filtration barrier is the capillary fenestrae, followed by the glomerular basement membrane, and finally the inner visceral layer of the Bowman's capsule being the foot processes of podocytes which interdigitate to form what is called the slit diaphragm. Once the filtrate filters across these selective barriers into the lumen of the Bowman's capsule, it is known as the glomerular filtrate. The glomerular filtrate then flows from the Bowman's capsule to the proximal convoluted tubule. Here, the glomerular filtrate is modified as molecules and water are exchanged between the lumen of the renal tubule and the peritubular capillaries that line the proximal tubule through the process of reabsorption and secretion. The solute concentration of the filtrate is further modified as it travels through the descending and ascending limbs of the Loop of Henle. More substances are reabsorbed by the peritubular capillaries once the filtrate enters the distal convoluted tubule. Substances such as toxins and drugs are also secreted from the peritubular capillaries into the filtrate at the distal convoluted tubule. This modified

glomerular filtrate then travels through the collecting duct where more water can be reabsorped into the blood. As the filtrate drains into the minor calyces it is finally excreted as urine [2] (Supplementary 3).

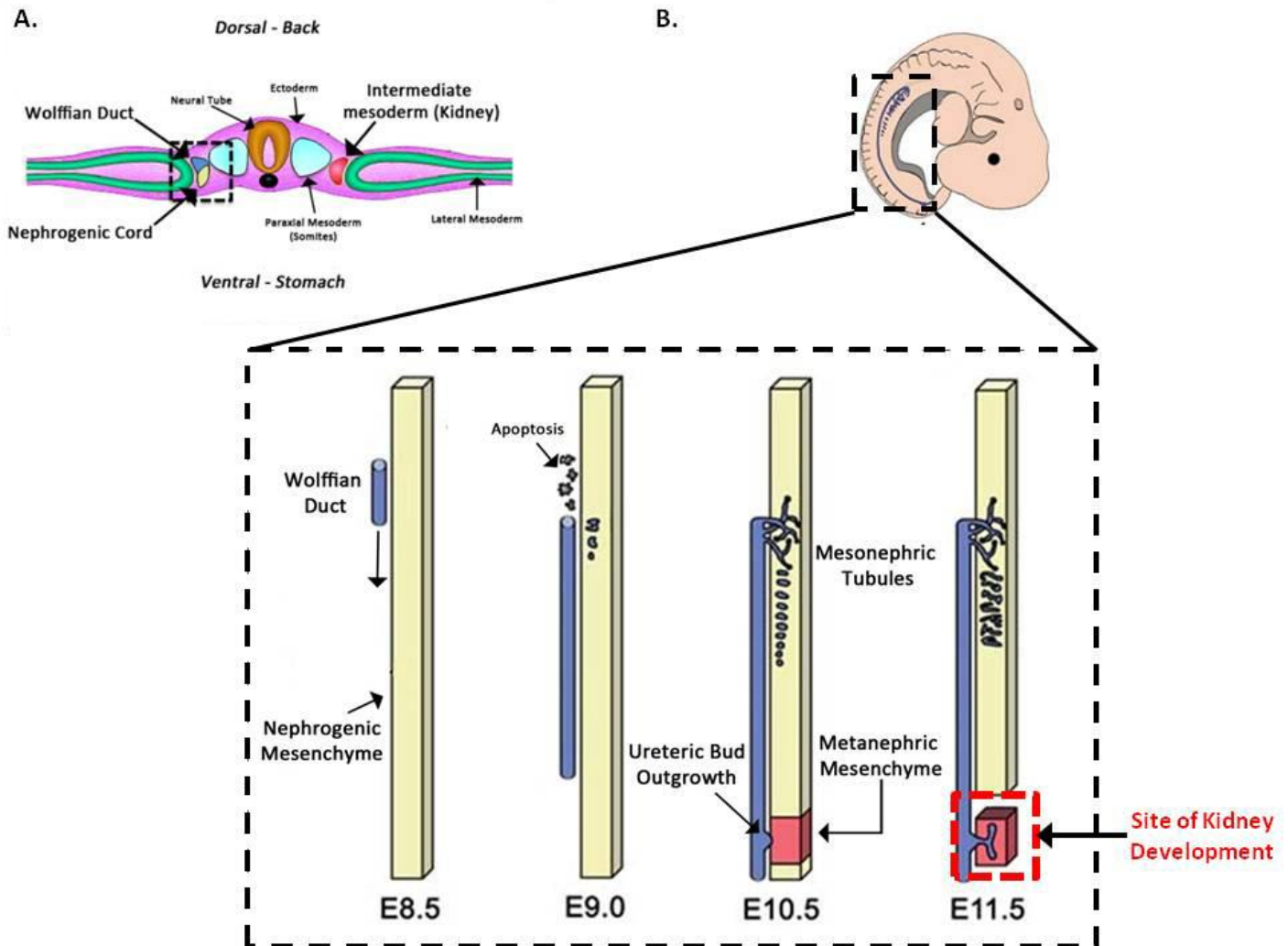
The nephron is a complex and critical structure that is able to expel unnecessary or harmful substances from the blood by filtration and secretion into the filtrate. It is also crucial for the reabsorption of substances back into the bloodstream that are useful for the body.

1.2 Kidney Development

1.2.1: Pre metanephric (kidney) development

Mammalian kidney development begins when the intermediate mesoderm divides into two primitive renal structures. Cells in the dorsal intermediate mesoderm form the Wolffian duct, while the ventral intermediate mesoderm forms the nephrogenic cord [3] (Supplementary 4A,B). At E8.5 in mice and 22 days gestation in Humans, the Wolffian duct begins to grow caudally along the dorsal aspect of the embryo. While migrating, the Wolffian duct induces the formation of tubules of the pronephric and mesonephric kidneys in the adjacent nephrogenic mesenchyme. These are transient organs in higher vertebrates, and later degrade via apoptosis [4].

Supplementary 4: Establishment of the Wolffian duct and nephrogenic cord



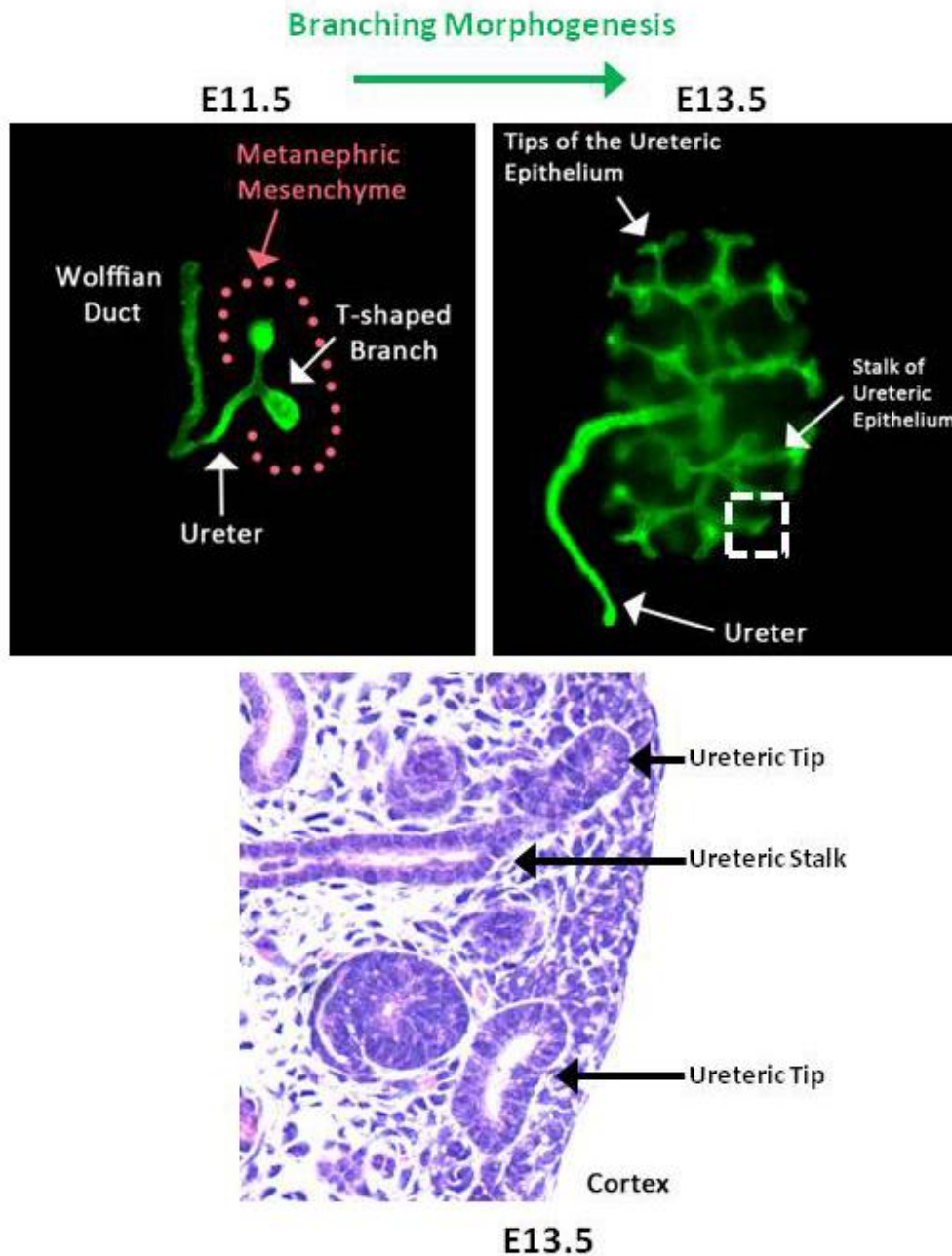
Establishment of the Wolffian Duct and Nephrogenic Cord: (A) Illustrations of the establishment of the precursors to kidney development in mice. The Wolffian duct (blue) and Nephrogenic cord (yellow) arise from the intermediate mesoderm. (B) The Wolffian duct forms at E8.5, migrates caudally along the dorsal end of the body inducing the formation of mesonephric tubules. Mesonephric tubules degrade via apoptosis in higher vertebrates. At E10.5, signals emanating from the metanephric mesenchyme cause an outgrowth off the Wolffian duct to form, called the ureteric bud. The ureteric bud then migrates into the Metanephric Mesenchyme. At E11.5 the ureteric bud has undergone branching morphogenesis to give rise to a T-shape branch. Red outline is the site of Metanephros (mammalian kidney development). (A) Image adapted [5]

1.2.2: Mammalian metanephric kidney development

The formation of the permanent kidney, metanephros, is initiated in the mouse at E10.5 and 5 weeks gestation in humans. An outgrowth off the caudal Wolffian duct known as the ureteric bud migrates into the adjacent metanephric mesenchyme, a specialized region of cells within the nephrogenic mesenchyme. Once the ureteric bud has invaded the metanephric mesenchyme, it undergoes a process termed branching morphogenesis and bifurcates to form a T-shaped branch at E11.5 in the mouse [4] (Supplementary 4). Ureteric branching morphogenesis will continue to occur for 10 cycles in mice [6] and 15 cycles in humans [4]. These repeated cycles of ureteric bud elongation and bifurcation branching events will eventually generate the metanephric collecting duct system, renal calyx and ureter (Supplementary 5).

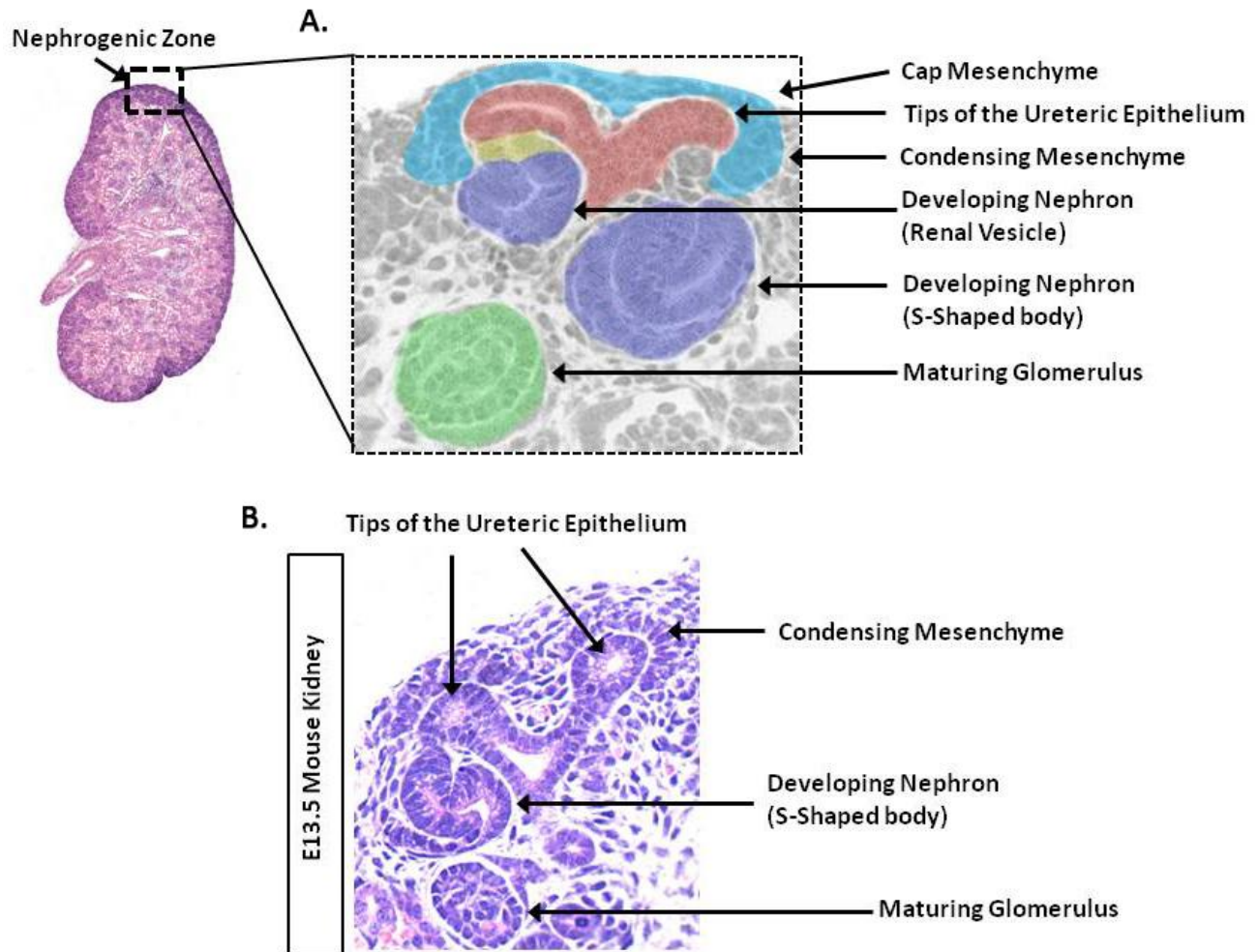
Migration of the ureteric epithelium into the metanephric mesenchyme also induces a subset of metanephric mesenchymal cells to begin the formation of nephrons. During the process of branching morphogenesis, the tips of the ureteric epithelium will become surrounded by a cap of metanephric mesenchyme. A subset of these metanephric mesenchymal cells will undergo nephrogenesis to form the filtering units of the kidney. The first stage of nephrogenesis is the formation of mesenchymal cell aggregates under the tips of the ureteric epithelium. These induced cells will undergo a transition from mesenchymal to epithelial cells and form renal vesicles. These renal vesicles subsequently differentiate into distinct morphological structures, termed the comma-shaped, s-shaped, and developing nephron, to ultimately become functional nephrons [4]. Nephrogenesis occurs in a region termed the 'nephrogenic zone', which is located in the cortex of the developing kidney (Supplementary 6).

Supplementary 5: Morphology of the branching ureteric bud/epithelium



Morphology of the branching ureteric bud/epithelium: (A) Typical T-shape branch formation at E11.5. (B) Branching morphogenesis results in continuous bi-fid branching of the ureteric epithelium giving rise to a branched collecting duct system. The pattern of branching morphogenesis is characterized by a swelling of each ureteric bud tip which is then remodeled to form two tips that extend and generate new branches (C) Histology demonstrating the morphology of ureteric epithelial tips and stalk.

Supplementary 6: Morphology of Nephrogenesis



Morphology of nephrogenesis: (A) E15.5 Kidney with the nephrogenic zone outlined. Within the nephrogenic zone, nephrogenesis occurs. Blown up area is a cartoon depiction of the different regions involved in nephrogenesis. Different morphological stages of nephrogenesis include in this order: condensing mesenchyme; pre-tubular aggregate (omitted); renal vesicle; comma-shaped body (omitted); S-shaped body; formation of glomerulus. (B) Example of the morphology of some of these formations in an actual mouse kidney histological section.

1.3 Gdnf/Ret Signalling

1.3.1: Gdnf/Ret signalling in ureteric bud formation

The first event in mammalian kidney development is characterized by the formation of a ureteric bud, an outgrowth off the Wolffian duct, which then invades the adjacent metanephric mesenchyme. The formation of the ureteric bud and subsequent invasion of the metanephric mesenchyme is essential, as normal renal development and function relies on the correct positioning and number of ureteric buds. A bud that forms too caudally or rostrally will invade the metanephric mesenchyme at suboptimal positions and impede kidney development [7]. In addition, the generation of multiple ureteric buds along the Wolffian duct will result in the formation of multiplex kidneys and multiple ureters that fail to insert properly in the bladder [8]. Since the correct positioning of the initial ureteric bud outgrowth from the Wolffian duct is crucial in maintaining proper development of the kidney, it requires stringent regulation. Ureteric bud formation is controlled by a number of stimulatory and inhibitory factors expressed in the mesenchyme and Wolffian duct. Central to ureteric budding is the Gdnf/Ret signalling pathway, which is also involved in the subsequent growth and elongation of the ureteric bud [9].

The expression of Gdnf (Glial derived neurotrophic factor) is restricted to the metanephric mesenchyme by E10.5. Gdnf secreted by the metanephric mesenchyme acts as a ligand when it binds to its cell surface co-receptors, c-Ret (receptor tyrosine kinase Ret) and GFR α 1 (Gdnf family receptor alpha-1), which are co-expressed by the Wolffian duct epithelium and, later, by the tips of the ureteric bud [9]. Ret is a receptor tyrosine kinase comprised of a ligand-binding extracellular region, a transmembrane region, and a cytoplasmic kinase domain. The cytoplasmic kinase domain is responsible for autophosphorylation of intracellular tyrosine

residues that interact with adaptor proteins responsible for downstream cell signalling [10]. The activation of Ret by Gdnf results in the activation of the Ras/Erk MAP kinase, phosphatidylinositol-3-kinase (PI3K) and phospholipase C (PLC)- γ pathways [10]. Together, these pathways lead to changes in gene expression that promote cell proliferation and movement, leading to the outgrowth of the ureteric bud and its subsequent branching [11, 12] (Supplementary 7).

The importance of the Gdnf/Ret signalling pathway in the formation of the ureteric bud is highlighted by mice deficient in either Gdnf (*Gdnf*^{-/-}), Ret (*Ret*^{-/-}), or GFR α 1 (*GFR α 1*^{-/-}). These null mice exhibit renal aplasia caused by a failure in ureteric budding [13]. Conversely, studies in which the Gdnf expressional domain was expanded, using either genetic mouse models or exogenously placed beads, led to the formation of ectopic ureteric buds off the Wolffian duct and caused abnormal branching morphogenesis, impeding normal kidney development [14]. Therefore, is not surprising that the spatial and temporal control of Gdnf expression requires numerous factors that positively regulate its expression and factors that restrict its spatial domain. The activation and maintenance of Gdnf expression in the metanephric mesenchyme are positively regulated by the transcription factors Eya1, Pax2 and Sall1 [14-16]. In contrast, the transcription factors Foxc1, Foxc2 and the Slit2/Robo signalling system act to negatively limit the expressional domain of Gdnf [8, 17].

1.3.2: Gdnf/Ret signalling in branching morphogenesis

In addition to promoting ureteric bud outgrowth off the Wolffian duct, Gdnf/Ret signalling also plays a central role in the subsequent branching of the ureteric epithelium [13]. Following the invasion of the metanephric mesenchyme by the ureteric bud in normal renal

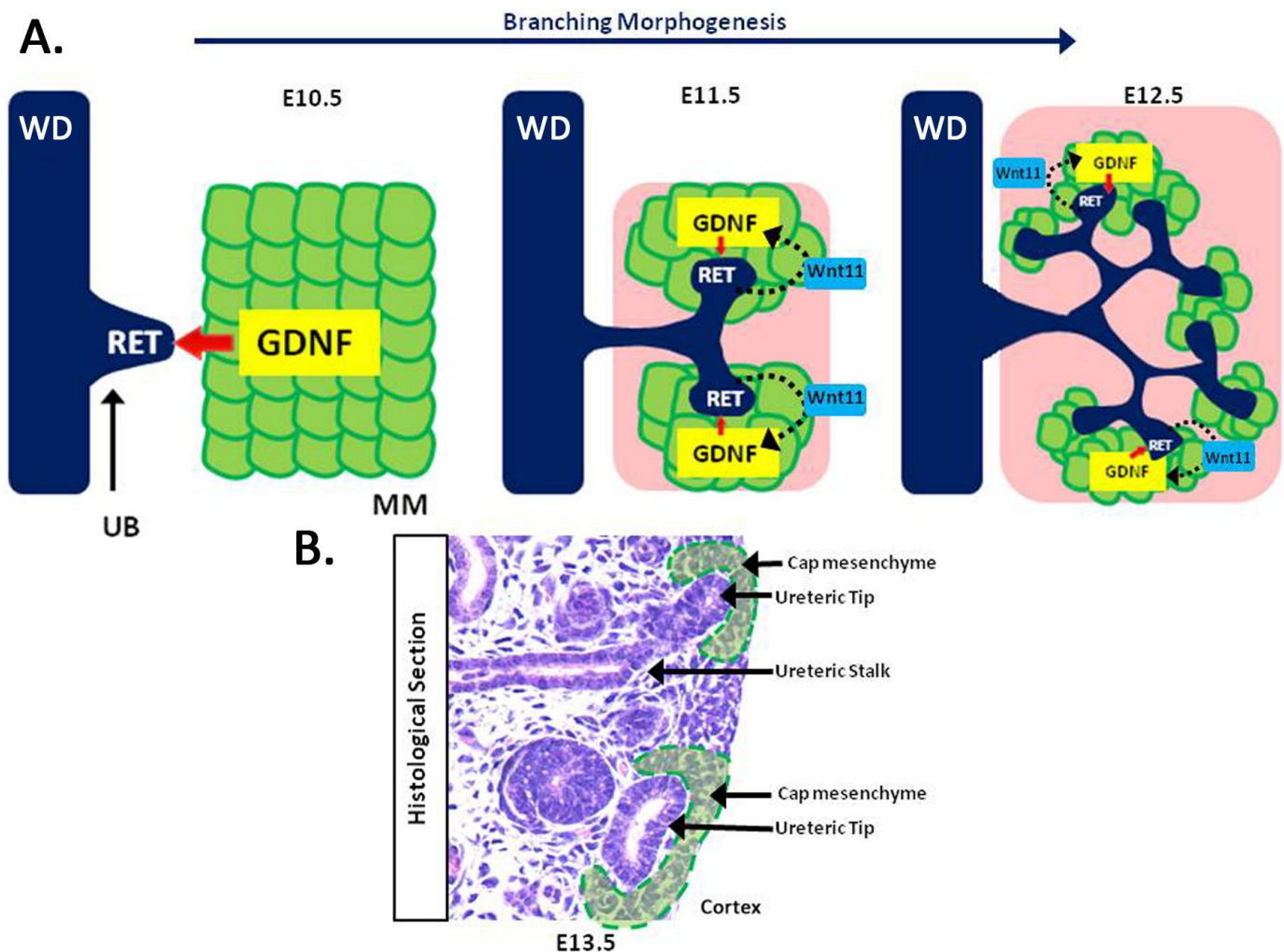
development, *Gdnf* expression becomes restricted to the cap mesenchyme surrounding each ureteric bud tip [18, 19]. In addition, the expression of *Ret* also becomes localized to the tips of the ureteric bud as *Ret*-expressing cells migrate toward the source of *Gdnf* [20]. This pattern of *Gdnf* and *Ret* expression persists throughout normal kidney development. In this regard, continued activation of the *Gdnf/Ret* signalling pathway leads to changes in gene expression which promote branching morphogenesis, specifically at the tips of the ureteric epithelium [9, 13]. However, to date, the cellular events that lead to the bifurcation of the ureteric bud epithelium remain unclear[21].

The importance of *Gdnf* signalling via *Ret* in the continuation of branching morphogenesis has been highlighted by studies in which the levels of *Gdnf* were reduced. Mice heterozygous for *Gdnf* (*Gdnf*^{+/-}), while demonstrating the formation of a normal ureteric bud, display a marked reduction in branching morphogenesis, resulting in renal hypoplasia[22]. In addition, kidneys cultured in the presence of anti-*Gdnf* antibodies, which reduce *Gdnf/Ret* signalling, also demonstrate decreased branching morphogenesis[13]. In contrast, a study in which *Gdnf* expression was increased resulted in abnormally large ureteric epithelial tips and abnormal ectopic branching patterns [23].

There are a number of target genes that are up-regulated in the ureteric epithelium following the activation of *Ret* by *Gdnf* [9]. One target of the *Gdnf-Ret* signalling pathway is the transcriptional activation of the *Ret* gene itself [24]. This finding demonstrates a positive feedback loop that reinforces tip-specific expression of *Ret*, which further propagates branching morphogenesis. An additional player in this positive feedback loop is *Wnt11* [25, 26]. In response to the activation of *Ret* by *Gdnf*, *Wnt11* is expressed and secreted by the tips of the

ureteric epithelium, where it increases transcriptional activation of *Gdnf* in the metanephric mesenchyme and reinforces branching morphogenesis [25] (Supplementary 7).

Supplementary 7: *Gdnf/Ret* signalling and branching morphogenesis



***Gdnf/Ret* Signalling and branching morphogenesis:** (A) The *Gdnf/Ret* signalling pathway controls ureteric budding and branching morphogenesis of the ureteric epithelium. *Gdnf* is expressed in the metanephric mesenchyme at E10.5 and activates *Ret* signalling which results in the outgrowth of the ureteric bud from the Wolffian duct. Downstream of *Ret* signalling is *Wnt11*. *Wnt11* is expressed at the tips of the ureteric epithelium. *Wnt11* is secreted and acts on the metanephric mesenchyme where it increases the expression of *Gdnf*. In this manner the *Gdnf/Ret/Wnt11* signalling axis makes up a positive feedback loop. (B) Histological section of a 13.5 kidney which marks the tips of the ureteric epithelium and the metanephric mesenchyme (dotted green area).

1.4: Wnts/Wnt Signalling

1.4.1: General Overview of Wnt signalling

The Wnt signalling pathway regulates a wide range of cellular events, including cell fate determination, cell migration, cell polarity and organogenesis during embryonic development [27]. Wnts comprise a large family of 19 secreted proteins that play key roles as intercellular signalling molecules [27]. Wnt proteins elicit their functions by binding to members of the frizzled (Fz) receptor family, of which there are 10 [27]. In addition to the interaction between the Wnt ligand and Fz receptor, co-receptors are also required for mediating Wnt signalling. There are several known co-receptors that mediate Wnt signalling, one being the lipoprotein receptor-related protein 5/6 (LRP5/6) [27]. Depending upon which Wnt ligand, Fz receptor and co-receptor are involved, different intracellular signal transduction cascades are activated, which have distinct biological consequences [27, 28]. There are two major signalling branches downstream of the Fz receptor activation by Wnt: the canonical Wnt/ β -catenin dependent pathway, and the non-canonical Wnt/ β -catenin independent pathway. The non-canonical Wnt/ β -catenin independent branch can be further divided into the Wnt/ Ca^{2+} and Wnt/Planar cell polarity (PCP) pathways. In the developing kidney, several known members of the Wnt family are expressed [27]. Wnt6, Wnt7b, Wnt9b and Wnt11 are expressed in the cells of the ureteric epithelium [25, 29-31]. Wnt4 is expressed in the metanephric mesenchyme [32] and Wnt2b is expressed in the cortical stroma [33]. Studies have demonstrated that these Wnt proteins can activate either the canonical or non-canonical signalling pathways during renal development. However, the canonical Wnt/ β -catenin dependent signalling pathway is of particular importance to our study.

1.4.2: Canonical Wnt/ β -catenin signalling

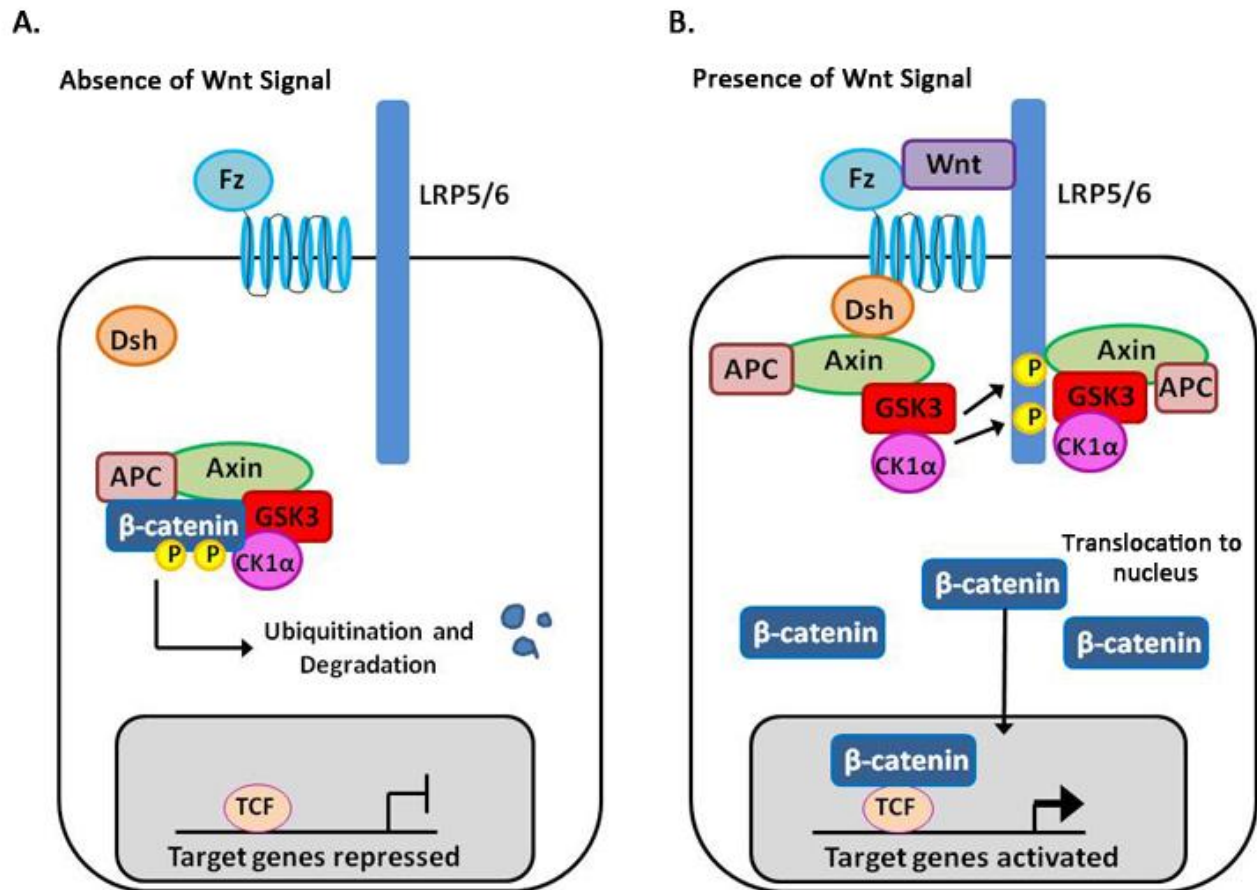
The canonical Wnt signalling pathway involves the cytoplasmic accumulation and translocation of the multifunctional protein β -catenin into the nucleus, where it activates specific genes.

In the absence of a Wnt ligand (signal), cytoplasmic β -catenin is targeted for degradation by a complex of proteins known as the destruction complex. The destruction complex is made up of multiple proteins, which include the scaffolding protein axin, adenomatous polyposis coli (APC), glycogen synthase kinase 3 (GSK3) and casein kinase 1 α (CK1 α). Cytoplasmic β -catenin is recruited and anchored by APC within this destruction complex. The trapped β -catenin is then phosphorylated at serine/threonine residues by the resident protein kinases GSK3 and CK1 α . The phosphorylation of β -catenin creates binding sites for E3 ubiquitin ligase. This leads to the ubiquitination of β -catenin, which subsequently targets it for proteolytic destruction by the proteosomal machinery[34]. This continual elimination of β -catenin prevents β -catenin from reaching the nucleus, and Wnt target genes are thereby repressed [35] (Supplementary 8A).

The canonical Wnt signalling pathway is activated upon binding of Wnt to its receptor complex, composed of the Fz receptor and the LRP5/6 co-receptor. This results in the recruitment and phosphorylation of a protein named dishevelled (Dsh). Dsh then directly interacts with the Fz receptor and recruits the Axin complex to the cell membrane [36]. Upon membrane translocation of Axin, it binds to the intracellular tails of LRP5/6, catalyzed by the phosphorylation of LRP5/6. The phosphorylation of the intracellular tails of LRP5/6 provides docking sites for additional Axin complexes thereby sequestering the cytosolic destruction complexes. These events lead to the inhibition of Axin-mediated β -catenin phosphorylation, thereby stabilizing β -catenin [36]. β -catenin accumulates in the cytoplasm and then translocates

into the nucleus. In the nucleus, β -catenin binds to members of the TCF/LEF family of DNA-bound transcription factors. This complex then binds to the promoter of target genes and regulates transcription [35] (Supplementary 8B).

Supplementary 8: Canonical Wnt/ β -catenin signalling



Canonical Wnt/ β -catenin signalling: (A) In the absence of a Wnt signal, the destruction complex made up of: Axin, APC, GSK3, CK1 α phosphorylates β -catenin, which is then targeted for degradation by the proteasome. β -catenin therefore does not translocate to the nucleus to activate target genes. (B) In the presence of a Wnt signal, Dsh binds to the Fz receptor which facilitates the translocation of the Axin complex from the cytosol to the plasma membrane. In addition LRP5/6 becomes phosphorylated and provides additional docking sites for other Axin complex. Cytosolic β -catenin is therefore not degraded by the axin complex as it is sequestered away. β -catenin then translocates to the nucleus where it complexes with TCF/LEF family members to induce transcription of target genes.

1.4.3: β -catenin

β -catenin is a multifunctional protein that has two major cellular functions. First, β -catenin is involved in cell adhesion by linking E-cadherin to the actin cytoskeleton. Together, β -catenin and actin, along with p120-catenin, α -catenin, and E-cadherin, control the formation, maintenance and functions of adherens junctions. Second, as mentioned above, β -catenin can act as a transcriptional co-regulator, in the presence of Wnt signals[35].

β -catenin is encoded by a gene called *Ctnb1*. The *Ctnb1* gene contains 14 coding exons [37]. Exon 3 of the *Ctnb1* gene encodes the serine/threonine residues found on the β -catenin protein [35], which are phosphorylated by GSK3 in the absence of a Wnt signal, consequently leading to the degradation of β -catenin [35]. Multiple studies have genetically deleted exon 3 in order to stabilize β -catenin, which results in constitutive activation of the canonical Wnt signalling pathway [32, 38, 39]. In contrast, studies have demonstrated that the genetic deletion of exons 2-6 of the *Ctnb1* gene result in the generation of a non functional β -catenin protein[40-42]. We have utilized both of these principles in order to generate our transgenic mouse models of β -catenin stabilization and loss of function, respectively.

1.5 Canonical Wnt/ β -catenin signalling in kidney development

To understand the spatio-temporal pattern of canonical Wnt signalling activity in kidney development, kidneys from transgenic mice containing TCF/LEF consensus binding sites upstream of a β -galactosidase reporter transgene were studied. These studies demonstrated β -catenin-mediated transcriptional activity in the Wolffian duct, ureteric bud, branching ureteric epithelium and metanephric mesenchyme [34, 41].

1.5.1: Wnt/ β -catenin signalling in the ureteric epithelium

Within the Wolffian duct, Wnt/ β -catenin signalling plays an important role in maintaining Gata3 expression [43]. Gata3 is a transcription factor that controls the proper proliferation and extension of the Wolffian duct along the dorsal aspect of the embryo [44]. In addition, Gata3 also regulates the expression of c-Ret [44]. Studies have demonstrated that a loss of β -catenin from the Wolffian duct leads to a reduction in Gata3 expression and, as a result, c-Ret expression and signalling is also lost [43]. Consequently, branching morphogenesis fails to progress normally and is severely delayed. These studies place Wnt/ β -catenin signalling upstream of Gata3 [43].

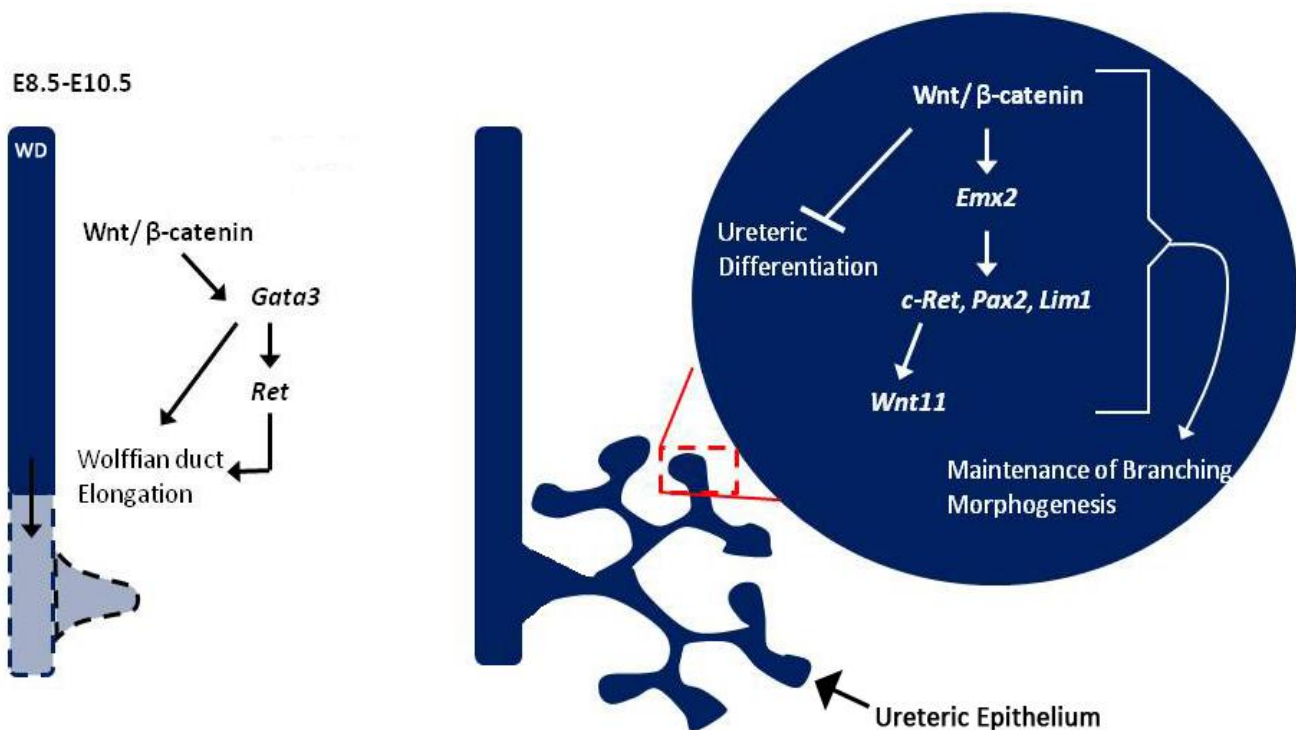
Numerous studies have also demonstrated that a loss of β -catenin specifically in the ureteric epithelium results in renal aplasia or severe hypodysplasia [41, 42]. Within the ureteric epithelium, β -catenin-mediated canonical Wnt signalling maintains the tips of the ureteric bud in an undifferentiated precursor state permissive for branching morphogenesis [42]. Loss of β -catenin from the ureteric epithelium leads to the premature expression of gene products that are normally associated with the differentiated kidney collecting duct system. Normally, Aquaporin-3, a water channel protein and marker of the differentiated collecting duct is not expressed until after E14.5. However, in β -catenin mutant Wolffian duct cells, Aqp-3 is expressed as early as E11.5 [42].

Another study demonstrated that loss of β -catenin leads to a decrease in Emx2 expression, causing an arrest in branching morphogenesis by E13.5 [41]. Emx2 is a transcription factor that is expressed in the Wolffian duct and ureteric bud, where it regulates the expression of key branching factors; Lim1, c-Ret, Pax2 and Wnt11 (discussed above) [41, 45]. Furthermore, the Emx2 promoter region contains TCF consensus binding sequences, where β -catenin can bind

and regulate transcription [41]. This study establishes that β -catenin signalling lies upstream of *Emx2* activation and as such regulates a hierarchy of gene expression (*Lim1*, *c-Ret*, *Pax2*) required in the maintenance of tip cell identity and branching morphogenesis [41].

Taken together, these studies demonstrate that *Wnt*/ β -catenin signalling maintains the ureteric epithelium in a precursor or undifferentiated state which allows for normal branching morphogenesis to occur and prevents the premature differentiation of these cells (Supplementary 9).

Supplementary 9: *Wnt*/ β -catenin signalling in the ureteric epithelium



***Wnt*/ β -catenin signalling in the ureteric epithelium:** A selection of pathways regulated by *Wnt*/ β -catenin signalling within the Wolffian duct prior to ureteric bud formation and ureteric epithelium during branching morphogenesis. In the Wolffian duct *Wnt*/ β -catenin signalling acts upstream of *Gata3* expression. *Gata3* controls *Ret* expression and together they maintain Wolffian duct elongation. During branching morphogenesis, *Wnt*/ β -catenin signalling maintains the tips of the ureteric epithelium in an undifferentiated state and regulates key genes necessary in the continuation of branching morphogenesis.

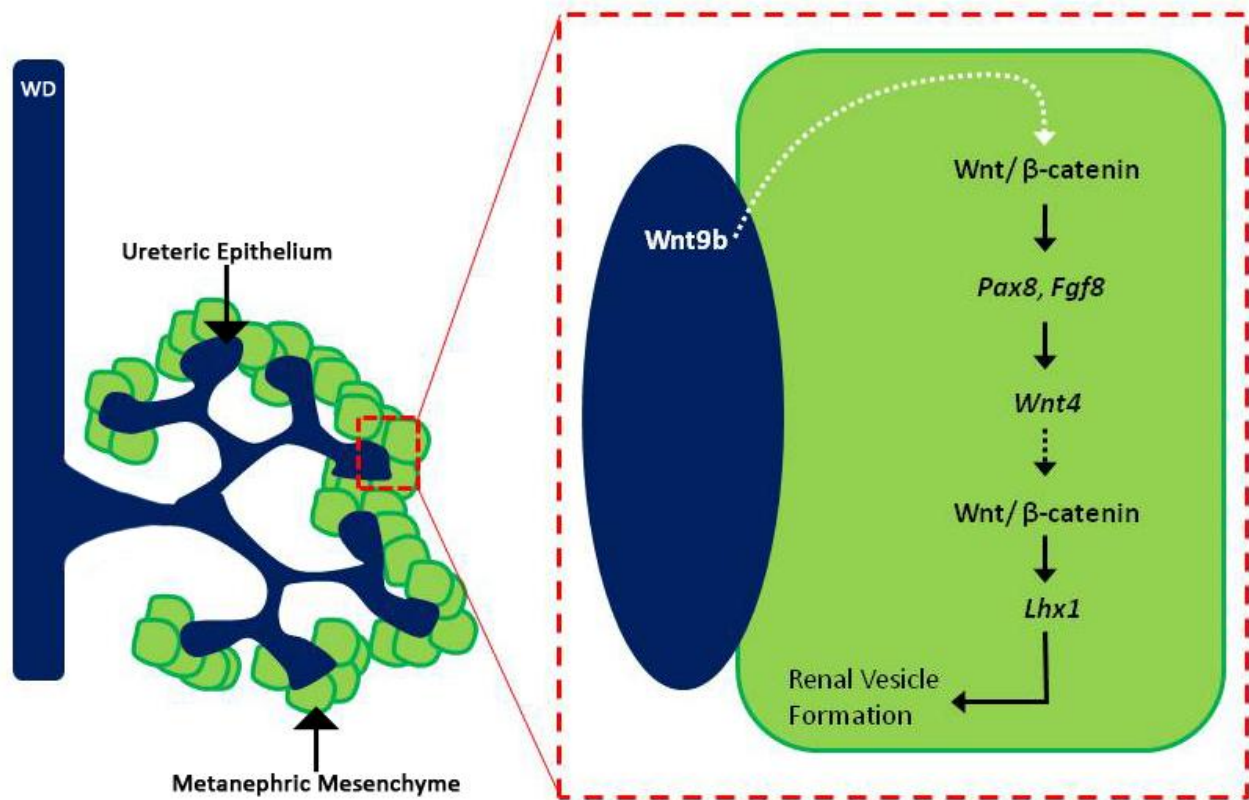
1.5.2: Wnt/ β -catenin signalling in the cap mesenchyme/nephron progenitors

Most research concerning Wnt/ β -catenin signalling in the metanephric mesenchyme has been focused on its role in nephrogenesis. Nephrogenesis is dependent upon a number of *Wnt* genes, including *Wnt9b* and *Wnt4* [29, 32, 39]. *Wnt9b* is expressed and secreted by the ureteric epithelium, and induces a subset of mesenchymal cells to condense around the tips of the ureteric branches [29]. The cap mesenchyme is composed of *six2*-expressing nephrogenic progenitors, a subset of which, upon induction by the ureteric epithelium, will cluster to form a pre-tubular aggregate (PTA) and express *Wnt4* [32]. *Wnt4* further induces these PTAs to undergo mesenchymal to epithelial transition (MET) and form epithelial structures known as renal vesicles (RVs), which will eventually give rise to mature nephrons [32]. A study conducted by Park et al demonstrated that Wnt/ β -catenin signalling is required for the formation of nephrons. More specifically, this study demonstrated that β -catenin mediates the early inductive actions of both *Wnt9b* and *Wnt4* in the transition of mesenchymal nephron progenitors to an epithelial renal vesicle [32]. Loss of β -catenin from nephron progenitors (cap mesenchyme) results in reduced expression of key genes required in the early inductive response (nephrogenic program) including: *Fgf8*, *Pax8*, *Wnt4*, *Lhx1* and as such no renal vesicle forms and nephrogenesis is absent [32] (Supplementary 10). On the other hand, over-expression of β -catenin within these nephron progenitors leads to an ectopic activation of the early inductive response genes (*Fgf8*, *Pax8*, *Wnt4* and *Lhx1*). While the early inductive response is initiated when β -catenin is stabilized, no renal vesicles form, which consequently leads to renal agenesis. Park et al suggested that while β -catenin is necessary for the induction of the early nephrogenic program, a down-regulation or loss of canonical Wnt activity may be necessary for the mesenchymal to epithelial transition (MET) and the subsequent formation of nephrons [32]. In contrast to their

findings, multiple studies have also shown that nephrogenesis progresses normally in the presence of sustained β -catenin activity within the metanephric mesenchyme [46]. Earlier work has shown that isolated metanephric mesenchyme from normal/wildtype mice cultured in the presence of LiCL (a GSK3 inhibitor) demonstrate the formation of not only renal vesicles but also comma-shaped bodies [46]. More recently, studies by Kuure et al demonstrated that metanephric mesenchyme in which β -catenin was stabilized, using a transgenic mouse model, displayed the formation of pretubular aggregates which then differentiated into nephron epithelium [47]. Based on these conflicting reports, it is still not clear as to the role mesenchymally expressed β -catenin has in nephron development.

However, more important to our study is that there are numerous signals emanating from the metanephric mesenchyme which control branching morphogenesis [9]. Yet, despite their importance in normal renal development, previous studies have not defined whether β -catenin regulates these mesenchymal expressed factors.

Supplementary 10: Wnt/ β -catenin signalling in nephrogenesis



Wnt/ β -catenin signalling in nephrogenesis: Model of Wnt/ β -catenin signalling in the metanephric mesenchyme in the control of Nephrogenesis proposed by Park et al[32]. In this model, Wnt/ β -catenin signalling mediates Wnt9b signalling and activates the expression of key genes required in the early nephrogenic program.

1.6 Renal dysplasia

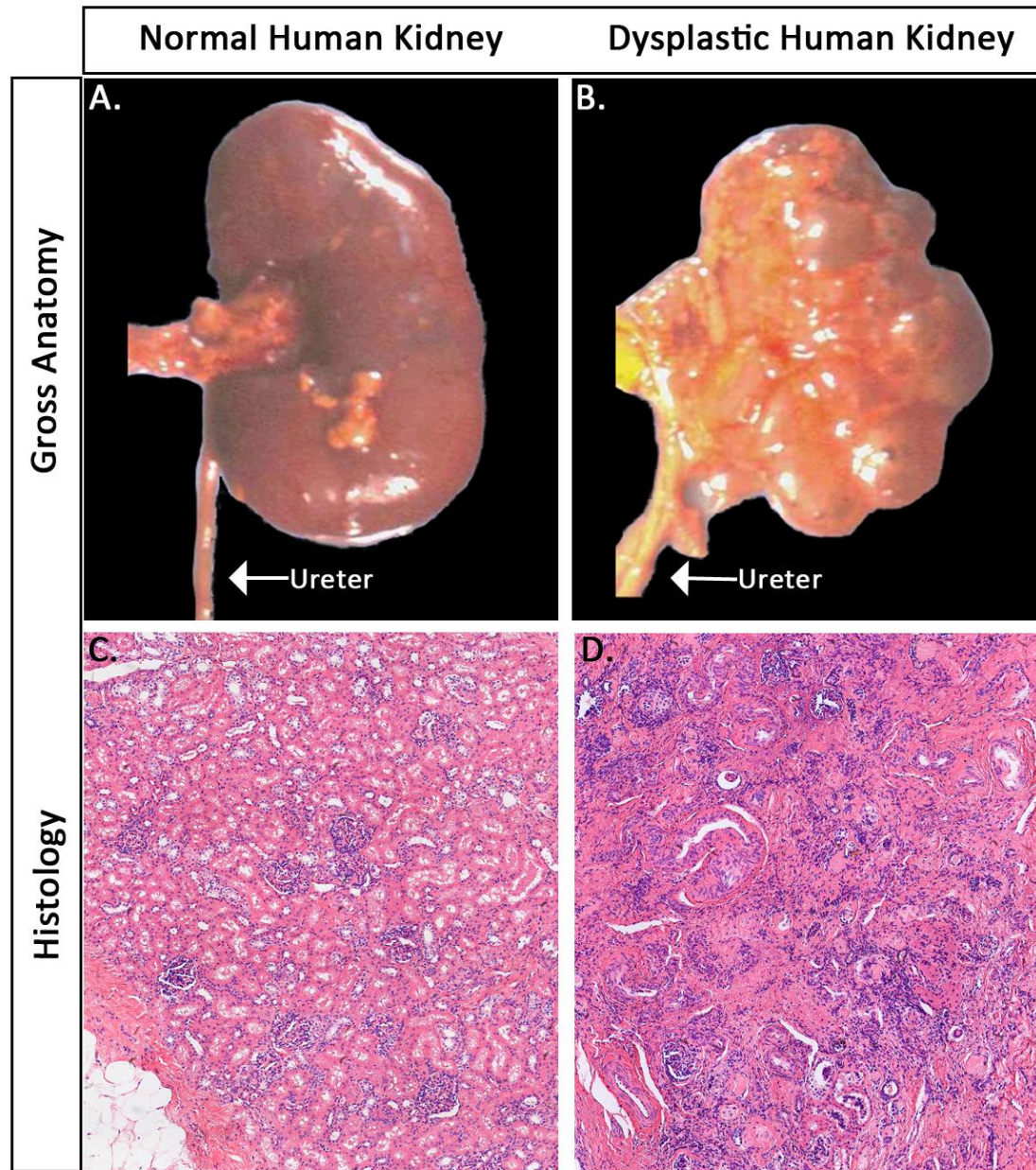
1.6.1: Human Renal Dysplasia

Congenital anomalies of the kidney and urinary tract (CAKUT) rank among the most common of all birth defects, with an incidence of 1 in 250 live births [48]. Included in these anomalies is renal dysplasia. Human renal dysplasia is a severe form of congenital kidney malformation which affects up to 1 in 1000 of the general population [49] and is one of the leading causes of childhood end-stage kidney disease [50]. The label ‘dysplasia’ is often given to kidneys that are misshapen and include abnormal structures not seen in normal tissue [49, 51, 52]. In this sense, renal dysplasia describes a range of disorders, from renal agenesis to massive cystic kidneys. Renal dysplasia arises from aberrant inductive interactions between the ureteric bud and surrounding mesenchyme during kidney development. Consequently, this interruption leads to abnormal collecting duct development and loss of functioning nephrons [49, 51, 52]. Renal dysplasia is associated with many different, yet distinct recognizable patterns of malformed kidney tissue (histological features of renal dysplasia are outlined in the next section) [49, 51, 52]. In this regard, while renal dysplasia may describe the presence of small kidneys, renal hypoplasia is considered a separate entity [49, 51]. Renal hypoplasia is described as small kidneys which consist a low number of structurally normal nephrons, yet maintain normal kidney architecture [53].

1.6.2: Characteristics of Human Renal Dysplasia

Renal dysplasia is characterized by the presence of malformed kidney tissue elements amidst some normal appearing renal parenchyma. There are a host of malformations which characterize dysplastic kidney tissue. Grossly, dysplastic kidneys are misshapen and cystic [51]. Histological characteristics of dysplastic kidneys include: abnormal cortical and medullary patterning [54], disorganization of the collecting system and nephron elements [49, 55], dilated/cystic epithelial tubules and collecting ducts [56-58], focal regions of undifferentiated tubules and mesenchyme [49], cystic glomeruli [53], loosely arranged stroma [49, 52], and the formation of metaplastic cartilage [52]. While these abnormalities characterize renal dysplasia, the degree of these malformations and their focal versus diffuse nature within dysplastic renal tissue varies among cases.

Supplementary 11: Human renal dysplasia



Human renal dysplasia: (A,B) Gross anatomy of human kidneys, Image adapted [51]. (A) Normal healthy human kidney at birth. (B) Dysplastic kidney at birth which is severely misshapen and lobular with multiple cyst formations. (C-D) Histology of human kidney tissue. (C) Normal human kidney section with organized tubules and glomeruli. (D) Dysplastic kidney tissue with a complete disorganization of kidney parenchyma. Formation of cystic glomeruli, dilated and cystic tubules. Focal regions of undifferentiated mesenchyme and epithelial tubules and dysplastic stroma.

1.6.3: β -catenin in Renal Dysplasia

While the exact causes of renal dysplasia are not known, the literature suggests hereditary factors and changes in gene expression are involved. Ten percent of children who display dysplastic kidneys have a first degree relative that is affected by a renal or urinary tract disease [59]. Various genomic mutations in the *HNF1B*, *PAX2*, and *RET* genes have been linked to a small proportion of cases of human renal dysplasia [60, 61]. However, in many cases of human renal dysplasia, a clear genomic alteration is not often ascertained. This should not be surprising considering the vast number of factors that are mis-expressed in dysplastic human kidney tissue [62]. Determining which changes in expression are causative and which are downstream consequences is therefore very difficult. To name a few mis-expressed factors, *TGF β 1*, *GDNF*, *PAX2* and *GATA3* have all been shown to be dysregulated in dysplastic human renal tissue [62, 63]. Interestingly, several of the genes that have been implicated in renal dysplasia are known to be regulated by β -catenin, including *Tgf β 1* and *Gata3* [38, 43]. In addition, our lab has mapped the promoter regions of multiple dysregulated genes in renal dysplasia and found that some contain β -catenin binding sites (personal communication, Bridgewater), suggesting that β -catenin is involved in the mis-regulation of these genes. In further support of this notion, a study by Hu et al demonstrated that β -catenin is over-expressed in ureteric derived epithelium in human renal dysplasia [58]. To determine the role of β -catenin over-expression in the pathogenesis of renal dysplasia, Bridgewater et al generated a mouse model in which β -catenin was over-expressed specifically in the ureteric epithelium [38]. These studies showed that elevated levels of β -catenin targeted to the ureteric epithelium during renal development leads to the up-regulation of *Tgf β 2* and *Dkk1*, negative regulators of branching morphogenesis and Wnt signalling respectively [38]. The over-expression of these factors inhibits branching morphogenesis and

increases metanephric mesenchyme cell apoptosis, resulting in severe renal hypodysplasia [38]. These studies have established the role of over-expression of β -catenin in the ureteric epithelium in the pathogenesis of renal dysplasia. However, whether β -catenin is over-expressed in other cells of kidney dysplastic tissue has not yet been assessed; thus, the role of β -catenin in renal dysplasia has not been fully explored.

2.0 Hypothesis and objectives

2.1: Overall hypothesis

The overall hypothesis of this study is that *mesenchymal over-expression of β -catenin causes renal dysplasia.*

2.2: Study objectives

1. Investigate β -catenin expression in human renal dysplasia

Hypothesis: *β -catenin is over-expressed in the metanephric mesenchyme and stroma in dysplastic human kidney tissue*

2. Generate and characterize a mouse model of human renal dysplasia

Hypothesis: *β -catenin over-expression in the metanephric mesenchyme will cause renal dysplasia*

3. Define a mechanism that leads to human renal dysplasia

Hypothesis: *β -catenin regulates the expression of key renal developmental genes in the metanephric mesenchyme.*

3.0 MATERIALS AND METHODS

Mice:

We utilized the Cre-LoxP system to generate transgenic mice. *Rarβ2-Cre* (*Cre* expression limited to the metanephric mesenchyme) male mice were crossed with female mice containing LoxP sites flanking exon 3 of the β -catenin allele (β -cat ^{$\Delta 3/\Delta 3$}) [64] to generate β -catenin gain-of-function mutant progeny, termed β -cat^{GOF-MM} (Fig. 2A). The Cre transgene was detected in mouse tail DNA using primers 5'-GCGGCATGGTGCAAGTTGAAT-3' and 5'-CGTTCACCGGCATCAACGTTT-3'. TCF- β -galactosidase reporter mice [65] were crossed with β -cat ^{$\Delta 3/\Delta 3$} to generate female *TCF/LacZ*; β -cat ^{$\Delta 3/+$} mice. Female β -TCF/LacZ; β -cat ^{$\Delta 3/+$} mice were then crossed with male *Rarβ2-Cre* mice to generate TCF/LacZ; β -cat^{GOF-MM} and used to visualize branching morphogenesis [38, 41]. To generate β -catenin loss-of-function mutants, *Rarβ2-Cre* male mice were crossed with female mice containing LoxP sites flanking exons 2 through 6 [40] to generate *Rarβ2-Cre*; β -cat^{+/-} males. These males were then mated to homozygous β -catenin conditional knockout females to generate *Rarβ2-Cre*; β -cat^{-/-} termed β -cat^{LOF-MM}. The Cre transgene was detected in mouse tail DNA using primers 5'-GCGGCATGGTGCAAGTTGAAT-3' and 5'-CGTTCACCGGCATCAACGTTT-3'. To detect the β -catenin floxed allele, primers 5'-AAG GTA GAG TGA TGA AAG TTG TT- 3' and 5' -CAC CAT GTC CTC TGT CTA TTC- 3' were used [40]. To analyze *Rarβ2-Cre* expression, male *Rarβ2-Cre* mice were crossed with *Gt(ROSA)26Sor(ROSA)* mice [66]. In all instances, 12:00pm on the day of vaginal plug detection was considered to be E0.5. Animal studies were done in accordance with animal care and institutional guidelines.

Micro dissection of mouse embryonic kidneys

Mouse embryos were collected on required embryonic day. Kidneys were resected using Dumont #5 inox surgical forceps in PBS pH 7.4 under EZ4D Leica microscope.

PCR conditions for genotyping:

To isolate DNA, mouse tails were heated at 95°C in 50mM NaCl for 40 minutes or until in solution and then 0.5M Tris-HCL pH 8.0 was added into solution. PCR conditions for each primer set were the same and were as follows:

Step1: 94°C, 3minutes

Step2: 94°C, 45seconds

Step3: 58°C, 40seconds

Step4: 72°C 40seconds

Step5: 72°C 5minutes

Steps2-4 for 35 cycles.

β-galactosidase staining:

Kidneys were fixed in LacZ fixing solution (0.2% gluteraldehyde, 100mM EGTA pH 7.3, 1M MgCl₂, 0.1M sodium phosphate buffer pH 7.3, 1.5% formaldehyde) for 5 minutes. Kidneys were washed in LacZ washing buffer (1M MgCl₂, 0.1M sodium phosphate buffer pH 7.3, 0.25% nonidet P-40). Whole kidney tissue was incubated X-galactosidase stain (25mg/ml X-gal (Bethesda Research labs), 0.25mM potassium ferrocyanide, 0.25mM potassium ferricyanide) until staining was complete. Kidneys were washed in wash buffer and fixed in 4% paraformaldehyde and visualized on LeicaEZ4D microscope.

Human kidney dysplastic tissue

1 year post-natal human renal dysplastic tissue was obtained from McMaster archived pathology in accordance with the Hamilton integrated research ethics board (13-160-T).

Histology:

Whole kidney tissue was fixed in 4% paraformaldehyde for at least 24 hours at 4 °C. Kidneys were Paraffin-embedded sectioned (4 µm) and mounted on slides. Samples were incubated overnight at 37°C Paraffin embedded kidney sections were deparaffinized using xylene washes and rehydrated using graded ethanol washes (100%, 95%, 75%, 50%, H₂O). Tissue sections were stained using haematoxylin and eosin (Sigma, MHS16).

Immunofluorescence and Immunohistochemistry:

Paraffin embedded kidney sections were deparaffinized and rehydrated using graded ethanol washes. Antigen retrieval was performed by boiling tissue sections for 5 minutes in 10mM sodium citrate solution pH 6.0, followed by blocking with 7.5% normal goat serum/4.5% BSA. Sections were incubated with primary antibodies to Six2 (Proteintech Group, 11562-1-AP; 1:250), Pax2 (Covance, PRB-276P; 1:200 dilution), Cytokeratin (Sigma, C2562; 1:200 dilution), WT-1(SantaCruz, sc-192; 1:200 dilution), Nephlin (Sigma, PRS2265; 1:200 dilution) overnight at 4°C. Tissue sections were washed in PBS pH 7.4, incubated with secondary antibodies Alexafluor 488, 568 (Invitrogen; 1:1000 dilution) for 1 hour at room temperature and stained with Dapi (Sigma, D9542; 1:1000 dilution) for 5 minutes and coverslipped using Fluoromount (Sigma, F4680). Immunohistochemistry was performed using the Vectastain elite ABC kit (Vector Labs, PK7100). After antigen retrieval, endogenous peroxidase activity was blocked

using 3% H₂O₂ for 10 minutes followed by blocking endogenous biotin binding activity using a biotin/avidin blocking kit (Vector Labs, SP-2001) as described by company protocol. Incubation with primary antibodies including, Activated β -catenin, which detects nuclear β -catenin (Millipore, 05-665; 1:100 dilution), Pax2 (Covance, PRB-276P; 1:200 dilution) and GDNF (R&D systems, AF-212-NA; 1:100) were incubated overnight at 4°C. Sections were washed and incubated in biotinylated secondary antibodies (Vector labs, BA1400) for 30 minutes at room temperature. Colour reaction was visualized using DAB (Vector Labs, SK4100) and slides were mounted using Permount (Fischer, SP15-500). Slides were viewed and photographed on a Nikon 90i-eclipse upright microscope.

Whole-mount immunofluorescence:

Kidneys were flattened on 0.4 μ m transwell filters (Falcon) for 4 hours at 37°C in wells containing DMEM and stored in 100% methanol at -20 degrees. Kidneys were washed 3X with PBS, blocked in 10% normal goat serum followed by incubation with primary antibodies to Cytokeratin (Sigma, C2562; 1:200 dilution) Pax2 (Covance, PRB-276P; 1:200 dilution) at 37°C for 1.5 hours. Kidneys were washed in PBS pH 7.4 and incubated with secondary antibodies Alexafluor 488, 568 (Invitrogen; 1:200 dilution) for 1.5 hours at 37°C. Kidneys were viewed and photographed on a Nikon 90i-eclipse inverted microscope.

In-situ hybridization:

Non-radioactive in-situ hybridization was performed using digoxigenin (DIG)-labeled cRNA probes on whole kidney tissue. cDNA encoding *Gdnf*, *C-Ret* and *Wnt11* were provided by the Rosenblum lab. *Gdnf* was linearized and a 0.33kb antisense RNA transcript was synthesized

with SP6 polymerase (Roche). *C-Ret* was linearized and a 1.8kb antisense RNA transcript was synthesized with T7 polymerase (Roche). *Wnt11* was linearized and a 0.55kb antisense RNA transcript was synthesized with T3 polymerase (Roche).

Kidneys were fixed in 4% paraformaldehyde overnight at 4 °C, then washed with PBS and stored at -20°C in 100% methanol. Kidneys were rehydrated using PBS pH 7.4 and treated with 4µg/ml Proteinase K (ThermoScientific) for 8 minutes at room temperature, washed with 2mg/ml Glycine (GE Healthcare) for 10 minutes at room temperature. Kidneys were washed with PBS and refixed with 4% Paraformaldehyde for 20 minutes at room temperature and washed in PBS. Prehybridization was performed on kidneys for 2 hours at 70°C, followed by hybridization with probe overnight at 70°C. Prehybridization and Hybridization solution was 50% formamide, 5X SSC (pH 4.5), 50 µg/ml yeast tRNA (Ambion), 50 µg/ml Heparin (Sigma), 1% SDS. Kidneys were washed in solution 1 for 1 hour at 70°C, followed by a wash in 50% solution 1: 50% solution 2 for 5 minutes at room temperature, washed in solution 2 for 10 minutes at room temperature. Solution 1 contained 50% formamide, 4X SSC, 1% SDS and solution 2 was made up of 0.5M NaCl, 0.01M Tris (pH 7.5), 1% Tween-20. Whole kidneys were treated with 100 µg/ml RNase A (Thermoscientific) for 30 minutes at 37°C. Kidneys were washed in 1X MABT solution and blocked with 2% blocking reagent (Roche) followed by overnight incubation with Anti-digoxigenin- AP (Roche; 1:2000 dilution in blocking reagent with 0.1% goat serum) at 4°C. Kidneys were washed in 1XMABT with Levamisole for 4 hours at room temperature, followed by a 30 minute wash in 0.1M Tris (pH 9.5), 0.05M MgCl₂, 0.1M NaCl, 1% Tween-20. Alkaline phosphatase (colour reaction) was developed by incubating kidneys in BM Purple AP Substrate precipitating (Roche) at room temperature. Kidneys were

washed in PBS and fixed in 4% paraformaldehyde. Kidneys were viewed and photographed using a Leica EZ4D microscope.

Chromatin immunoprecipitation (ChIP):

Embryonic kidney E14.5 was dissected and fixed (crosslinked) in 4 % formaldehyde. Addition of glycine to final concentration of 125mM stopped fixation. Fixed tissue was homogenized in lysis buffer (1%SDS, 10mM EDTA, 50MmTris pH 8.0) and sonicated to generate DNA fragments of 200-1000bp. Soluble chromatin was precleared by Protein G agarose /salmon sperm DNA beads (Millipore, CA,USA). 2µg of mouse anti-β-catenin antibody (BD, Canada) was added to every 100µl of soluble chromatin to immunoprecipitate β-catenin-binding DNA. This complex was separated with unbound fraction by G agarose /salmon sperm DNA beads followed by a series of washing buffer with protein inhibitors. Crosslinked protein-DNA compound was disassociated by incubation with DNase-free proteinase K and RNA residual was removed by RNase A. DNA was finally purified with Zymo ChIP DNA clean & concentrated kit (Zymo Research, USA).

Qualitative analysis of ChIP DNA:

Three fragments having the TCF binding sites of interest on the 5'UTR and one fragment including the TCF binding site on the 3'UTR were examined by PCR. A fragment enclosing GDNF coding region was used as a negative control. All primers were designed with Primer 3 software. PCRs were performed using the same PCR program:

Step1: 94°C, 2minutes

Step2: 94°C, 30seconds

Step3: 58°C, 30seconds

Step4: 72°C 10seconds

Step5: 72°C 4minutes

Steps2-4 for 35 cycles.

Primer sequences for ChIP:

Primer sequences were as followings:

4.9kb site on 5' UTR (forward) 5'-TCTCAGCTGCTGTGCCTATG-3' and (reverse) 5'GGCAGGTCAGGAGTAAGCAA-3'.

2.5kb site on 5' UTR (forward) 5'-GCAAACCAGCTCTTTCAACA-3' and (reverse) 5'-AATTGCTGGACTGAACATGGA-3'.

2.3 kb site on 5' UTR (forward) 5'-GGGTAATGTGTGTGGCAATG-3' and (reverse) 5'-CTTCCCTGCAAGGTGTTGTT.

3'UTR site 5'-TGGACCCTTGTTCTCAATGTT-3' and (reverse) 5'-TCACCAGTGACCACAGAAGC-3'.

GDNF coding region (forward) 5'- ACATGCCTGGCCTACTTTGT-3' and (reverse) 5'-GACTTGGGTTTGGGCTATGA-3'.

Constructs of plasmids:

A 560bp Mlu I/Hind III fragment of the Gdnf promoter including the TCF binding site TTCAAAG was amplified from human 293 genomic DNA with a pair of primers of 5' ACGCGTTGAGGGGACATTCCAGGCT 3' (FP) and 5' AAGCTTATCTCCCTTGCCAATGTCAGGA 3' (RP) and cloned into pGLuc-Basic vector

(NEB, MA, USA) to create pGluc-Gdnf. TATA box oligonucleotides were annealed and ligated into BamH I site to create the pGluc-Gdnf-TATA. All the inserts were sequenced after plasmids were constructed and all the sequences were correct.

Cell Culture:

HEK293 cells were obtained from American Type Cell Collection (ATCC, Rockville, MD, USA) and cultured in Dulbecco's minimal essential medium (DMEM) (Hyclone) with 4mM L-glutamine, supplemented with 10% fetal bovine serum (FBS) (PAA, Etobicoke, ON, CA) at 37°C in a 5%CO₂ water-jacketed incubator.

Transfection:

HEK293 cells were seeded into a 24-well plate at 1.0×10^5 /well in 0.5 ml of growth medium without antibiotics. Twenty-four hours later, HEK293 cells were transfected with three indicated plasmids (pGluc-Basic, pGluc-Gdnf, pGluc-Gdnf-TATA) following the instructions of LipofectamineTM 2000 by the manufacturer (Invitrogen, Carlsbad, CA): 0.8 µg of each plasmid DNA was diluted in 50 µl of DMEM in one eppendorf tube and gently mixed and then 2.0 ul of Lipofectamine 2000 was added into 50 µl DMEM in another eppendorf tube and gently mixed. After five minute incubation, diluted plasmid DNA and diluted Lipofectamine 2000 were mixed gently and incubated at room temperature for 20 minutes. One hundred microliters of the DNA-Lipofectamine 2000 complexes were added drop-wise to each well containing cells and medium.

Activation by LiCl:

Twenty-four hours after transfection, media were collected and then completely changed to serum-free medium (DMEM only). Cells were serum-starved overnight (16hrs) and subsequently activated by 40 mM lithium chloride (LiCl) (Sigma, St. Louis, MO, USA). Medium were collected at 0, 6, 8, 10, 12 and 24 hours. Cells were lysed in lysis buffer (150 mM NaCl, 20 mM Tris, 1% NP40, pH 8.0) and lysates were harvested for protein assay.

***Gaussia* Luciferase activity assay**

Gaussia Luciferase assays were performed with BioLux® *Gaussia* Luciferase Flex Assay Kit from New England BioLabs (MA, USA). Twenty microliters of culture medium were added into a 96-well opaque plate and 50µl of Gluc substrate working solution were injected and relative light units (RLUs) were measured by a LB luminometer (Thermo Fisher, USA). *Gaussia* Luciferase activity was calculated as total RLUs in the medium and standardized by the total protein of the cells in corresponding wells.

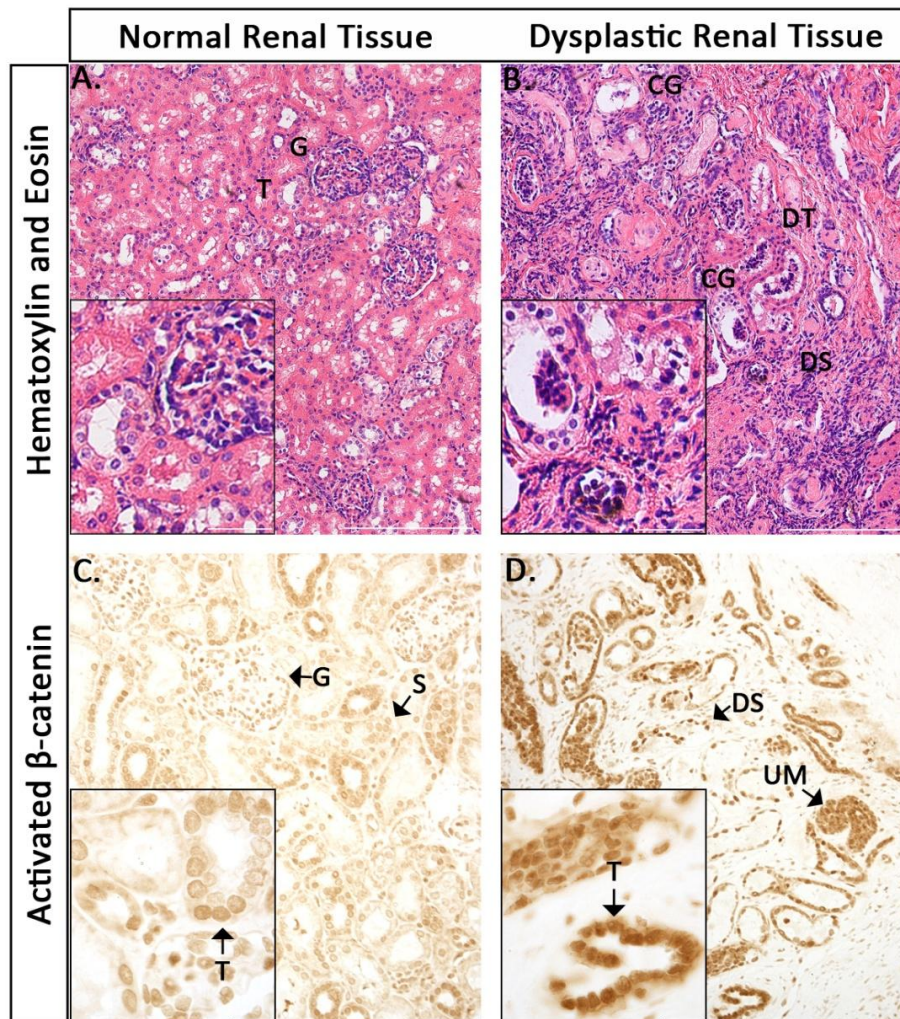
Statistical Analysis

Analysis included determination of mean signal intensity and positive staining area of *Gdnf* expression in β -cat^{GOF-MM} mutants and WT using NIS elements software. The data was analyzed using 2-tailed Student's *t* test using GraphPad Prism software (version 5.0c). A probability of less than 0.05 was considered to indicate statistical significance. Values are given as mean +/- SEM.

4.0 RESULTS

4.1: β -catenin is over-expressed in human renal dysplasia

Normal human kidney tissue at 1 year post natal reveals the formation of an organized cortex and medulla, containing tubules and glomeruli (Fig. 1A). In contrast, histological analysis of Human dysplastic renal tissue at one year post natal demonstrates a lack of cortical/medullary patterning, undifferentiated dilated and cystic tubules, cystic glomeruli and the expansion and disorganization of stromal cells (Fig. 1B). Previous studies have shown over-expression of β -catenin in the ureteric epithelium of dysplastic human renal tissue [58], however in these studies it was not clear whether β -catenin was over-expressed in other cells of the kidney. To analyze the expression of β -catenin in dysplastic human renal tissue, we utilized an antibody that detects the transcriptionally active form of β -catenin. In normal renal tissue we observed the expression of β -catenin in the nuclei of epithelial tubules, epithelial cells of the glomeruli and in stromal cells (Fig. 1C). In contrast, in dysplastic renal tissue we observed a marked increase in the expression of β -catenin within the nuclei of dysplastic epithelium; dilated and cystic epithelial tubules and glomeruli, and in sporadic regions of undifferentiated mesenchyme and stromal cells (Fig. 1D). These results demonstrate for the first time that in addition to the ureteric epithelium, activated β -catenin is mis-expressed within the mesenchyme and stroma of dysplastic renal tissue. In addition, these studies suggest that over-expression of β -catenin may have an important pathological role in the progression of renal dysplasia and therefore warrants further study.

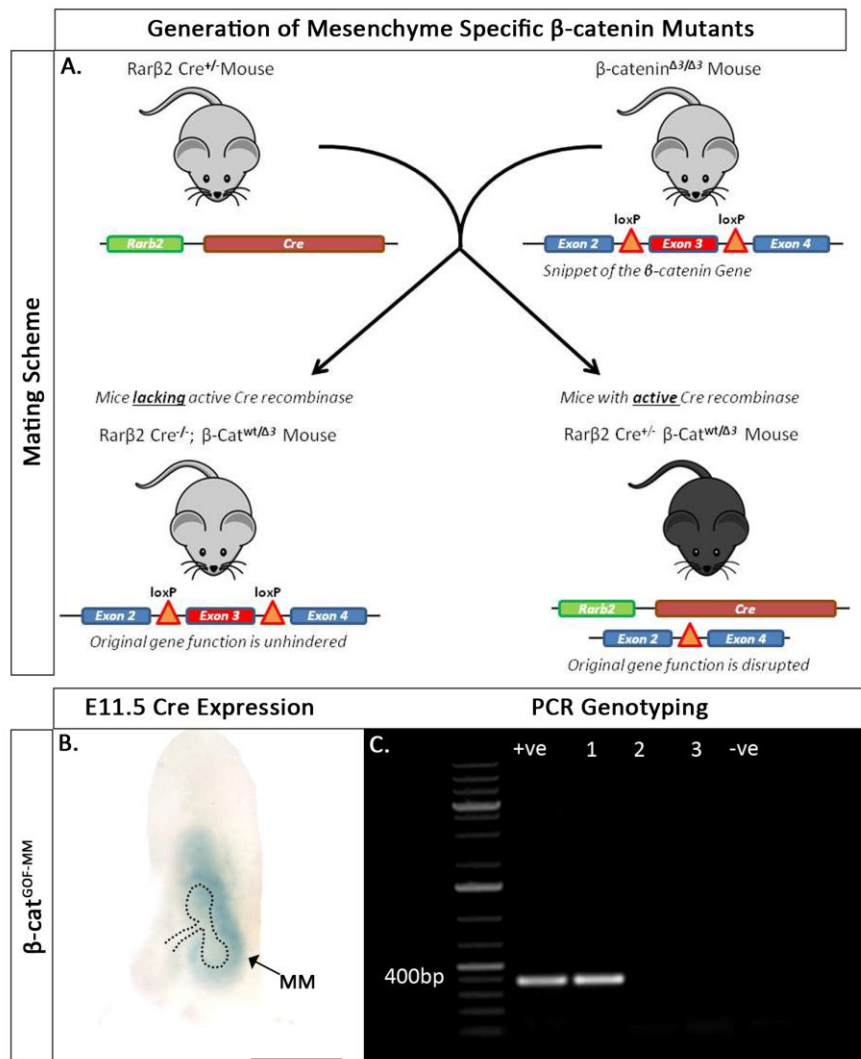
Figure 1: β -catenin levels are elevated in Human Renal Dysplasia

Levels of active β -catenin are elevated in human renal dysplastic tissue. (A,B) Postnatal human kidney tissue stained with hematoxylin and eosin (scale bar = 200 μ m, Inset scale bar = 100 μ m). **(A)** Normal human renal tissue showing glomeruli (G) and tubular structures (T) within the renal parenchyma (Inset: high power image of a glomerulus and adjacent tubules). **(B)** Human dysplastic kidney tissue characterized by disorganized renal parenchyma, dysplastic dilated cystic tubules (DT), cystic glomeruli (CS), and disorganized stroma (DS). **(C,D)** Activated β -catenin expression was detected by immunohistochemistry using anti-active β -catenin and HRP-conjugated secondary antibodies (scale bar = 50 μ m, Inset scale bar = 10 μ m). **(C)** β -catenin is weakly expressed in normal human kidney tissue epithelial tubules and surrounding stroma (Inset: Nuclear β -catenin is moderately expressed in epithelial tubules). **(D)** Levels of β -catenin are markedly increased in the nuclei of epithelial tubules, undifferentiated mesenchyme (UM) and stroma in human renal dysplastic tissue (Inset: β -catenin is expressed at high levels in the tubule epithelial nuclei).

4.2: Generation of mesenchyme specific β -catenin Gain-of-function mutants

To understand the pathological significance of β -catenin over-expression in the mesenchyme of dysplastic tissue, we generated a mouse model in which β -catenin was over-expressed specifically in the metanephric mesenchyme. The $Rar\beta 2$ promoter drives expression of Cre specifically in the metanephric mesenchyme of the developing kidney [45, 67]. To confirm that $Rar\beta 2$ Cre expression was specific to the metanephric mesenchyme we crossed $Rar\beta 2$ Cre mice with a ROSA reporter mouse strain. ROSA reporter mice contain a LoxP flanked DNA segment (stop segment) that prevents the expression of a β -galactosidase gene (LacZ). However, when ROSA mice are crossed with a Cre transgenic mouse, the “stop site” will be genetically deleted by Cre and β -galactosidase will be expressed wherever Cre is active [66]. In $Rar\beta 2$ -cre;ROSA mice, Cre was expressed specifically in the metanephric mesenchyme surrounding the T-shape ureteric epithelium at E11.5 (Fig. 2B). Mutants, termed β -catenin gain of function-metanephric mesenchyme (β -cat^{GOF-MM}) were generated by crossing homozygous mice that had exon 3 of the β -catenin gene flanked (“floxed”) by LoxP sites with mice expressing Cre recombinase under the control of the $Rar\beta 2$ promoter (the genetic cross is outlined in Fig. 2A). The offspring will have genetic deletion of exon 3 mediated by Cre, thus generating a β -catenin protein lacking phosphorylation sites which are required for β -catenin degradation. This results in the stabilization (over-expression) of β -catenin exclusively in the metanephric mesenchyme.

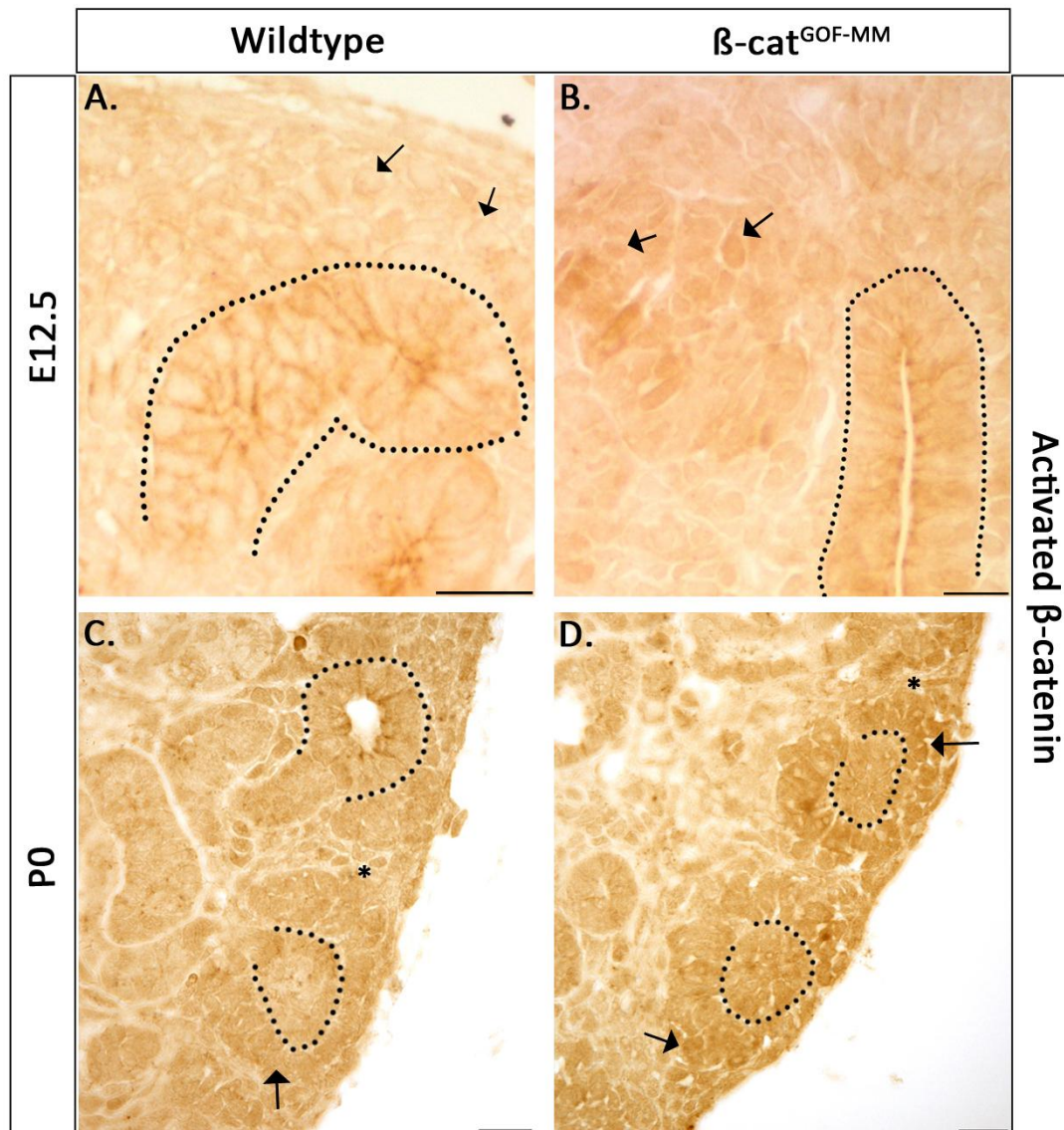
To identify β -cat^{GOF-MM} mutant and wildtype embryos, we performed PCR using primers specific to the $Rar\beta 2$ Cre transgene. The PCR amplification of the $Rar\beta 2$ -Cre transgene generated a 400bp amplicon. The absence of an amplicon was considered wildtype (Fig 2C).

Figure 2: Generation of mesenchyme specific β -catenin gain of function mutants

Generation of mesenchyme specific β -catenin gain-of-function mutants. (A) Mating scheme to generate mice with over-expression of β -catenin in the metanephric mesenchyme. (B) At E11.5, Rar β 2 drives Cre expression specifically in the metanephric mesenchyme (scale bar = 250 μ m). (C) PCR genotyping to detect the Cre transgene. Primers for Rar β 2cre were used to detect β -cat^{GOF-MM} mutants, indicated by the presence of a 400bp amplicon band. A known mutant (+ve) was used to determine if the PCR reaction was successful. The presence of a band in lane 1 indicated that the Cre transgene was present resulting in a β -cat^{GOF-MM} mutant. No band in lane 2 and 3 indicated that the Cre transgene was not present and therefore β -catenin expression remained normal resulting in a wildtype phenotype. A negative control was used to establish that there was no contamination in the PCR reaction.

To determine if β -cat^{GOF-MM} mutants exhibited increased levels of β -catenin, antibodies detecting the transcriptionally active form of β -catenin were used during different developmental time-points. At E12.5, wildtype kidneys demonstrated cytoplasmic localization of β -catenin in both ureteric and mesenchymal cells, however the majority of metanephric mesenchymal cells lacked nuclear β -catenin or was expressed at low levels (Fig. 3A). In contrast, β -cat^{GOF-MM} mutants demonstrated increased nuclear accumulation of β -catenin within the metanephric mesenchyme (Fig. 3B). These findings demonstrate that very early during development β -cat^{GOF-MM} mutants exhibit increased levels of β -catenin in the metanephric mesenchyme. At post-natal day 0, β -cat^{GOF-MM} mutants displayed increased nuclear and cytoplasmic accumulation of β -catenin in mesenchymal, epithelial and stromal cells (Fig. 3D) as compared to wildtype (Fig. 3C). Together, these findings confirm increased levels of transcriptionally active β -catenin in β -cat^{GOF-MM} kidneys.

Figure 3: Levels of transcriptionally active β -catenin are increased in β -cat^{GOF-MM} mutants



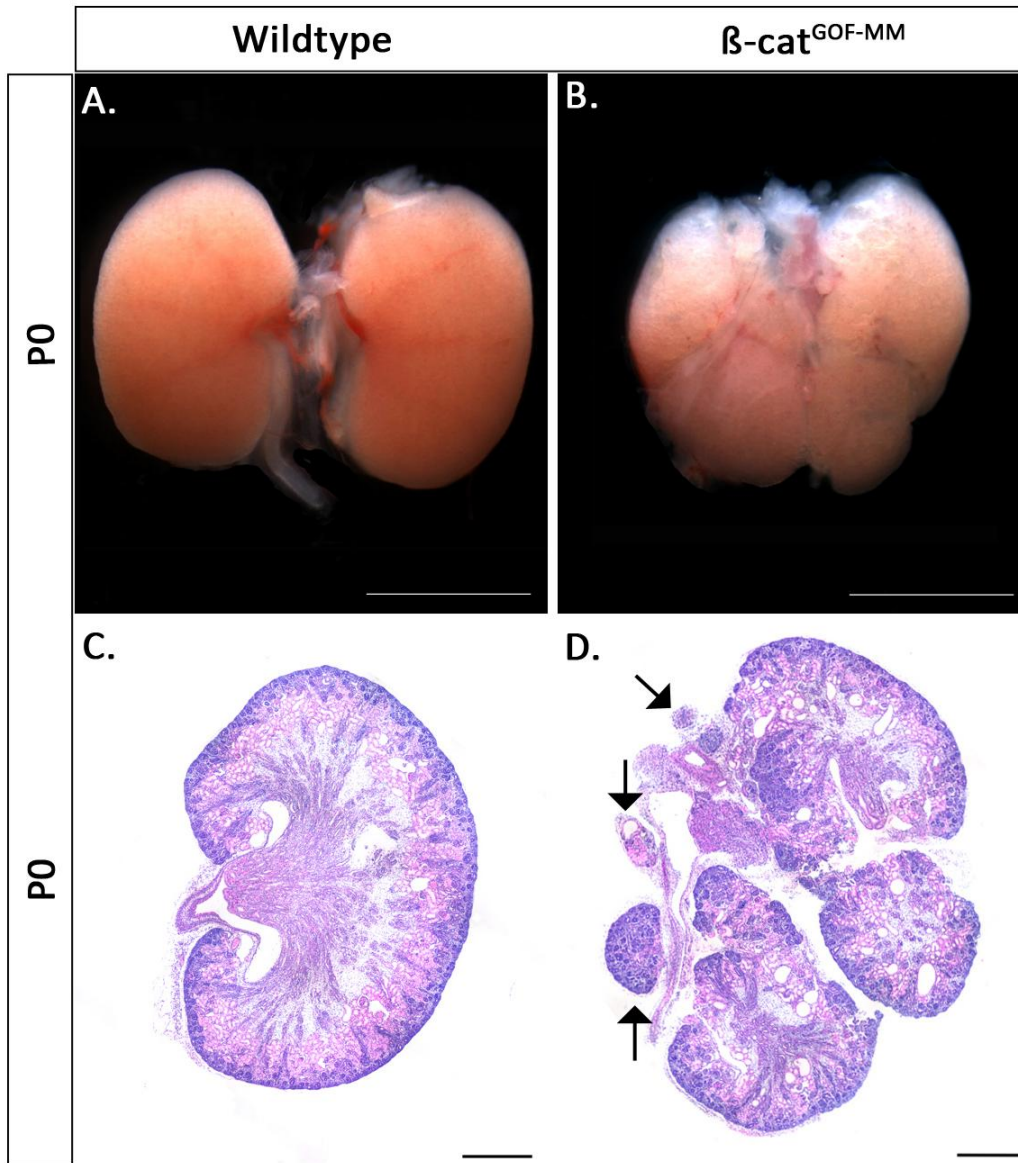
Levels of transcriptionally active β -catenin are increased in β -cat^{GOF-MM} mutants: (A,B) Analysis of activated β -catenin using Immunohistochemistry in E12.5 kidneys (scale bar = $10\mu\text{m}$). (A) Wildtype kidney tissue demonstrates low levels of β -catenin in mesenchymal and ureteric cells (dotted line represents ureteric bud epithelium) and lack of nuclear β -catenin in the mesenchyme (black arrows). (B) β -cat^{GOF-MM} mutants display high levels of β -catenin in mesenchymal cells (dotted line represents ureteric bud epithelium). In addition β -cat^{GOF-MM} mutants demonstrate increased nuclear levels of β -catenin in the mesenchyme (black arrows) as compared to wildtype. (C,D) Analysis of activated β -catenin using Immunohistochemistry in P0 kidneys (scale bar = $10\mu\text{m}$). As compared to Wildtype (C), β -cat^{GOF-MM} kidneys demonstrate increased nuclear and cytoplasmic accumulation of β -catenin within mesenchymal (black arrows), epithelial and cortical stromal cells (black star).

4.3: β -cat^{GOF-MM} mutants demonstrate renal dysplasia

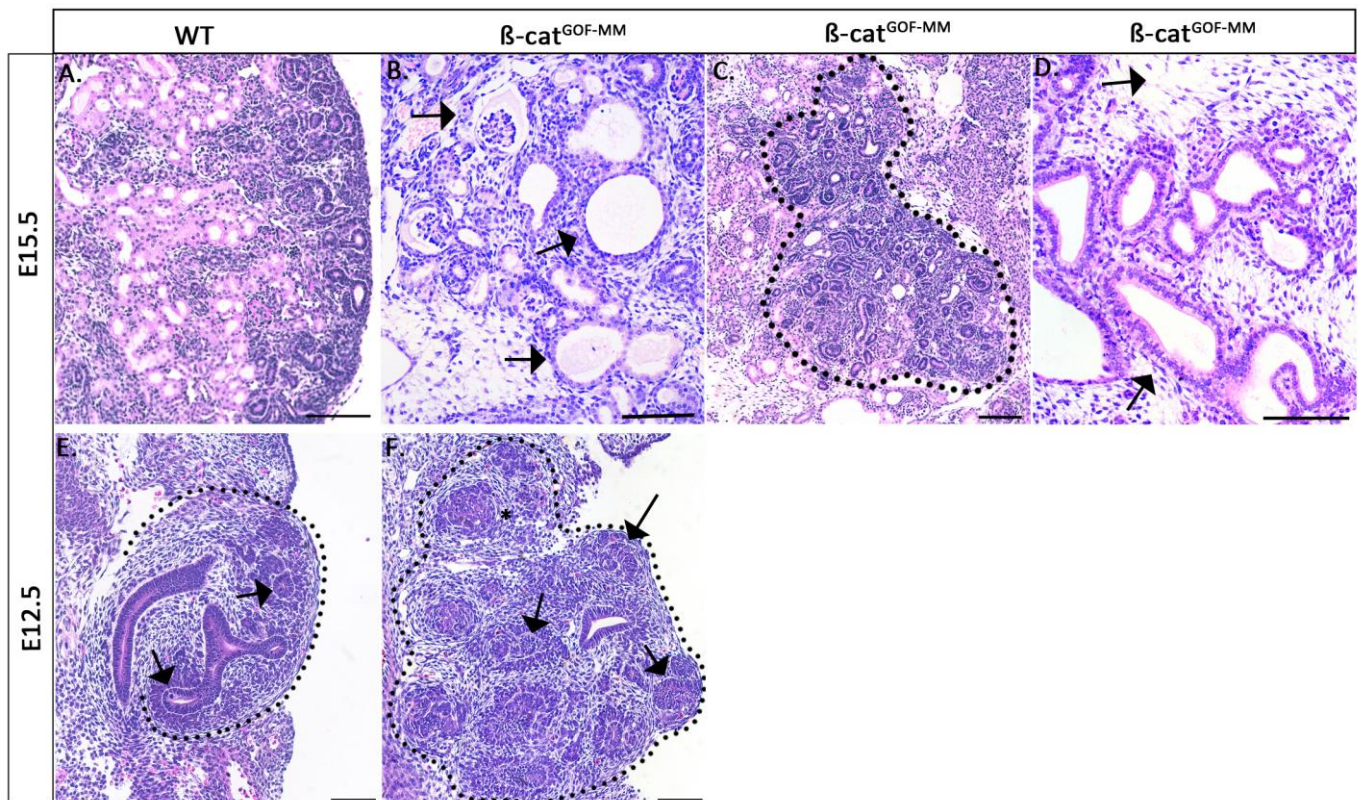
β -cat^{GOF-MM} mutants developed to term but died shortly after birth. Gross anatomical analysis of newborn pups (P0) revealed that β -cat^{GOF-MM} mutant kidneys were lobular and misshapen when compared to wildtype (Fig. 4A,B). Further analysis of β -cat^{GOF-MM} kidneys by histology confirmed the lobular phenotype and also revealed disorganized collecting ducts and irregular patterning of nephrogenic structures (Fig. 4D). Interestingly we also observed multiple kidney-like structures located around the periphery of the kidney (Fig. 4D). The kidney irregularities observed in newborn β -cat^{GOF-MM} mutants are in stark difference to the normalcy of wildtype kidney tissue (Fig 4A,C), which suggests that β -cat^{GOF-MM} mutants experience severe renal developmental defects. Consequently histological analysis was performed at E15.5. In contrast to wildtype (Fig. 5A), β -cat^{GOF-MM} mutant kidneys demonstrated the formation of multiple large cystic tubules and cystic glomeruli (Fig. 5B), disorganized nephrogenic zone, focal regions of undifferentiated mesenchyme (Fig. 5C), and undifferentiated dilated epithelial tubules surrounded by loosely arranged stroma (Fig 5D). These histopathological characteristics are remarkably similar to human renal dysplasia [49, 51, 52]. In order to address how early developmental defects arise in β -cat^{GOF-MM} mutants, histological analysis was performed at earlier embryological time-points. At E12.5, β -cat^{GOF-MM} mutants demonstrate several renal abnormalities. First, β -cat^{GOF-MM} kidneys are severely misshapen and lobular as compared to wildtype (Fig. 5F). Second, β -cat^{GOF-MM} kidneys display sporadic regions of undifferentiated pockets of mesenchyme (Fig. 5F). Third, β -cat^{GOF-MM} kidneys demonstrate abnormally spaced ureteric duct tips (Fig. 5F). During branching morphogenesis the ureteric epithelium branches and forms tips at the cortex of the developing kidney [4]. In wildtype, the tips of the ureteric duct are located at the cortex of the developing kidney and capped by metanephric mesenchyme (Fig.

5E). While the ureteric tips are capped by metanephric mesenchyme in β -cat^{GOF-MM} mutants, the tips are also located sporadically throughout the kidney, outside the nephrogenic zone. Some tips reside deep inside the developing kidney, while several extend further outward than others (Fig 5F). These findings suggest that kidney development is altered very early in β -cat^{GOF-MM} mutants. Taken together, β -cat^{GOF-MM} mutants clearly demonstrate phenotypic characteristics consistent with human renal dysplasia. Therefore we have generated a novel mouse model of renal dysplasia to utilize in understanding the mechanisms that lead to the disorder.

Figure 4: Kidneys from new born β -cat^{GOF-MM} mutants are severely abnormal



Kidneys from new born β -cat^{GOF-MM} mutants are severely abnormal: (A,B) Gross anatomy of wild type and β -cat^{GOF-MM} mutant kidneys at P=0 (scale bar = 2mm). In Contrast to wildtype (A) β -cat^{GOF-MM} mutants demonstrate misshapen lobular kidneys (B). (C,D) Histological analysis of P0 kidneys reveals abnormal kidney architecture: irregular patterning of nephrogenic structures, cystic tubules, and disorganized and dilated collecting ducts. In addition β -cat^{GOF-MM} mutants demonstrate ectopic formation of kidney-like tissue. (black arrows, scale bar = 500 μ m).

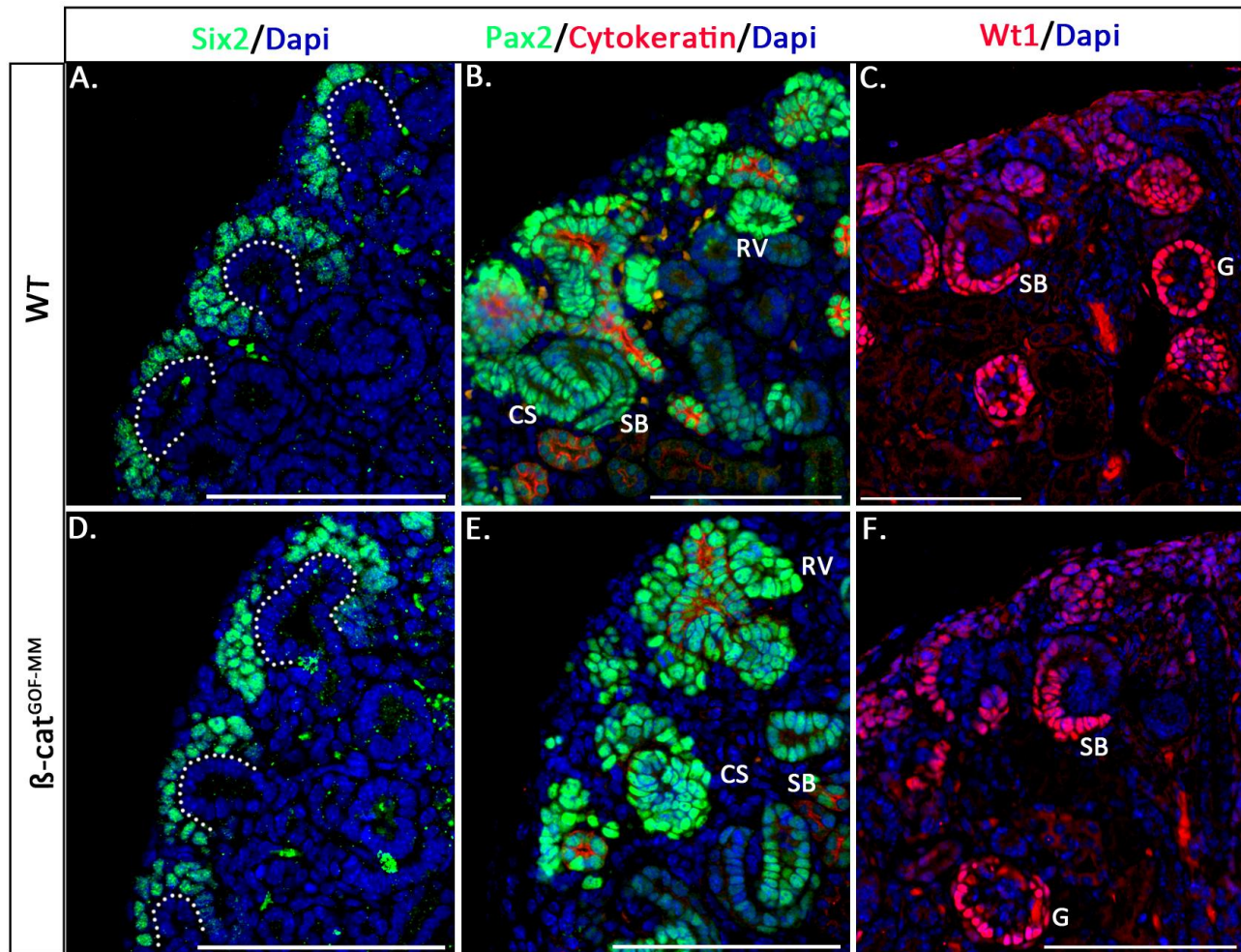
Figure 5: β -cat^{GOF-MM} mutants demonstrate Renal Dysplasia **β -cat^{GOF-MM} mutants demonstrate Renal dysplasia**

(A-D) Histological analysis of E15.5 mouse kidney tissue, stained with hematoxylin and eosin (scale bar = 100 μ m). In contrast to wildtype (A), which displays normal morphology, β -cat^{GOF-MM} kidney demonstrates numerous characteristics consistent with human renal dysplasia including: (B) multiple large cysts (black arrow: bottom) and cystic glomeruli (black arrow: top); (C) disorganized nephrogenic zone (dotted black line) with undifferentiated mesenchyme and tubules; (D) undifferentiated dilated epithelial tubules (black arrow: bottom) surrounded by loosely packed stroma (black arrow: top). (E,F) Histological analysis of E12.5 mouse kidney tissue, stained with hematoxylin and eosin (scale bar = 100 μ m). In contrast to wildtype (E), β -cat^{GOF-MM} kidneys are misshapen and lobular. In addition β -cat^{GOF-MM} kidneys demonstrate regions of undifferentiated mesenchyme (black star) and disorganized ureteric duct tip locations (black arrows).

4.4: Nephrogenesis is maintained in β -cat^{GOF-MM} mutants

Renal dysplasia arises from a failure of nephrogenesis and branching morphogenesis, two processes that guide kidney development. Previous work conducted by Park et al demonstrated that the stabilization of β -catenin within the Six2 positive nephrogenic progenitor population lead to renal agenesis caused by a failure in nephrogenesis [32]. This is in stark difference to the phenotype we observed in newborn β -cat^{GOF-MM} mutants (P0). P0 β -cat^{GOF-MM} kidneys while severely misshapen and dysplastic still display mature nephrogenic structures (Fig. 5B). To determine whether nephrogenesis progressed normally in β -cat^{GOF-MM} mutant kidneys, we analyzed the expression of proteins necessary for the development of nephrogenic structures at E15.5 (Fig. 6A-F). We chose E15.5 since both developing and mature nephrons are present at this stage. We first used an antibody against Six2, a marker of the mesenchymal progenitor population [68]. As compared to wildtype (Fig. 6A), β -cat^{GOF-MM} mutant kidneys demonstrated a similar expression pattern of six2 positive cells surrounding each ureteric tip (Fig. 6D). This suggested no alteration in the mesenchyme progenitor population. We next analyzed Pax2, a marker for the induced mesenchyme that identifies cells in aggregating pre-tubular cells, renal vesicles, comma and s-shaped bodies and ureteric bud epithelium. A Cytokeratin antibody was used to distinguish ureteric bud cells from the induced mesenchymal cells. We observed normal nephrogenesis within the nephrogenic zone of the cortical region in wildtype kidneys as several renal vesicles and s-shaped bodies could be observed under the ureteric tips of the collecting duct (Fig. 6B). Similarly in β -cat^{GOF-MM} mutant kidneys, renal vesicles were observed under the tips of the ureteric collecting duct in addition to comma and s-shaped bodies (Fig. 6E). Finally, we used an antibody against WT-1, a marker for developing and mature podocytes. WT-1 expression was localized to the cleft of the proximal end of developing S-shaped bodies and in a

circular pattern in mature glomeruli in wildtype renal tissue (Fig 6C). Likewise WT-1 expression followed the same normal pattern in β -cat^{GOF-MM} kidneys (Fig. 6F). This analysis indicates that nephrogenesis is unaltered when β -catenin is stabilized in the metanephric mesenchyme during renal development.

Figure 6: Nephrogenesis progresses normally in β -cat^{GOF-MM} mutant kidneys**Nephrogenesis progresses normally in β -cat^{GOF-MM} mutant kidneys**

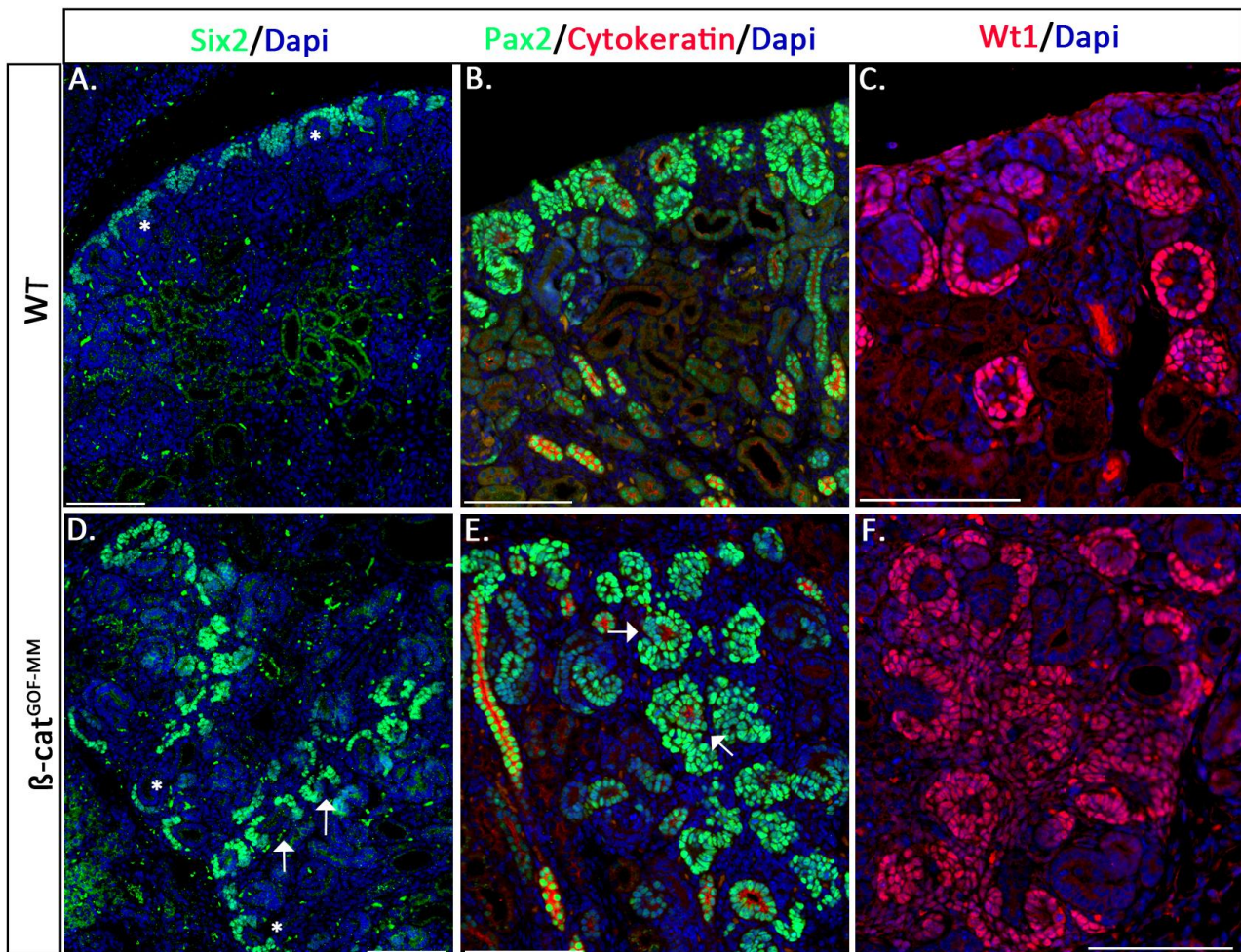
(A-F) Analysis of nephrogenesis in the cortical region of wildtype and β -cat^{GOF-MM} kidney tissue at E15.5 using immunofluorescence microscopy (scale bar = 100 μ m, dapi marks nuclei blue). (A,D) Analysis of the six2 cell population in wildtype (A) and in β -cat^{GOF-MM} kidney (D) tissue using anti-six2 (green) antibody demonstrates similar expression patterns. (B,E) Analysis of the cortical region of wildtype (B) and β -cat^{GOF-MM} tissue (E) using anti-pax2 (green) antibody, anti-cytokeratin (red) antibody demonstrates the condensing mesenchyme, the formation of renal vesicle (RV), comma shaped bodies (CS) and s-shaped bodies (SB). (C-F) Analysis of developing glomeruli in wildtype (C) and β -cat^{GOF-MM} kidneys (F) using anti-wt1 (red) antibody. Both wildtype (C) and β -cat^{GOF-MM} (F) kidneys express wt1 in similar patterns in developing glomeruli (SB) and mature glomeruli (G).

4.5: β -cat^{GOF-MM} mutants display sporadic zones of disorganized nephrogenic structures and ectopic kidney formation

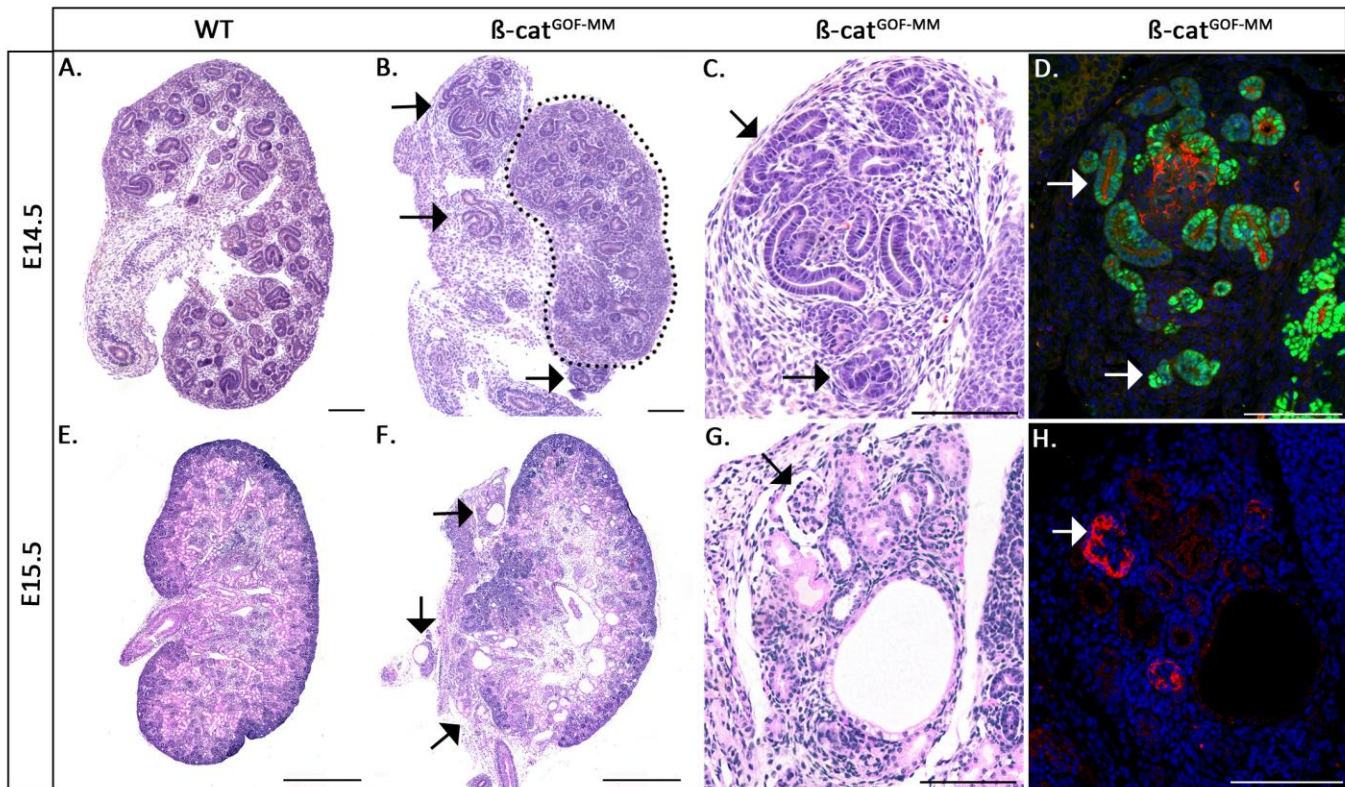
During normal renal development the tips of the branching ureteric epithelium localize to the cortex of the kidney [4, 69]. Each tip is surrounded by a cap of six2 positive metanephric mesenchyme, termed the ‘cap mesenchyme’[68]. A subset of cells within the cap mesenchyme will form the nephrons of the kidney[39]. Together, the cap mesenchyme and tips of the ureteric duct make up part of the nephrogenic zone, which is located around the periphery of the cortex[4]. This normal patterning is seen within wildtype kidneys, as nephron progenitors and ureteric tips are localized to the outer cortex of the kidney (Fig. 7A) and the induced mesenchyme and developing glomeruli localize to the nephrogenic zone (Fig 7B,C), while the stalk of the ureteric epithelium extends into the medulla (Fig. 7B). Our results demonstrate that the formation of nephrons remained intact in β -cat^{GOF-MM} mutants (Fig. 6A-F). However, the organization of the mesenchymal progenitor population (Fig. 7D), induced mesenchyme (Fig. 7E), and developing glomeruli (Fig. 7F) demonstrated focal zones that were expanded into the medulla of β -cat^{GOF-MM} mutant kidneys. In addition, β -cat^{GOF-MM} mutant kidneys also demonstrated ureteric duct tips and surrounding cap mesenchyme in the medulla (Fig. 7E). This irregular patterning of the mesenchyme and ureteric epithelium has been previously attributed to abnormal branching morphogenesis [8]. Interestingly, we also observed ectopic formation of renal tissue around the kidney periphery in β -cat^{GOF-MM} mutants at early stages of development (Fig. 8B,F). Close examination of these regions revealed the formation of what appeared to be tubules (Fig. 8C) and glomeruli (Fig. 8G). In order to confirm that they were in fact kidneys, we performed immunofluorescence using antibodies that detect Pax2 and Cytokeratin (Fig. 8D), which marks mesenchymal and ureteric derived tubules, and Nephtrin (Fig. 8H), which marks the

slit diaphragm of a mature glomerulus. This approach confirmed that developing and mature nephrogenic structures form around the periphery in kidneys from β -cat^{GOF-MM} mutants.

Figure 7: β -cat^{GOF-MM} mutants display sporadic zones of disorganized nephrogenic structures



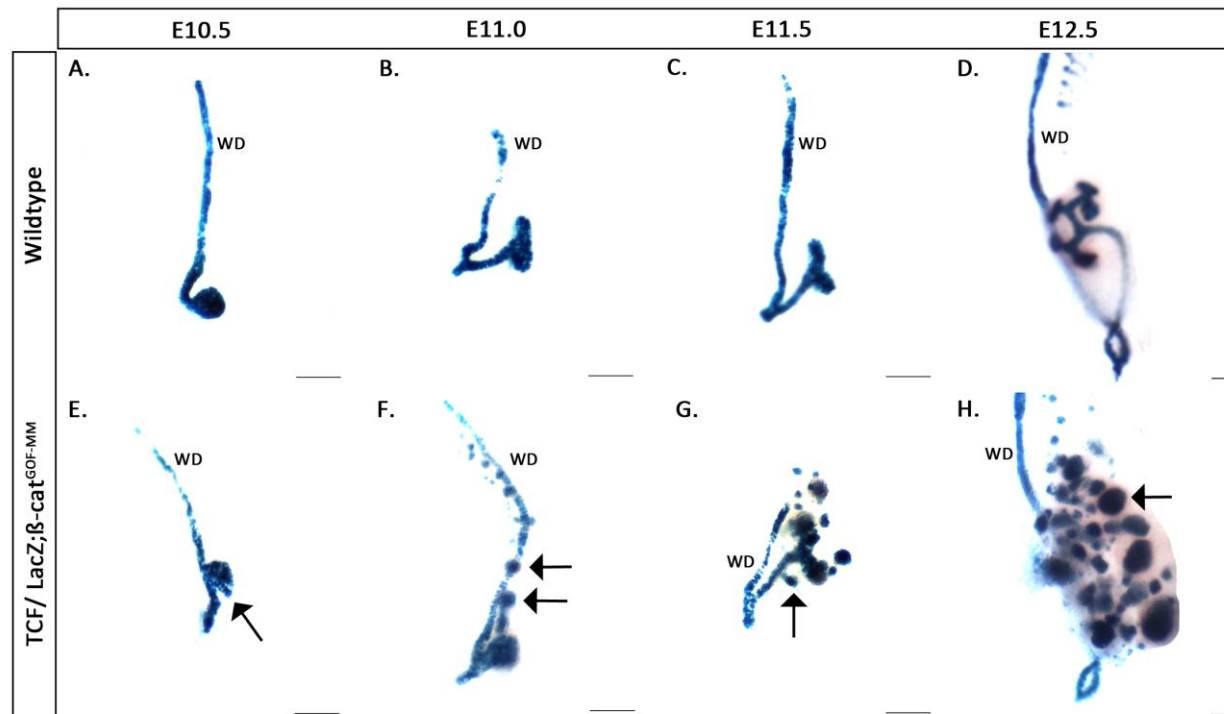
β -cat^{GOF-MM} mutants display sporadic zones of disorganized nephrogenic structures: (A-F) Analysis of nephrogenic structures in wildtype and β -cat^{GOF-MM} kidney tissue at E15.5 using Immunofluorescence microscopy (scale bar = 100 μ m, dapi marks nuclei of cells). (A,D) Analysis of cortical region of β -cat^{GOF-MM} and wildtype tissue using anti-six2 (green) antibody. (white star indicates normal positioning of ureteric tip and surrounding cap mesenchyme). (A) Wildtype tissue demonstrates normal patterning of six2 nephrogenic progenitors around the periphery of the cortex. (D) β -cat^{GOF-MM} mutants demonstrates a disorganization of the self-renewing progenitor population and their expansion into the medulla (white arrows). (B,E) Analysis of induced mesenchyme in wild type and β -cat^{GOF-MM} kidney tissue using anti-pax2 (green) antibody and anti-cytokeratin (red) antibody. (B) Wildtype demonstrates normal pattern of ureteric tips and developing nephrogenic structures in the nephrogenic zone of the kidney. (E) β -cat^{GOF-MM} demonstrates the medullary expansion of nephrogenic structures and ureteric duct tips (white arrow). (C,F) Analysis of developing and mature podocytes using anti-wt1 (red) antibody displays disorganized expression pattern and medullary expansion in β -cat^{GOF-MM} mutant (F) as compared to wildtype (C).

Figure 8: β -cat^{GOF-MM} mutants display ectopic kidney formation

β -cat^{GOF-MM} mutants display ectopic kidney formation: (A-H) E14.5-E15.5 β -cat^{GOF-MM} kidneys demonstrate ectopic renal tissue residing around the periphery of the major developing kidney. (A,B) Histological analysis of E14.5 kidneys stained with hematoxylin and eosin reveals ectopic kidney-like formation in β -cat^{GOF-MM} mutants (black arrows, scale = 100 μ m). (C) High power image of ectopic candidate renal tissue in β -cat^{GOF-MM} reveals the formation of tubulogenic structures (black arrow: top) and what appears to be a comma/s-shaped body (black arrow: bottom)(scale bar = 100 μ m). (D) Immunofluorescence analysis of ectopic renal tissue in β -cat^{GOF-MM} mutants with anti-cytokeratin (red) and anti-pax2 (green) antibody confirms the presence of ureteric (white arrow: top) and mesenchymally derived structures (white arrow: bottom) (scale bar = 100 μ m). (E,F) Histological analysis of E15.5 kidneys stained with hematoxylin and eosin reveals ectopic kidney-like formation in β -cat^{GOF-MM} mutants (black arrows, scale = 500 μ m). (G) High power image of ectopic candidate renal tissue in β -cat^{GOF-MM} reveals the formation of mature nephrogenic structures including glomeruli (black arrow) and other tubulogenic structures (scale bar = 100 μ m). (H) Immunofluorescence analysis of ectopic renal tissue in β -cat^{GOF-MM} mutants with anti-nephrin (red) antibody confirms the presence of glomeruli (scale bar = 100 μ m).

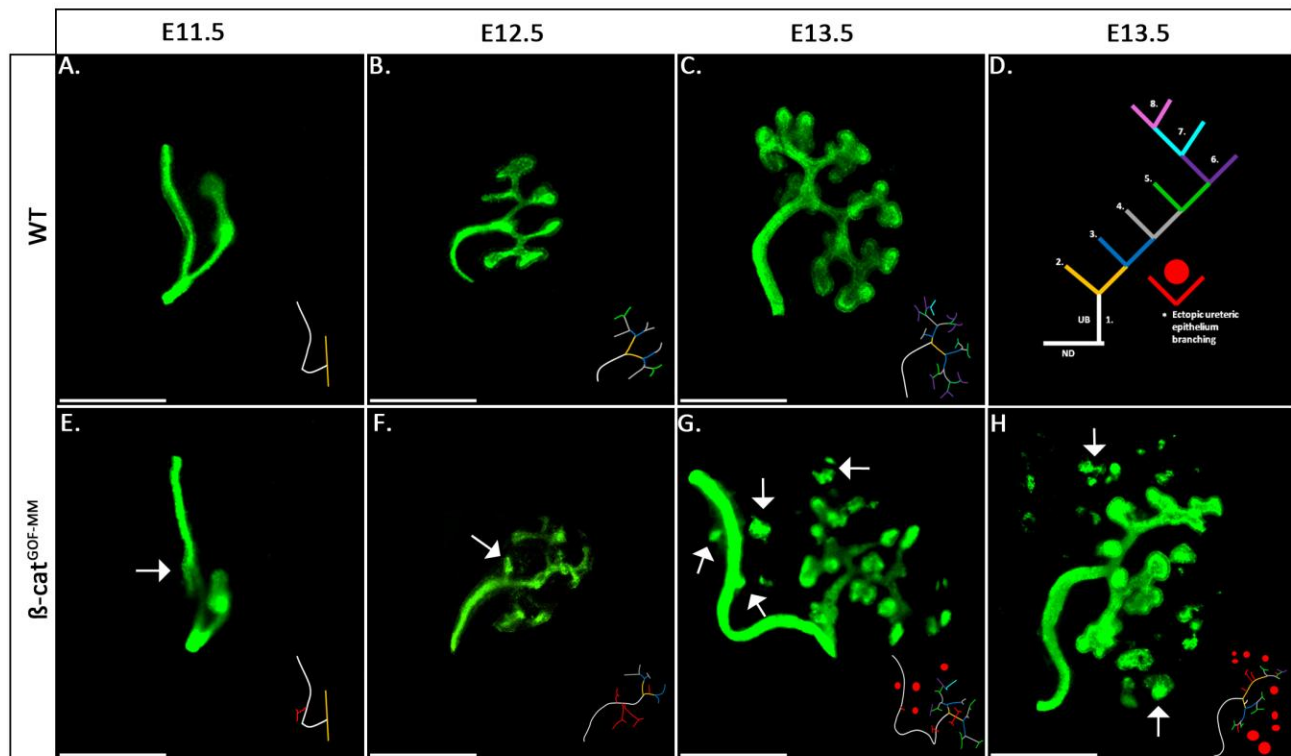
4.6: Abnormal branching morphogenesis in β -cat^{GOF-MM} mutants

Previous work has shown that renal dysplasia can be caused by alterations in branching morphogenesis [38]. Since expression of cytokeratin was observed in ectopic kidneys in β -cat^{GOF-MM} mutants (Fig. 8D), along with a disorganization of nephrogenic structures within the renal parenchyma (Fig. 7D-F), we sought to determine whether abnormal/disorganized branching morphogenesis contributed to the phenotype observed in β -cat^{GOF-MM} mutants. To initiate our analysis of branching morphogenesis, we utilized a TCF/LEF reporter mouse model. The TCF/LEF reporter mouse demonstrates high levels of β -galactosidase in the ureteric epithelium. Therefore by using an X-gal stain, the TCF/LEF reporter mouse is an excellent model for visualizing branching morphogenesis [38]. To analyze branching morphogenesis using an X-gal stain we generated β -cat^{GOF-MM} mutants that contained TCF sites linked to a LacZ reporter gene termed, TCF/LacZ; β -cat^{GOF-MM} (see materials and methods for the mating scheme). This technique provided us with valuable insights into the branching phenotype at very early stages of development. As expected, wildtype mice showed a single normal ureteric bud outgrowth from the caudal end of the nephric duct characterized by a thin stalk and swollen ampulla at E10.5 (Fig. 9A) and the subsequent formation of a T-branch at E11.5 (Fig. 9B,C). In contrast, TCF/LacZ; β -cat^{GOF-MM} mutants demonstrated an expanded initial ureteric bud. We also observed formation of ectopic buds in 3/3 β -cat^{GOF-MM} mutants at variable sites, off the Wolffian duct (Fig. 9E,F) and ureter (Fig. 9G) between E10.5-E11.5. No ectopic buds were ever observed in wildtype mice (0/5). At E12.5, branching morphogenesis progressed normally in the wildtype (Fig. 9D), however we could not establish a branching phenotype in TCF/LacZ; β -cat^{GOF-MM} mutants as the urogenital ridges were cluttered with aggregates of increased β -catenin activity (Fig. 9H).

Figure 9: Abnormal branching morphogenesis in TCF/LacZ; β -cat^{GOF-MM} mutants

Abnormal Branching Morphogenesis in TCF/LacZ; β -cat^{GOF-MM} mutants: (A-D) Wildtype demonstrates normal branching morphogenesis (scale bar = 125 μ m, WD represents Wolffian duct). (A) At E10.5 wildtype demonstrates a single normal ureteric bud outgrowth. (B,C) At E11.0-E11.5 the ureteric bud undergoes branching morphogenesis to form a normal T-branch in wildtype. (D) Wildtype demonstrates normal bifid branching morphogenesis at E12.5. (E-H) Analysis of ureteric bud outgrowth in TCF/LacZ; β -cat^{GOF-MM} mutants (scale bar = 125 μ m). (E) TCF/LacZ; β -cat^{GOF-MM} mutant at E10.5 reveals a thick initial ureteric bud with an ectopic bud coming off the initial ureteric stalk (black arrow). (F) Ectopic ureteric buds stemming off the Wolffian duct at E11.0 (black arrows) in TCF/LacZ; β -cat^{GOF-MM} mutant kidney. (G) Ectopic ureteric bud off the initial stalk in TCF/LacZ; β -cat^{GOF-MM} mutant at E11.5 (black arrow). (H) Cluster of β -catenin active aggregates in TCF/LacZ; β -cat^{GOF-MM} mutant kidney at E12.5 (black arrow).

We therefore performed whole-mount immunofluorescence using an anti-cytokeratin antibody to mark the ureteric bud at early time points during development (Fig. 10A-H). At E11.5, In contrast to wildtype, β -cat^{GOF-MM} mutants demonstrated ectopic budding off the Wolffian duct in 1/3 kidneys analyzed (Fig. 10A,E). Analysis of ureteric branch pattern at E12.5 revealed ectopic budding off the initial ureteric stalk (1/3) and disorganized ureteric branching (3/3) in β -cat^{GOF-MM} kidneys (Fig. 10F). To establish whether branching morphogenesis would undergo progressive disorganization over-time, we analyzed branching morphogenesis at E13.5, and as expected, found disorganized branch pattern in the β -cat^{GOF-MM} kidneys (4/4) (Fig. 10G,H). Additionally, these kidneys also demonstrated ectopic buds off the nephric duct (1/4) (Fig. 10G) and surprisingly, the formation of ectopic cytokeratin positive structures around the periphery of the developing collecting duct system (4/4) (Fig. 10G,H). No ectopic ureteric budding or cytokeratin positive structures residing outside the normal developing kidney were observed in wildtype mice (Fig. 10A-C). Beyond E13.5 we were unable to establish a branching pattern in β -cat^{GOF-MM} mutants using this method due to high background signal caused by ectopic renal tissue in the urogenital ridge. Together, these analyses demonstrate that over-expression of β -catenin in the metanephric mesenchyme leads to ectopic ureteric budding and disorganized branching morphogenesis during the early stages of renal development.

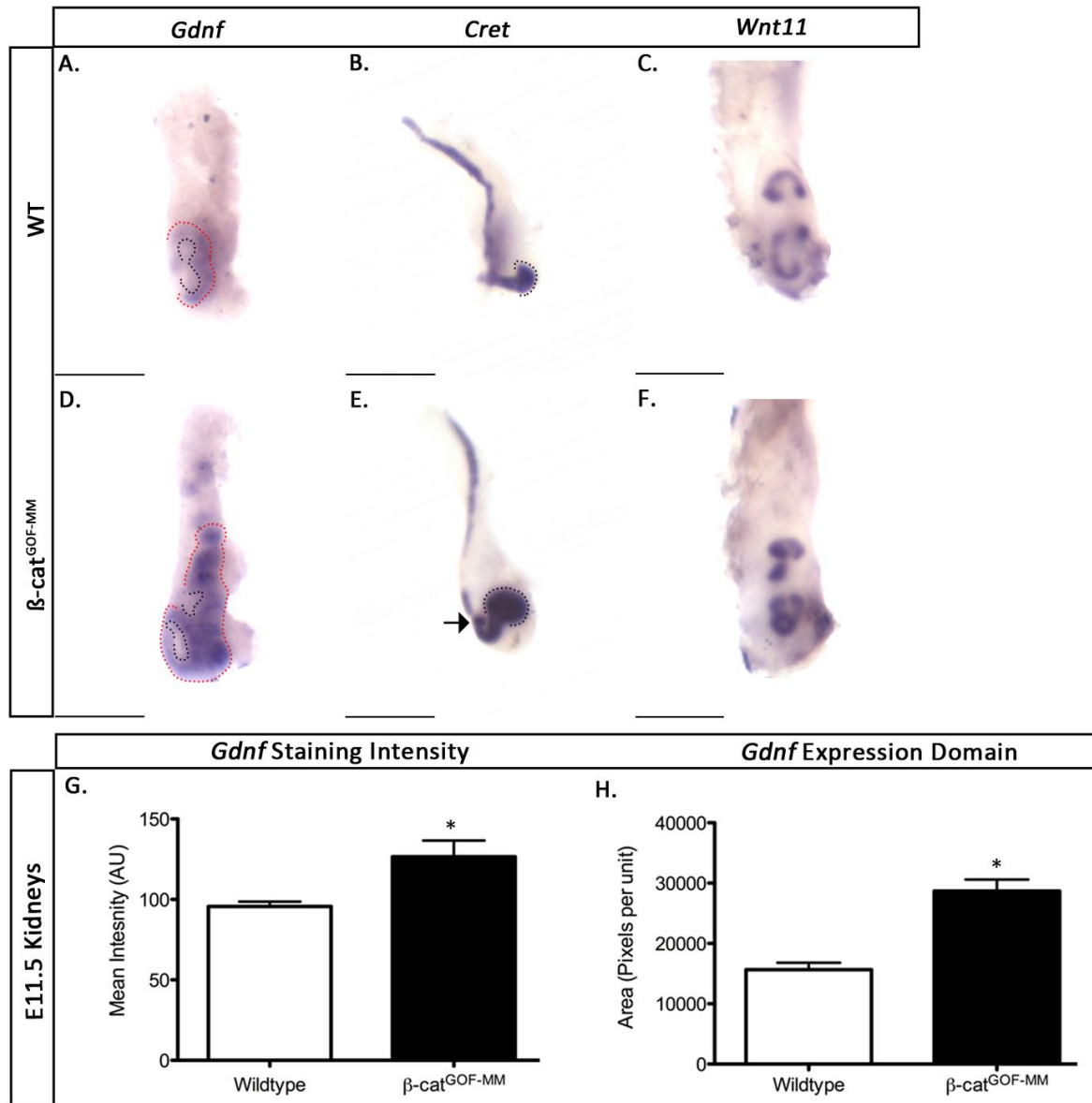
Figure 10: Abnormal branching morphogenesis in β -cat^{GOF-MM}

Abnormal Branching Morphogenesis in β -cat^{GOF-MM} mutants: (A-H) Whole mount immunofluorescence using anti-cytokeratin antibody to mark the ureteric bud (white arrow indicates ectopic ureteric budding, scale bar = 250 μ m). (D) Line diagram using a colour code to represent branch generation. The primary bud from the Wolffian duct is considered the “first generation” (white); the first two branches that form from the primary bud are the second generation (yellow) etc. Red line represents ectopic branching morphogenesis.. (A,E) As compared to Wild type, β -cat^{GOF-MM} mutant displays ectopic branching off the Wolffian duct and a normal T-branch at E11.5. (B,F) As compared to Wild type, β -cat^{GOF-MM} mutant displays ectopic branching off the initial ureteric stalk and disorganized branching morphogenesis at E12.5. (C,G,H) Analysis of branching morphogenesis at E13.5 reveals an ectopic ureteric bud growth, disorganized branching pattern and ectopic cytokeratin positive structures outside developing collecting duct system in β -cat^{GOF-MM} mutants.

4.7: Increased *Gdnf* Expression in β -cat^{GOF-MM} mutants

Next, we investigated how β -catenin over-expression in the metanephric mesenchyme was altering branching morphogenesis. Previous studies have demonstrated that ectopic expression of *Gdnf* induces the formation of ectopic ureteric buds and disorganized ureteric bud branching [8, 14, 17], a phenotype very similar to that seen in β -cat^{GOF-MM} mutants. We first analyzed *Gdnf* expression at E11.5 by whole mount in-situ hybridization. The intensity of *Gdnf* expression was markedly increased in the metanephric mesenchyme of β -cat^{GOF-MM} mutant kidney tissue compared to that of wildtype (expression intensity: wildtype mean=95.68 versus β -cat^{GOF-MM} mean=126.5, $p < 0.0267$) (Fig. 11A,C,G). The spatial domain of *Gdnf* expression was also dramatically increased in β -cat^{GOF-MM} mutant kidney (expression domain: wildtype mean=15660 versus β -cat^{GOF-MM} mean = 28700 arbitrary units, $p < 0.0041$) (Fig. 11A,C,H). These findings demonstrate that *Gdnf* is expressed at higher levels and in ectopic locations within β -cat^{GOF-MM} kidneys. Next, we investigated the expression of *c-Ret*. *c-Ret*, the receptor for *Gdnf*, is expressed in the Wolffian duct, the ureteric bud, and tips of the branching ureteric epithelium [70]. Previous studies have demonstrated that over-expression of *Gdnf* leads to the ectopic activation of the *Ret/Gdnf* pathway, which induces ectopic ureteric bud formation, and consequently *c-Ret* expression [14, 17]. In comparison to wildtype (Fig. 11B), *c-Ret* expression was expanded and more intense in the ureteric tip in β -cat^{GOF-MM} mutants (Fig. 11E). Of note, *c-Ret* was also expressed in an ectopic bud off the Wolffian duct in β -cat^{GOF-MM} mutants (Fig. 11E) consistent with earlier data demonstrating ectopic ureteric buds (Fig. 9,10). Next we analyzed the expression of *Wnt11* due to its involvement in a positive feedback loop with *Gdnf* and *c-Ret* [25]. Analysis of *Wnt11* demonstrated an increase in expression intensity and domain in β -cat^{GOF-MM} mutant kidneys (Fig. 11C) when compared to wildtype (Fig. 11F). Taken together, β -cat^{GOF-}

^{MM} mutants exhibit alterations in *c-Ret*, *Wnt11* and most notably *Gdnf* expression at very early stages during kidney development.

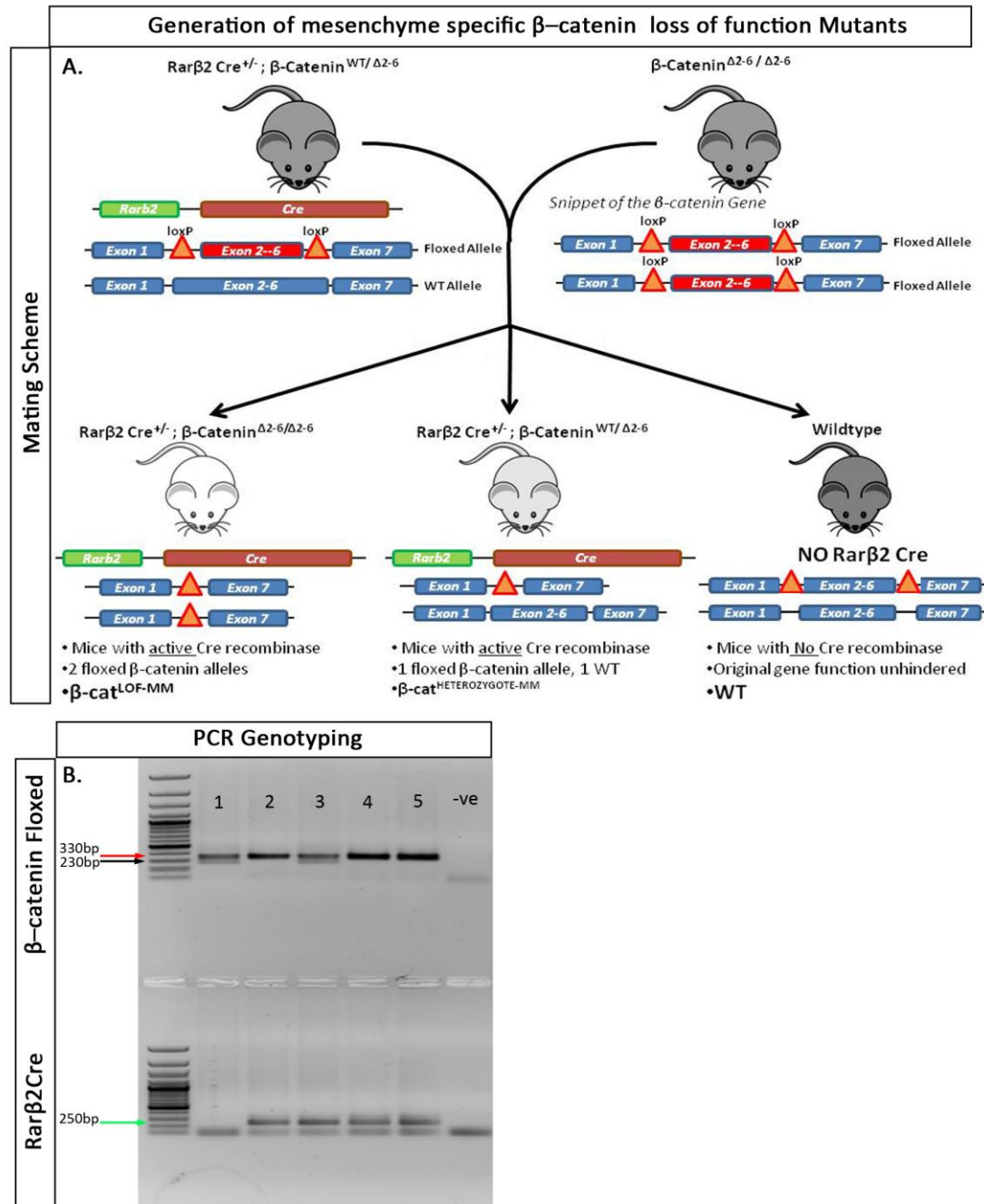
Figure 11: Increased *Gdnf* Expression in β -cat^{GOF-MM} mutants

Increased *Gdnf* Expression in β -cat^{GOF-MM} mutants: (A-F) Wholemount in-situ hybridization for *Gdnf*, *Ret* and *Wnt11* in E11.5 wildtype and β -cat^{GOF-MM} kidneys (scale bar = 250 μ m, black dotted line = ureteric bud). (A,D) In contrast to wild type littermate, *Gdnf* expression levels were higher based on staining intensity and encompassed a larger domain (red dotted line) in β -cat^{GOF-MM} kidney (B,E) In contrast to the wild type, *Ret* expression is expanded in the ureteric bud tip and stalk of β -cat^{GOF-MM} kidney, and is observed in an ectopic pattern (black arrow). (C,F) *Wnt11* is expressed in the tips of the ureteric epithelium at higher levels based on staining intensity in β -cat^{GOF-MM} kidneys. (G,H) Quantification of *Gdnf* staining intensity (Wt mean=95.68 versus β -cat^{GOF-MM} mean=126.5, $p < 0.0267$). and *Gdnf* expression domain (wt mean=15660 versus β -cat^{GOF-MM} mean = 28700 arbitrary units, $p < 0.0041$) demonstrates significantly increased *Gdnf* expression in β -cat^{GOF-MM} mutants.

4.8: Generation of mesenchyme specific β -catenin Loss-of-function mutants

Both *c-Ret* and *Wnt11* are expressed in the ureteric epithelium [9, 25], therefore their alteration is likely secondary to changes in *Gdnf* expression. Thus we hypothesized β -catenin may have a role in the regulation of *Gdnf* expression during kidney development. To examine this possibility we generated a mouse model in which β -catenin was specifically deleted from the metanephric mesenchyme. These mutants, termed β -catenin loss of function-metanephric mesenchyme(β -cat^{LOF-MM}) were generated by crossing homozygous mice that had exon 2-6 of the β -catenin gene flanked (“floxed”) by LoxP sites with Rar β 2Cre mice that were heterozygous for the loss of function β -catenin allele (the genetic cross is outlined in Fig. 12A). The offspring will have Cre mediated genetic deletion of exon 2-6, thus generating a non-functional β -catenin protein [40] exclusively in the metanephric mesenchyme [39].

To identify β -cat^{LOF-MM} mutant and wildtype embryos, we performed PCR using primers that detected the Rar β 2Cre gene and the β -catenin floxed allele (Fig. 12B). The PCR amplification of the Rar β 2Cre transgene generated a 250bp amplicon. Depending upon the genotype of the embryo, the PCR amplification using primers specific to the β -catenin floxed allele would generate a 330bp amplicon and/or 230bp amplicon. The 330bp amplicon corresponded to the β -catenin floxed allele, while the 230bp amplicon indicated a wildtype allele. In this regard, this cross would generate three different genotypes: 1) mice containing the Rar β 2Cre and two β -catenin floxed alleles (β -cat^{LOF-MM}); 2) mice containing Rar β 2Cre with one β -catenin floxed allele and one wildtype allele (β -cat^{HETEROZYGOTE-MM}); and 3) mice containing no Rar β 2Cre (wildtype), which were used as wildtype littermates.

Figure 12: Generation of mesenchyme specific loss of function β -catenin mutants

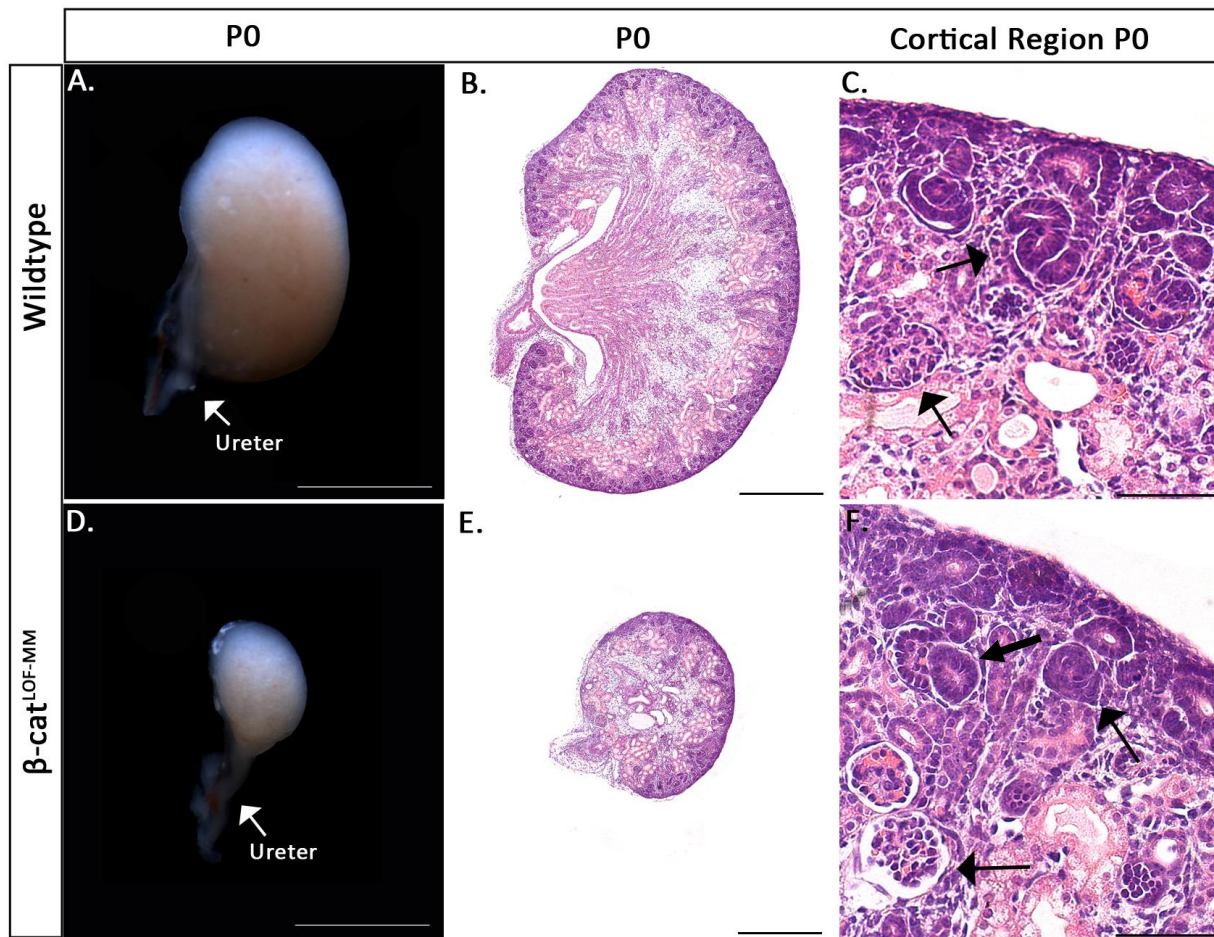
Generation of mesenchyme specific β -catenin loss of function mutants: (A) Mating scheme to generate β -catenin loss of function mice specific to the metanephric mesenchyme. (B) Genotyping of embryos using primers specific the Cre transgene and floxed β -catenin allele. Top Panel: Primers amplify both the floxed β -catenin allele (330bp) and the wildtype β -catenin allele (230bp). Bottom Panel: Primers amplify the Cre transgene (250bp). Genotypes for following embryo/lanes: 1) Wildtype; 2) β -cat^{LOF-MM}; 3) β -cat^{Heterozygote-MM}; 4) β -cat^{LOF-MM}; 5) β -cat^{LOF-MM}. A negative control (-ve) was used to establish that there was no contamination in the PCR reaction.

4.9: β -cat^{LOF-MM} demonstrate renal hypoplasia

Gross anatomical analysis of newborn pup (P0) kidneys revealed that β -cat^{LOF-MM} mutant kidneys were markedly smaller, approximately a quarter of the size of wildtype and was confirmed by histology (Fig. 13A,C,B,D). Further histological analysis of β -cat^{LOF-MM} mutants revealed normal kidney anatomy and patterning of the cortex with an active nephrogenic zone, and medulla (Fig. 13D). Closer inspection of the cortical region/nephrogenic zone in β -cat^{LOF-MM} mutants revealed the formation of normal mature glomeruli and developing comma and S-shaped bodies, similar to that of wildtype (Fig. 13C,F). However, as compared to wildtype, newborn (P0) β -cat^{LOF-MM} mutants demonstrated a marked reduction in the number of nephrogenic structures and collecting ducts (Fig. 13B,D). In order to gain further insight into the developmental defects displayed by β -cat^{LOF-MM} mutants we analyzed earlier embryological time-points. At E13.5, β -cat^{LOF-MM} kidneys were noticeably smaller than wildtype (hypoplastic) (Fig. 14A,B). Histological examination of E13.5 mutant kidneys revealed that β -cat^{LOF-MM} kidneys contained an active nephrogenic zone (Fig. 14A,B). Similar to wildtype, β -cat^{LOF-MM} mutants demonstrated the formation of renal vesicles, comma and s-shaped bodies and developing glomeruli, suggesting that nephrogenesis progressed normally (Fig. 14C,D). However histological analysis revealed that the number of nephrogenic structures and ureteric epithelial tips in the cortex were reduced in β -cat^{LOF-MM} mutant kidneys based on observational analysis (Fig. 14A,B). These findings were confirmed at an earlier developmental time-point using Pax2 and Cytokeratin immunofluorescence (Fig. 14E,F). As early as E12.5 β -cat^{LOF-MM} kidneys were hypoplastic. Despite the formation of normal developing nephrogenic structures (Fig. 14G,H), their numbers were reduced, as were cytokeatin positive ureteric duct tips (Fig. 14E,F). Taken together, β -cat^{LOF-MM} mutants demonstrate smaller kidneys with reduced nephrons. Since

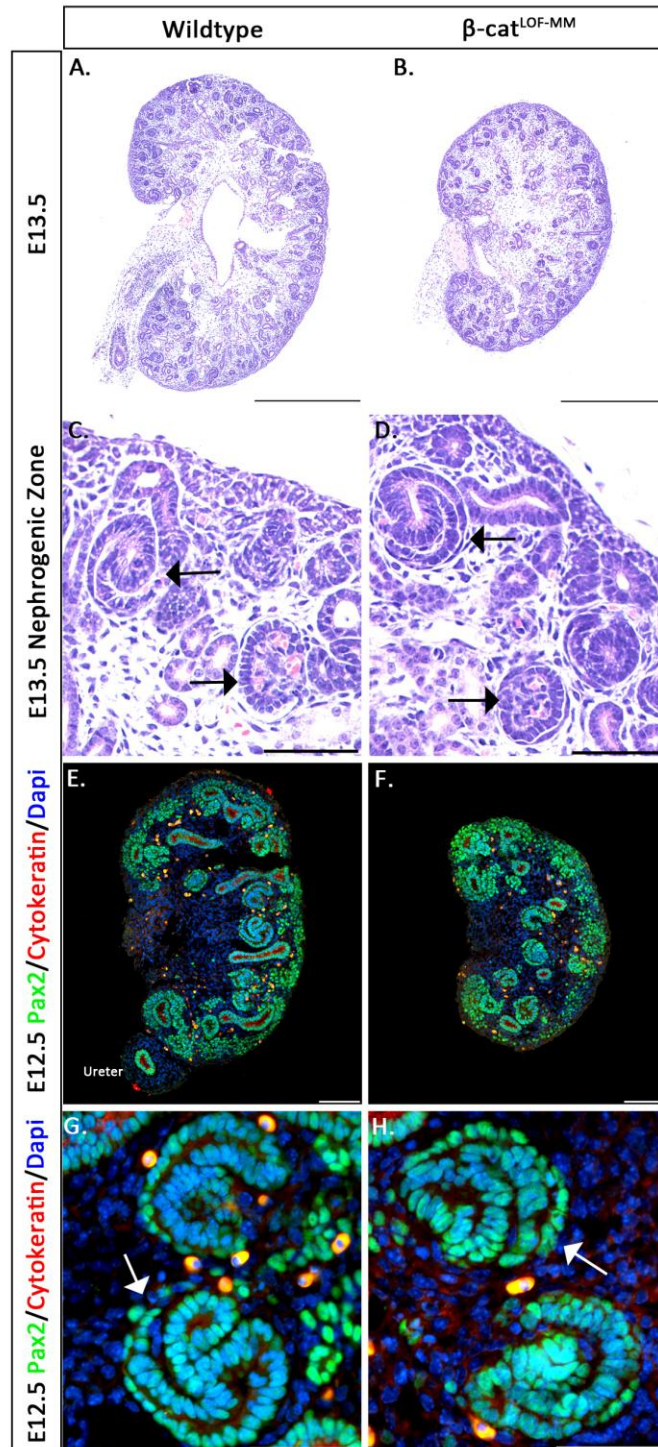
nephrogenesis progressed normally in $\beta\text{-cat}^{\text{LOF-MM}}$ mutants at multiple embryological time-points, the reduction in nephrons are likely the result of decreased branching morphogenesis [71, 72].

Figure 13: $\beta\text{-cat}^{\text{LOF-MM}}$ mutants demonstrate renal hypoplasia



$\beta\text{-cat}^{\text{LOF-MM}}$ mutants demonstrate renal hypoplasia: (A,D) Gross anatomy of newborn kidneys (P0) (scale bar = 2mm). As compared to wildtype (A), $\beta\text{-cat}^{\text{LOF-MM}}$ mutant kidneys are markedly smaller (D). (B,E) Histological analysis of newborn kidneys using hematoxylin and eosin stain (scale bar = 500µm). $\beta\text{-cat}^{\text{LOF-MM}}$ mutant kidneys are noticeably smaller than wildtype and have reduced nephrogenic structures. They maintain cortical medullary patterning and a distinct nephrogenic zone similar to wildtype (black star). (C,F) Histological analysis of newborn kidneys at higher magnification (scale bar = 100µm). Similar to wildtype (C), $\beta\text{-cat}^{\text{LOF-MM}}$ mutant demonstrate the formation of comma shaped bodies (black arrow: top), S-shaped bodies (black arrow: middle) and glomeruli (black arrow: bottom) (F).

Figure 14: β -cat^{LOF-MM} mutants demonstrate renal hypoplasia during kidney development

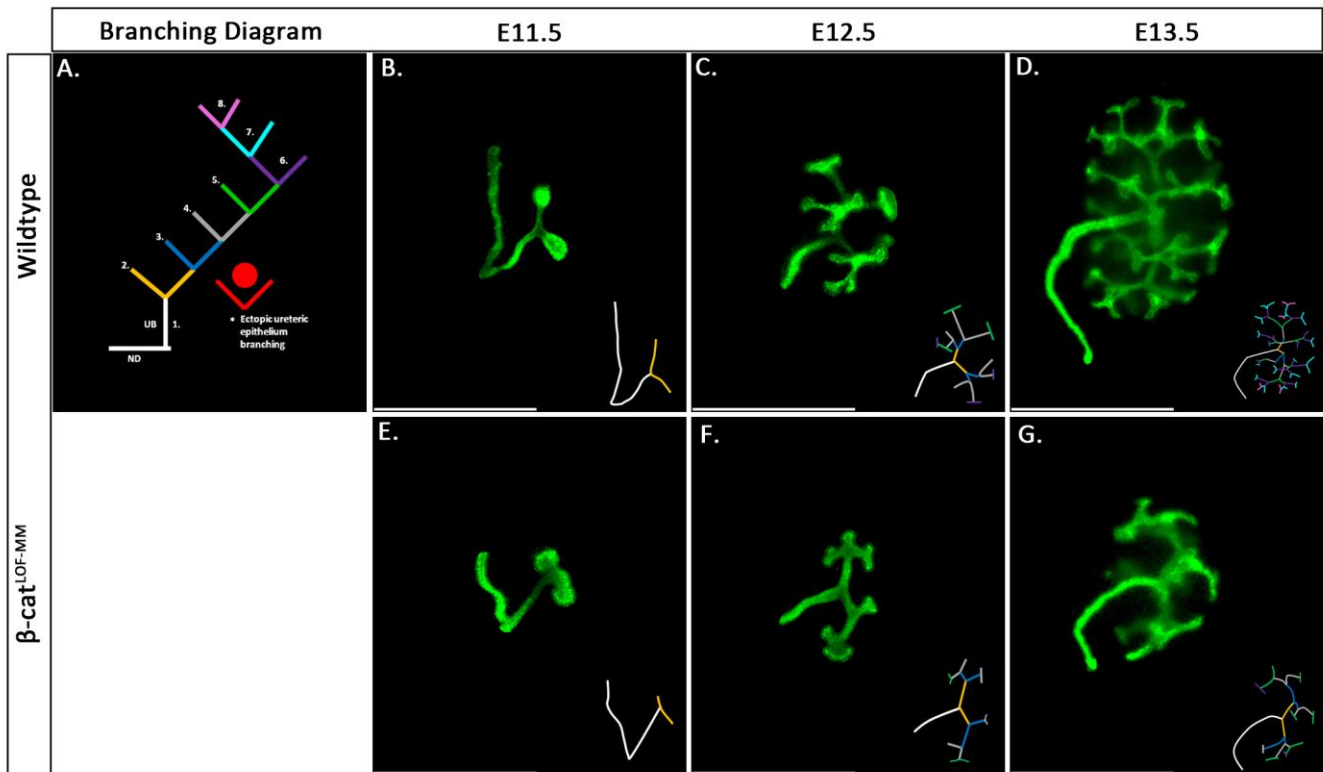


β -cat^{LOF-MM} mutants demonstrates renal hypoplasia during kidney development: (A,B) Histological analysis of newborn kidneys using hematoxylin and eosin stain (scale bar = 500 μ m). As compared to wildtype (A), β -cat^{LOF-MM} kidneys are markedly smaller than wildtype. (C,D) Histological analysis of E13.5 kidneys at higher magnification (scale bar = 100 μ m) reveals that β -cat^{LOF-MM} mutants maintain an active nephrogenic zone. Similar to wildtype (C), β -cat^{LOF-MM} demonstrate normal nephrogenesis with the formation of S-shaped bodies (arrow: top) and glomeruli (arrow: bottom), (E-H) Immunofluorescence analysis of E12.5 kidneys using Pax2 (green) and Cytokeratin (red) antibodies. As compared to wildtype (E), β -cat^{LOF-MM} demonstrate reduced kidney size and reduced number of cytokeratin positive ureteric duct tips (F) (scale bar = 100 μ m). (G,H) β -cat^{LOF-MM} demonstrate normal formation of developing nephrons, S-shaped bodies (white arrow).

4.10: β -cat^{LOF-MM} demonstrate delayed and reduced branching morphogenesis

Since the tips of the ureteric bud continually induce the formation of new nephrons as they branch, a reduction in branching morphogenesis can lead to renal hypoplasia with reduced nephron number [71]. In order to determine if the reduction of ureteric tips within β -cat^{LOF-MM} mutant kidneys was due to defects in branching morphogenesis, we performed whole-mount Cytokeratin immunofluorescence on kidney explants. At E11.5 the ureteric bud formed a T-branch containing 2 distinct tip regions in wildtype (Fig. 15B). β -cat^{LOF-MM} mutants also demonstrated the formation of a T-branch, however branching morphogenesis appeared slightly delayed as the tip regions were not as distinct (Fig. 15E). At E12.5, β -cat^{LOF-MM} mutants displayed a reduction in branching morphogenesis. As compared to wildtype which demonstrated the formation of 15 branch tips (Fig. 15C), β -cat^{LOF-MM} mutants formed 10 branch tips (Fig. 15F). By E13.5 branching morphogenesis was noticeably reduced in β -cat^{LOF-MM} mutants. While wildtype displayed the formation of approximately 43 ureteric branch tips (Fig. 15D), β -cat^{LOF-MM} mutants demonstrated the formation of only 16 ureteric branch tips (Fig. 15G). Taken together, these analyses confirm that β -cat^{LOF-MM} kidneys have a reduction in branching morphogenesis, which would account for the development of renal hypoplasia.

Figure 15: $\beta\text{-cat}^{\text{LOF-MM}}$ demonstrate delayed and reduced branching morphogenesis

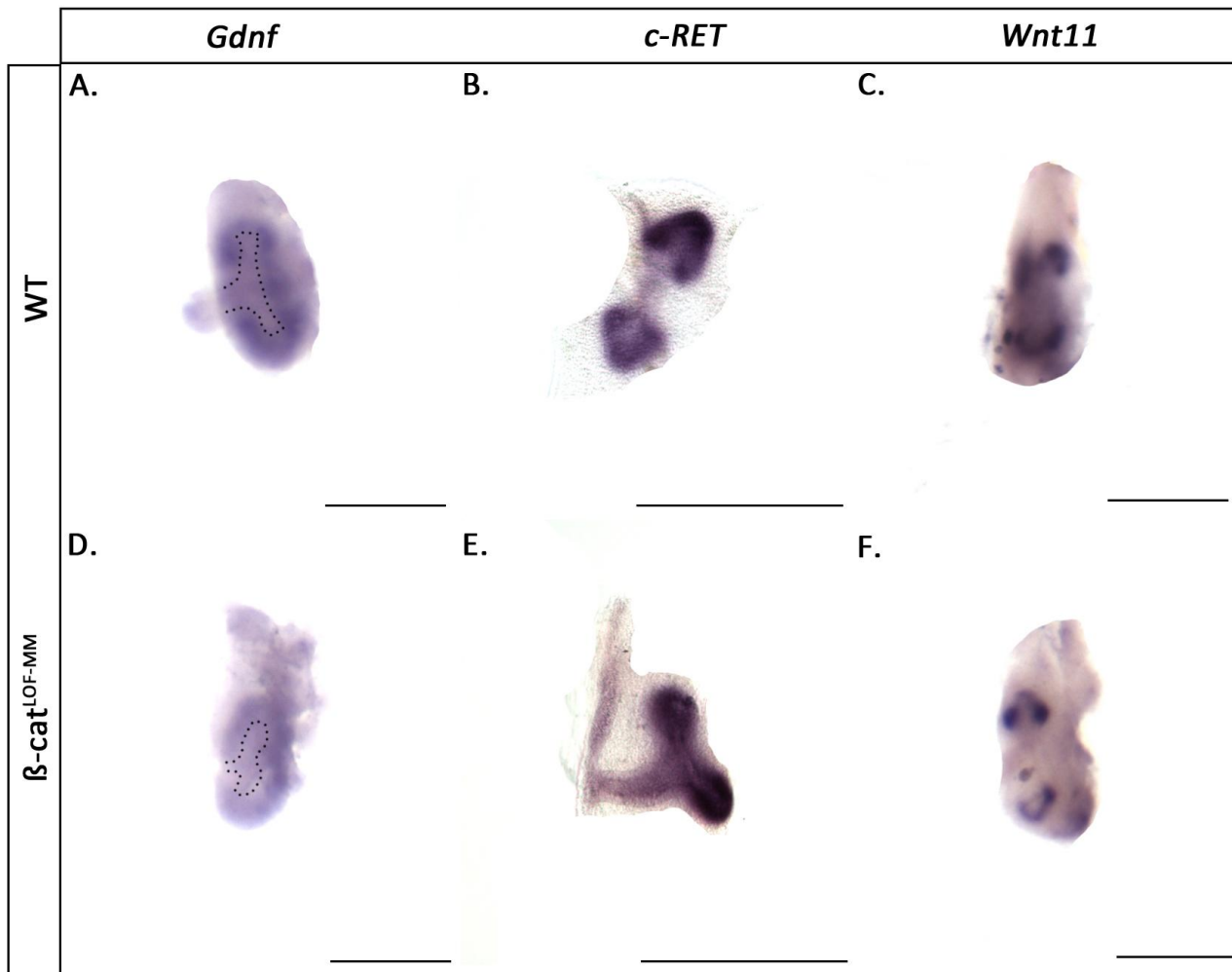


$\beta\text{-cat}^{\text{LOF-MM}}$ mutants demonstrate delayed and reduced branching morphogenesis: (A) Line diagram using a colour code to represent branch generation. The primary bud from the Wolffian duct is considered the “first generation” (white); the first two branches that form from the primary bud are the second generation (yellow) etc. Red line represents ectopic branching morphogenesis. (B-G) Wholemount immunofluorescence using anti-Cytokeratin antibody, demonstrating reduced branching morphogenesis in $\beta\text{-cat}^{\text{LOF-MM}}$ mutants (scale bar = 250 μm) (B) At E11.5, as compared to wildtype which shows two distinct tip regions, $\beta\text{-cat}^{\text{LOF-MM}}$ mutants demonstrate a delayed formation of a T-branch (E). At E12.5 as compared to wildtype (C), $\beta\text{-cat}^{\text{LOF-MM}}$ mutants demonstrate a reduction in ureteric branching (F). At E13.5 $\beta\text{-cat}^{\text{LOF-MM}}$ mutants display a marked reduction in branching morphogenesis as evidenced by a decrease in ureteric tip generation (G), as compared to wildtype (D).

4.11: Decreased *Gdnf* Expression in β -cat^{LOF-MM} mutants

Next, we investigated how a loss of β -catenin in the metanephric mesenchyme altered branching morphogenesis. *Gdnf* is expressed in the metanephric mesenchyme and regulates ureteric bud outgrowth and branching morphogenesis [9]. A reduction in *Gdnf* expression has been previously shown to reduce branching morphogenesis [23]. To determine if the reduction in branching morphogenesis observed in β -cat^{LOF-MM} mutants was a result of decreased *Gdnf* expression, we performed whole-mount in-situ hybridization at E11.5, as we observed branching defects at this age. In comparison to wildtype (Fig. 16A), *Gdnf* expression was markedly reduced in the metanephric mesenchyme of β -cat^{LOF-MM} mutant kidneys (Fig. 16B). We also analyzed the expression of *c-Ret*, and *Wnt11*. The intensity of *c-Ret* expression was similar between wildtype and β -cat^{LOF-MM} mutants (Fig. 16C,D). However the expression of *c-Ret* was not quite fully limited to the tips of the branching ureteric bud in β -cat^{LOF-MM} mutants (Fig. 16D). Finally we analyzed *Wnt11* expression. The expression *Wnt11* appeared slightly reduced in β cat^{LOF-MM} as compared to wildtype (Fig. 16E,F).

Taken together, these findings demonstrate that a loss of β -catenin in the metanephric mesenchyme leads to renal hypoplasia. This is likely caused by a delay in kidney development due to reduced branching morphogenesis as a result of decreased *Gdnf* levels. These data support our hypothesis that β -catenin, within the metanephric mesenchyme, controls the expression of *Gdnf*.

Figure 16: Decreased *Gdnf* expression in β -cat^{LOF-MM} mutants

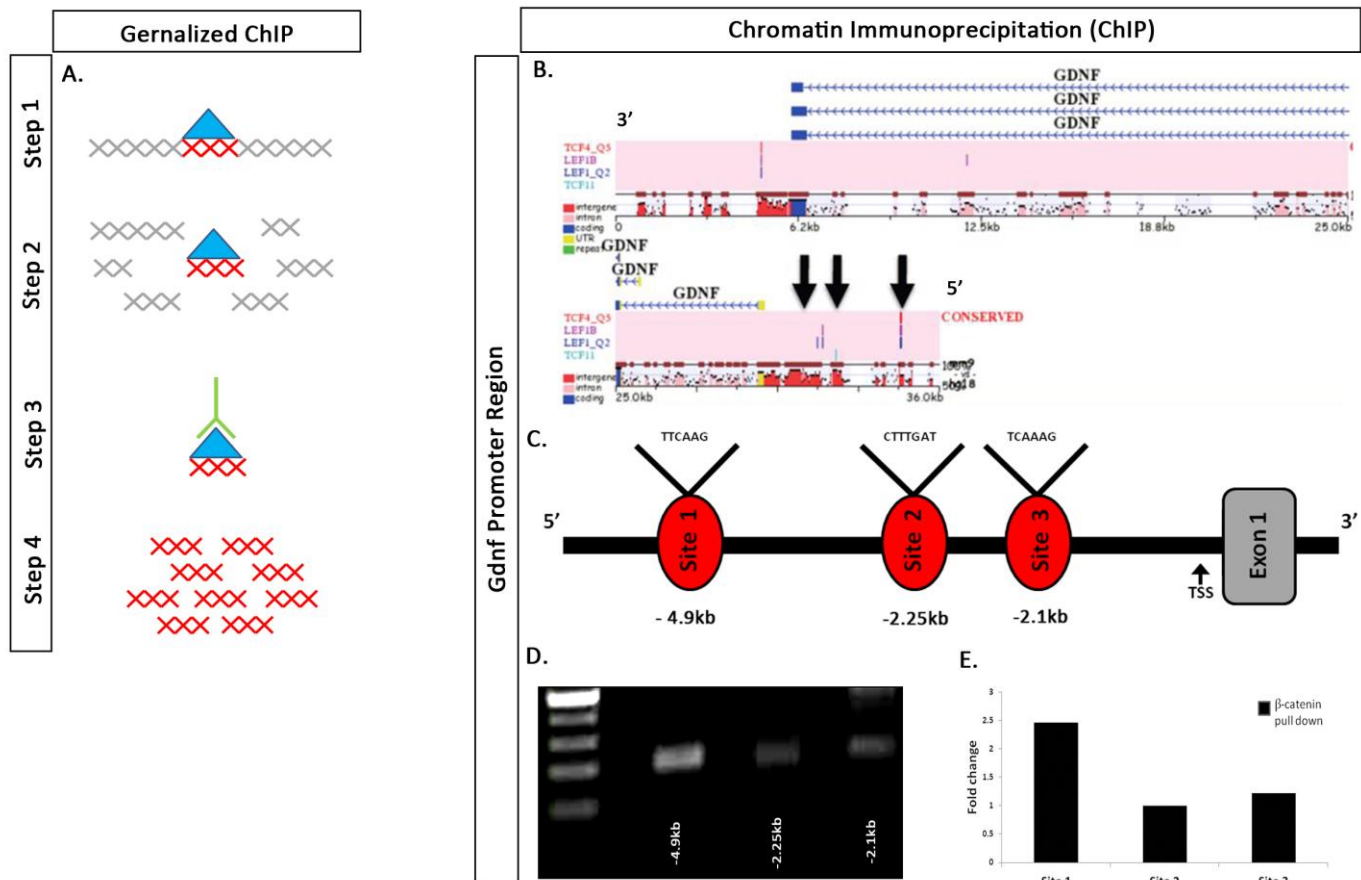
Decreased *Gdnf* Expression in β -cat^{LOF-MM} mutants: (A-F) Whole mount In-situ hybridization for *Gdnf*, *Ret* and *Wnt11* in E11.5 wildtype and β -cat^{LOF-MM} kidneys (dotted line indicates ureteric bud, scale bar = 250 μ m). (A,D) In contrast to wildtype littermate (A), the intensity of *Gdnf* expression levels are lower in β -cat^{LOF-MM} kidney (D). (B,E) The levels of *c-Ret* expression were similar between wildtype (B) and β -cat^{LOF-MM} mutants (E), however the expression was not fully limited to the tips in β -cat^{LOF-MM} mutants as it was in wildtype (black arrows). (C,F) *Wnt11* expression levels were similar between wildtype (C) and β -cat^{LOF-MM} mutants (F).

4.12: β -catenin binds TCF/LEF consensus sequences in the *Gdnf* promoter and regulates transcription

Up to this point, we have shown that 1) over-expression of β catenin within the metanephric mesenchyme leads to an increase in *Gdnf* expression and 2) deletion of β catenin within the metanephric mesenchyme leads to a loss in *Gdnf* expression. Together, these findings demonstrate that β catenin plays a role in the regulation of *Gdnf* expression. We next wanted to determine whether β -catenin has direct effects on the regulation of *Gdnf* transcription.

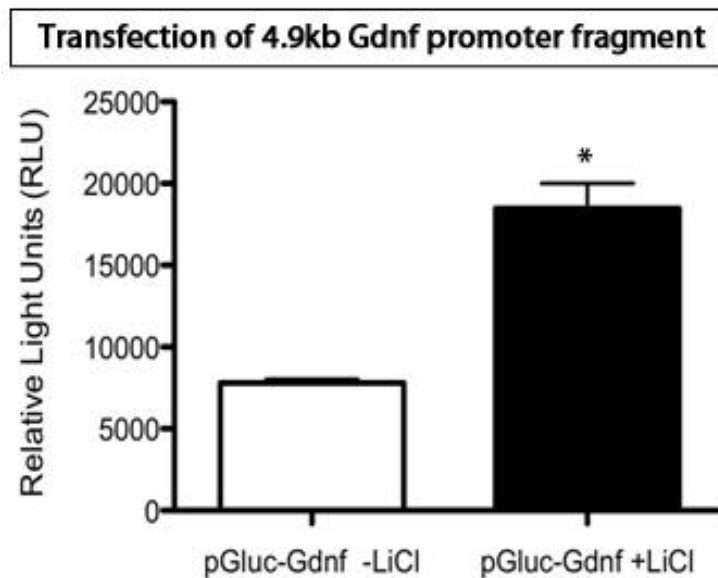
Once in the nucleus, β -catenin interacts with members of the TCF/LEF family of DNA bound co-transcriptional activators to regulate gene transcription. We first retrieved mouse, human and rat *Gdnf* genomic DNA sequences that contained approximately 25kb upstream of the *Gdnf* transcriptional start site (<http://genone.ucsc.edu/>). We then used the multiple sequence alignment tool (MULAN) (<http://mulan.dcode.org/analysis>) to align the sequences, which highlights conserved regions between mouse, human and rat DNA. Next we used Transfac professional V10.2 library. This library contains thousands of conserved transcription factor binding sites. Using these tools we searched the *Gdnf* 5' promoter region for TCF/LEF consensus binding sites, since β -catenin binds to TCF/LEF transcription factors to regulate gene transcription. We identified 3 TCF/LEF consensus binding sequences conserved between mouse, rat and human located within the *Gdnf* promoter. These 3 highly conserved TCF/LEF binding sites were located at 4.9kb (site 1), 2.25kb (site 2) and 2.1kb (site 3) upstream of the *Gdnf* start site (Fig. 17B,C). In order to determine whether β -catenin/TCF/LEF transcription factors directly bound to these sites, we performed chromatin immunoprecipitation (ChIP). ChIP refers to a procedure that is used to determine whether a given protein binds to a specific DNA sequence *in vivo*. This technique involves using antibodies specific to the DNA-binding protein,

which will then ‘pull-down’ the given protein/DNA complex. If PCR, using primers specific to the given DNA sequence, amplifies the region, it demonstrates that the protein of interest binds to that given DNA site (Refer to Fig. 17A for a visual representation of the procedure). Therefore, to determine whether β -catenin was physically associated with these three sites, we performed ChIP on E14.5 kidneys, as this was the earliest time point that yielded sufficient protein/DNA complexes. Protein/DNA complexes were ‘pulled-down’ using a ChIP grade β -catenin antibody. Next specific primers were designed to the 3 conserved TCF/LEF binding sites discovered from our *in-silico* analysis (Fig. 17B,C). Using these primer sets we performed PCR to amplify the candidate regions. Primer sets specific for site 1 generated a 159bp amplicon, site2 generated a 161 bp amplicon and site 3 generated a 190bp amplicon (Fig 17B) This indicates that these 3 TCF/LEF consensus binding sites were ‘pulled down’ with β -catenin. Together, these findings demonstrate that β -catenin/TCF/LEF molecular complexes directly interact with all 3 sites within the Gdnf promoter. The ChIP input DNA was carefully quantified using the nano-drop spectrophotometer. Exactly 100ng of DNA was utilized for site1, site2, and site3. Interestingly site 1 demonstrated a more intense PCR product, relative to site 1 and 2 (Fig. 17D,E), indicating that more DNA was precipitated at this particular site. This suggests that β -catenin/TCF/LEF molecular complexes bind to site 1 (4.9kb fragment) with greater affinity.

Figure 17: β -catenin binds TCF/LEF consensus sequences in the *Gdnf* promoter

β -catenin binds TCF/LEF consensus sequences in the *Gdnf* promoter: (A) Generalized ChIP protocol. Step 1) DNA-binding proteins are cross-linked to DNA following fixation process; Step 2) Isolate chromatin (protein/DNA). Shear protein/DNA into smaller fragments; Step 3) Bind antibodies specific to the DNA-binding protein to isolate the complex by precipitation. Reverse the cross-linking in step 1 to release the DNA and digest the proteins; Step 4) Use PCR to amplify specific DNA sequences to see if they were precipitated with the antibody. This will demonstrate that the protein in question binds to the DNA sequence. (B,C) In-silico analysis demonstrating the position and sequence of the conserved TCF/LEF transcription factor binding sites in the *Gdnf* promoter region (TSS = Transcriptional Start Site). (D) Chromatin immunoprecipitation of E14.5 kidney lysates followed by PCR of Site 1, 2 and 3. PCR amplification results in a 159bp PCR product at site 1, 161bp product at site 2, and 190bp product at site 3. (E) Quantification of ChIP demonstrates that β -catenin binds to site 1 (4.9kb fragment) with higher affinity than site 3, relative to site 2 (2.45 fold increase vs. 1.35 fold increase respectively).

Since β -catenin/TCF/LEF molecular complexes bound to site 1 (4.9kb fragment) with the highest affinity, we next determined if β -catenin by binding to this specific site could activate gene transcription. In order to accomplish this task we generated primers containing Mlu1 and Hind3 fragments that were specific to site 1 (see materials and methods for specific sequences). These primers amplified a 560bp fragment that included the TCF/LEF binding site (Site1). This fragment was then subcloned into a pGluc luciferase reporter vector to generate a pGluc-Gdnf plasmid. The pGluc-Gdnf plasmid was then transfected into human embryonic kidney (HEK293) cells using lipofectamine. HEK293 cells were incubated in the presence or absence of LiCl to activate the canonical Wnt/ β -catenin pathway. Transfected HEK293 cells that were treated with lithium chloride demonstrated a 2.37 fold increase in luciferase activity, compared to those cells without the addition of LiCl (Fig. 18). As a negative control we also generated pGluc vectors without the promoter fragment. Taken together, these studies indicate that β -catenin directly binds to the 4.9kb TCF/LEF consensus site in the Gdnf promoter, and that this site regulates gene transcription.

Figure 18: The 4.9kb Gdnf promoter fragment activates gene transcription

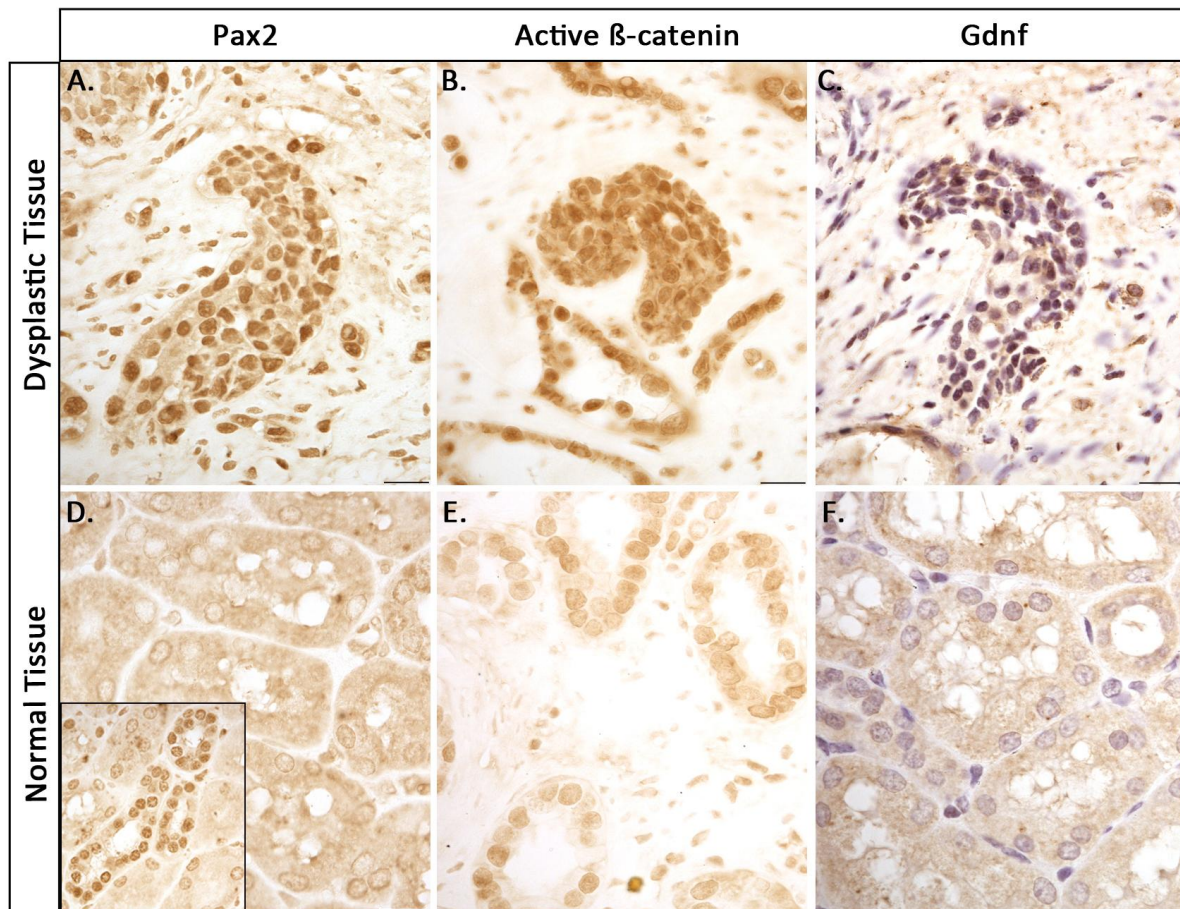
The 4.9kb Gdnf promoter fragment activates gene transcription: The 4.9 kb fragment was cloned upstream of a luciferase reporter gene. The construct was transfected into HEK293 cells and stimulated with or without LiCl. HEK293 cells stimulated with LiCl demonstrated a marked increase in light emission as compared to HEK293 with no treatment ($p < 0.013$). Stimulation of the canonical wnt/ β -catenin signalling pathway resulted in a 2.37 fold increase in luciferase activity compared to those cells without treatment.

4.13: Undifferentiated mesenchyme in dysplastic human renal tissue demonstrates both increased β -catenin and Gdnf levels

We next determined if the high levels of activated β -catenin we observed in 1 year post natal human dysplastic renal tissue was associated with increased GDNF protein expression. By utilizing a PAX2 antibody, we identified a population of undifferentiated metanephric mesenchyme (Fig. 19A,D). Within this population of cells, the levels of activated β -catenin was increased as compared to that of normal renal tissue (Fig. 19B,E). In the human dysplastic

kidney tissue the PAX2-positive mesenchyme cells expressing high levels of activated β -catenin also expressed high levels of GDNF (Fig. 19C,F). These studies support a mechanism by which an over-expression of β -catenin in the metanephric mesenchyme results in increased *Gdnf* expression thereby contributing to the genesis of renal dysplasia

Figure 19: Dysplastic kidney tissue demonstrates elevated levels of β -catenin and Gdnf



Dysplastic kidney tissue demonstrates elevated levels of β -catenin and Gdnf: (A-F) Immunohistochemistry on 1 year post natal human renal dysplastic tissue (scale bar = 10 μ m). (A) Pax2 marks undifferentiated mesenchyme in dysplastic human renal tissue. (D) Pax2 is rarely expressed in normal renal tubules (inset). (B) Within dysplastic renal tissue, undifferentiated mesenchyme demonstrates increased levels of activated β -catenin as compared to normal renal tubules (E). (C,F) Consistent with our mouse studies, Gdnf levels are increased within undifferentiated mesenchyme that demonstrate increased β -catenin activity in dysplastic tissue

5.0 DISCUSSION

5.1: Overall findings

Renal dysplasia is the abnormal development of the kidney encompassed by varying degrees of defective renal formation. Studies in mouse and human have demonstrated the importance of various growth factors, signalling pathways and transcription factors in the onset of renal dysplasia. However, despite the advancements in this field, the underlying molecular mechanisms regulating renal dysplasia are poorly understood. Previous reports have demonstrated that β -catenin is over-expressed in the ureteric bud derived epithelium of dysplastic human renal tissue [58]. Our studies extend these findings two fold. First, in addition to the ureteric epithelia, we have spatially localized the over-expression of β -catenin to the undifferentiated metanephric mesenchyme and renal stroma in dysplastic human renal tissue. Second, we utilized an antibody that specifically detects the activated form of β -catenin. In its activated form, β -catenin translocates to the nucleus where it interacts with members of the TCF/LEF family of DNA-bound transcription factors to activate gene transcription. In this regard we demonstrate that the activated form of β -catenin is over-expressed in the nuclei of ureteric, mesenchymal and stromal cells, which suggests that β -catenin may play an important role in the regulation of key genes responsible in the pathogenesis of renal dysplasia.

To determine the pathological role of mesenchymal over-expression of β -catenin in the development of renal dysplasia, we generated a mouse model of β -catenin stabilization specifically in the metanephric mesenchyme. β -cat^{GOF-MM} mutants demonstrated a number of histopathological characteristics consistent with human renal dysplasia. Phenotypical characterization of β -cat^{GOF-MM} mutants revealed disrupted and disorganized branching morphogenesis. β -cat^{GOF-MM} mutant mice exhibited an over-expression of *Gdnf*, *c-Ret* and *Wnt11*,

molecules critical in the regulation of branching morphogenesis. In addition, we demonstrated that β -catenin directly binds to the Gdnf promoter and regulates its transcription during kidney development. We propose a model by which β -catenin over-expression in the metanephric mesenchyme directly regulates Gdnf transcription. The over-expression of Gdnf causes ectopic and disorganized ureteric epithelial patterning and branching leading to renal dysplasia.

5.2: Maintenance of Nephrogenesis In β -cat^{GOF-MM} mutants

Several studies have assessed the role of β -catenin in nephrogenesis. In a study conducted by Park et. al [18], mice in which β -catenin was over-expressed exclusively in the cap mesenchyme exhibited renal agenesis and a lack of nephron formation. At the molecular level, stabilization of β -catenin within the cap mesenchyme induced the ectopic activation of key genes required in the early nephrogenic program; however, the formation of renal vesicles was blocked. Park et al concluded that while stabilization of β -catenin in the metanephric mesenchyme is sufficient to initiate nephrogenesis, a down-regulation of β -catenin activity may be required for the transition of mesenchymal nephron progenitors to an epithelial renal vesicle (MET). These findings are in contrast to the observations made in our study, which found that mice in which β -catenin was over-expressed in the metanephric mesenchyme exhibited large, misshapen and lobular kidneys with ectopic renal tissue formation. In addition, with respect to nephrogenesis, while β -cat^{GOF-MM} mutants demonstrate irregular patterning of developing nephrons, the nephrogenic program (i.e. the progression from renal vesicle to mature glomeruli), remained intact throughout the kidney. We believe that the drastic differences between these two studies, with respect to the phenotypes observed, is due to the distinct Cre mice lines used. In our study, we utilized the Rarb2-Cre driver rather than the Six2-Cre driver used by Park and

colleagues. In *Rarb-Cre* mice, Cre is expressed as early as E9.5 in the nephric mesenchyme and becomes restricted to the metanephric mesenchyme by E10.5 [45, 67]. At E12.5 Cre is expressed not only in the cap mesenchyme but also in the cortical stroma [39, 67]. In contrast, in the *Six2-Cre* mouse model, Cre is expressed in the cap mesenchyme (nephrogenic progenitors) beginning at E11.5 and is not active in the renal stroma [68]. Therefore, while Park et al stabilized β -catenin only in the cap mesenchyme, in our study β -catenin was over-expressed in all the metanephric mesenchyme and cortical stroma within β -cat^{GOF-MM} kidneys. In recent years, a number of studies have highlighted the importance of the cortical stroma in the regulation of nephrogenesis and MET [73-75]. Therefore, it is likely that we have altered the levels of stromally expressed factors and created an environment in which the formation of renal vesicles and nephrons are not perturbed. We are therefore currently elucidating the role β -catenin plays in the renal stroma during renal development.

Interestingly, a study conducted by Kuure et al also demonstrated that nephrogenesis remained intact when β -catenin was stabilized in the cap mesenchyme [47]. In this study, researchers isolated embryonic mouse mesenchymes from β -catenin gain of function mutants at E11.0 and cultured them for 5 days. These mutant mesenchymes formed pretubular aggregates and differentiated into nephron epithelium [47]. These findings by Kuure et al are also in contrast to those observed by Park et al, and complement what is seen in β -cat^{GOF-MM} kidneys. These conflicting reports highlight the uncertainties regarding the role of β -catenin in nephrogenesis. Consequently, researchers have begun to address the roles of other signalling pathways in nephron formation. For example, a number of recent studies have highlighted the importance of the non-canonical calcium/NFAT-Wnt signalling pathway in the regulation of nephrogenesis [72, 76]. The calcium/NFAT pathway is activated upon the Wnt-induced increase of

intracellular Ca^{2+} . This rise in Ca^{2+} levels leads to the activation of calcineurin (a phosphatase) which dephosphorylates the NFAT transcription factors, facilitating their translocation to the nucleus and subsequent transcriptional activation of target genes [77]. Ectopic activation of the Calcium/NFAT pathway in *Wnt4*^{-/-} kidneys rescues the nephrogenic defect and demonstrates the sufficiency of this pathway to overcome the block in MET caused by the absence of *Wnt4* [72]. Previous studies have demonstrated that over-expression of *Wnt5a* and *Wnt11* can trigger intracellular Ca^{2+} influx, which may lead to the activation of the Calcium/NFAT pathway [78, 79]. Since $\beta\text{-cat}^{\text{GOF-MM}}$ kidneys demonstrate elevations in *Wnt11* expression, it is possible that Calcium/NFAT signalling activity is increased. The elevation in Calcium/NFAT signalling activity may account for the progression of nephrogenesis observed in $\beta\text{-cat}^{\text{GOF-MM}}$ kidneys. Determining whether the Calcium/NFAT pathway is dysregulated in $\beta\text{-cat}^{\text{GOF-MM}}$ mutants will shed more light on the maintenance of nephrogenesis.

5.3: Transcriptional regulation of *Gdnf*

Gdnf is an essential regulator of ureteric bud outgrowth and branching morphogenesis [21]. As compared to wildtype, the levels of *Gdnf* expression are markedly higher in $\beta\text{-cat}^{\text{GOF-MM}}$ mutants. In contrast, $\beta\text{-cat}^{\text{LOF-MM}}$ mutant kidneys demonstrate reduced *Gdnf* expression. Taken together, these findings strongly suggest that β -catenin directly regulates *Gdnf* transcription. *In silico* analysis revealed three putative TCF/LEF consensus-binding sequences conserved between the mouse, rat and human in the *Gdnf* promoter. However, the physical binding or direct transcriptional regulation of β -catenin/TCF/LEF complexes in the *Gdnf* promoter has not been demonstrated in the kidney. Here we show that β -catenin directly binds to the TCF/LEF-consensus binding sites within the *Gdnf* promoter and directly regulates its transcription within

the kidney. Consistent with our findings, a previous study has shown that β -catenin regulates the expression of *Gdnf* at the transcriptional level within Sertoli cells [80]. Our studies demonstrate that this transcriptional regulation of *Gdnf* by β -catenin also occurs in the kidney.

The incomplete loss of *Gdnf* expression in β -cat^{LOF-MM} kidneys suggests that other key positive regulators of *Gdnf* expression are unaltered. Recent studies have demonstrated that Pax2, Eya1 and Hox11 form a molecular complex that directly regulates *Gdnf* expression in the metanephric mesenchyme [81]. Furthermore, in the absence of *Sall1*, the levels of *Gdnf* are also reduced, suggesting a role in the regulation of *Gdnf* expression [16]. Future studies will be aimed to address whether other positive regulators of *Gdnf* expression are dysregulated in β -cat^{LOF-MM} or β -cat^{GOF-MM} mutants.

5.4: Wnt proteins controlling *Gdnf* expression

Our findings place *Gdnf* downstream of β -catenin canonical Wnt signalling in the metanephric mesenchyme; however, the specific Wnt signal that activates β -catenin and thus *Gdnf* transcription is unknown. A number of *Wnt* genes are expressed during renal development and several regulate branching morphogenesis. Wnt9b is expressed and secreted by the ureteric epithelium, where it activates the transcription of genes in the cap mesenchyme [29, 39]. Loss of Wnt9b results in a severe branching deficiency and a reduction in *Gdnf* expression [29], a phenotype similar to that observed in β -cat^{LOF-MM} mutants. However, over-expression of Wnt9b in the ureteric epithelium also results in a reduction in branching morphogenesis [82]. Therefore, it is not likely that a Wnt9b specific response within the metanephric mesenchyme, mediated through β -catenin regulates *Gdnf* expression. Instead, Wnt11 appears to be a more suitable candidate. Wnt11 is expressed and secreted at the tips of the ureteric epithelium, where it

regulates the expression of specific genes within the cap mesenchyme [25]. Studies have shown that a loss of Wnt11 results in reduced *Gdnf* levels in the metanephric mesenchyme [25], a phenotype similar to that of β -cat^{LOF-MM} mutants. In addition, over-expression of Wnt11 leads to an increase in *Gdnf* expression [23], similar to what is observed in our β -cat^{GOF-MM} mutants. Therefore, it is more likely that a Wnt11 specific response within the metanephric mesenchyme mediated through β -catenin regulates the expression of *Gdnf*.

5.5: Ectopic and disorganized branching morphogenesis in β -cat^{GOF-MM} mutants

β -cat^{GOF-MM} mutants exhibit ectopic kidney formation outside the normal region of renal development. There are a few potential explanations that may account for this irregularity. Ectopic budding and branching of the ureteric epithelium has been previously shown to induce the formation of supernumerary kidneys that fuse together and disrupt normal renal development [8, 23]. Consistent with other studies, in which the *Gdnf* expressional domain was expanded, using either genetic mouse models [8, 17] or exogenously placed beads [14], we also demonstrate ectopic ureteric budding off the Wolffian duct and initial stalk in β -cat^{GOF-MM} mutants. These ectopic buds may then branch and fuse to the normal developing kidney, resulting in the development of renal tissue residing outside the kidney proper. In some instances no ectopic buds are clearly visible; however, branching morphogenesis remains severely disorganized. This discrepancy with respect to the branching phenotype may be explained by a physiological threshold that *Gdnf* levels must first overcome before inducing ectopic ureteric budding, as a number of factors exist that restrict the initial budding step [26]. For instance, loss of *Spry1*, a protein that has been postulated to inhibit Wnt11 signalling [23], can lead to the formation of supernumerary ureteric buds in the presence of *Gdnf*. However, this *spry1* null

phenotype is rescued when reducing the *Gdnf* gene dosage [83]. These results support the notion of a *Gdnf* threshold/dosage that, once surpassed, may induce the formation of ectopic buds in β -cat^{GOF-MM} mutants. Why these threshold levels are not always obtained in β -cat^{GOF-MM} mutants maybe in part due to some mesenchymal cells escaping Cre-recombination.

Apart from *Gdnf*-Ret signalling, FGF10, which is expressed and secreted by the metanephric mesenchyme, signals via FGFR2 on the ureteric bud and plays a secondary role in the control of branching morphogenesis [84, 85]. Ureteric buds cultured in the presence of increased FGF10 demonstrate abnormal branching patterns, resembling the branching phenotype observed in β -cat^{GOF-MM} mutant kidneys [84]. Furthermore, ectopic expression of FGF10 causes ectopic ureteric buds to form along the Wolffian duct [85]. Studies conducted in mouse anterior heart field progenitor cells have demonstrated that FGF10 is a direct target of Wnt/ β -catenin signalling [86]. Therefore, it is likely that we altered the levels of FGF10 in both our gain of function and loss of function transgenic mouse models. Whether FGF10 is increased in β -cat^{GOF-MM} mutant kidneys and contributes to the branching irregularity is an area that requires further investigation.

5.6: Ectopic kidney formation in β -cat^{GOF-MM} kidneys

β -cat^{GOF-MM} kidneys demonstrate abnormal formation of ectopic renal tissue, which consists of tubules, developing glomeruli, and mature glomeruli outside the capsule of the major developing kidney. As mentioned above, the development of supernumerary ectopic ureteric buds in β -cat^{GOF-MM} kidneys may account for the formation of ectopic renal tissue. The formation of ectopic ureteric buds may induce the adjacent metanephric mesenchyme to undergo nephrogenesis. However, it is also possible that these ectopic renal formations arise due to the

severe disorganized branching morphogenesis observed in β -cat^{GOF-MM} mutants. In this regard, one branch may extend further than normal or in an irregular direction. Then depending on the section of the mutant kidney, these formations, by histological or immunohistochemical analysis, would appear outside the kidney proper, when in fact they may be connected to the major developing kidney.

We have also shown that, in conjunction with ectopic ureteric budding and severe disorganized branching morphogenesis, stabilization of β -catenin within the uninduced mesenchyme leads to the formation of ectopic cytokeratin positive structures not connected to the developing collecting duct system. These ectopic cytokeratin positive structures may account for the formation of renal tissue outside the kidney proper. How does the stabilization of β -catenin within the uninduced metanephric mesenchyme lead to the spontaneous formation of tubules? One possibility is that mesonephric tubules, which stain positively for cytokeratin, fail to regress and degenerate. During the early stages of kidney development, two types of mesonephric tubules form: cranial mesonephric tubules that are attached to the Wolffian duct, and more caudal mesonephric tubules that arise adjacent to the Wolffian duct. Under normal conditions, both types of mesonephric tubules regress and undergo apoptosis [87]. However, depending on local extrinsic factors, mesonephric tubule lifespan can be greatly extended [88] or reduced [29]. Since *Rarb2-cre* is also expressed in the mesonephric mesenchyme and tubules [39, 67], along with transcriptionally active β -catenin [89], it is possible that we have created a local environment that acts to maintain these tubules and prevent them from undergoing apoptosis. Studies conducted in an avian model demonstrated that regressing mesonephric tubules have reduced levels of transcriptionally active β -catenin [90]; therefore, it is likely that

stabilization within these tissues prevents their degradation. However, the specific role β -catenin plays within the murine mesonephric mesenchyme/tubules remains to be identified.

This explanation may account for those tubules residing rostral to the kidney capsule in β -cat^{GOF-MM} mutants; however, the presence of tubules and mature nephrogenic structures adjacent and caudal to the kidney proper require further clarification. Caudal mesonephric tubules are derived from the mesonephric mesenchyme and their formation requires the inductive actions of Wnt9b.[29] Wnt9b is expressed by the Wolffian duct and signals via the canonical wnt pathway, thus implicating β -catenin in the formation of caudal mesonephric tubules.[29] Since Rarb2-cre expression is detected as early as E9.5-E10.5 in the mesonephric mesenchyme [45, 67], the canonical wnt signalling pathway mediated by β -catenin has been activated prior to ureteric bud invasion. The stabilization of β -catenin can replace the normal activity of Wnt9b and induce the mesenchymal cells to form mesonephric tubules in ectopic locations. However, mesonephric tubules lack both a glomerular apparatus and loop of henle[88], therefore determining whether the ectopic tubules in β -cat^{GOF-MM} mutants also lack these formations will provide us with further insight into the origins of these structures. Since glomeruli reside outside the kidney proper in β -cat^{GOF-MM} mutants, not all these ectopic structures can be derived from mesonephric tubules.

It is more likely that a combination of these mechanisms, rather than just one, contribute to the ectopic formation of renal tissue in β -cat^{GOF-MM} mutants. In order to narrow our focus and gain further insight into the generation of these ectopic formations, it is crucial that we first determine if they derive from the mesenchyme or Wolffian duct. This will be accomplished by crossing Rar β 2-Cre mice with a TomatoGFP Cre-reporter strain, which express green fluorescent protein (GFP) in cells that have undergone Cre-mediated recombination. Mice that express both

TomatoGFP and Rar β 2-Cre (TomatoGFP+/ Rar β 2Cre+) will be crossed with mice homozygous for the stabilized β -catenin allele (β -cat $^{\Delta 3/\Delta 3}$) to generate β -cat $^{\text{GOF-MM}}$ mutants that also express TomatoGFP. Since Rar β 2-Cre is not expressed in the Wolffian duct or ureteric bud, GFP will be absent from these cells during kidney development. In this regard, if GFP expression is observed in the ectopic renal tissue, it is more likely that they derive from the mesenchyme. These studies will undoubtedly be helpful in gaining a better understanding of these ectopic formations.

5.7: Conclusion

Consistent with our findings, human dysplastic kidney tissue demonstrates increases in *GDNF* expression [63]. However, genomic alterations within *GDNF* do not appear to promote these elevations in renal dysplasia [61]. As such, it is likely that defects in genes upstream of *GDNF* expression contribute to the development of the disorder. Here we have identified a novel role for β -catenin in renal dysplasia. Not only have we demonstrated that β -catenin directly binds to the *Gdnf* promoter and regulates transcription but also that increased levels of β -catenin leads to an over-expression of *Gdnf* and causes ectopic and disorganized ureteric epithelial branching leading to renal dysplasia. These studies identify a novel disrupted developmental pathway that may be targeted to reduce or alleviate the dysplastic renal phenotype.

6.0 REFERENCES

1. Vize, D.P., ed. *The Kidney: From Normal Development to Congenital Disease*. 2003, Elsevier Science: Journal of New England Medicine. 1-519.
2. Fox, I.S., *Physiology of the Kidneys*. Human Physiology. Vol. 10. 2008, New York, USA: McGraw Hill
3. De Robertis, E.M. and H. Kuroda, *Dorsal-ventral patterning and neural induction in Xenopus embryos*. Annu Rev Cell Dev Biol, 2004. **20**: p. 285-308.
4. Saxen, L. and H. Sariola, *Early organogenesis of the kidney*. Pediatr Nephrol, 1987. **1**(3): p. 385-92.
5. Davidson, A.J., *Mouse Kidney Development*, in *StemBook*, K.R. Chien, Editor. 2009, The Stem Cell Research Community.
6. Cebrian, C., et al., *Morphometric index of the developing murine kidney*. Dev Dyn, 2004. **231**(3): p. 601-8.
7. Airik, R. and A. Kispert, *Down the tube of obstructive nephropathies: the importance of tissue interactions during ureter development*. Kidney Int, 2007. **72**(12): p. 1459-67.
8. Grieshammer, U., et al., *SLIT2-mediated ROBO2 signaling restricts kidney induction to a single site*. Dev Cell, 2004. **6**(5): p. 709-17.
9. Bridgewater, D. and N.D. Rosenblum, *Stimulatory and inhibitory signaling molecules that regulate renal branching morphogenesis*. Pediatr Nephrol, 2009. **24**(9): p. 1611-9.
10. Takahashi, M., *The GDNF/RET signaling pathway and human diseases*. Cytokine Growth Factor Rev, 2001. **12**(4): p. 361-73.
11. Fisher, C.E., et al., *Erk MAP kinase regulates branching morphogenesis in the developing mouse kidney*. Development, 2001. **128**(21): p. 4329-38.

12. Tang, M.J., et al., *Ureteric bud outgrowth in response to RET activation is mediated by phosphatidylinositol 3-kinase*. *Dev Biol*, 2002. **243**(1): p. 128-36.
13. Costantini, F. and R. Shakya, *GDNF/Ret signaling and the development of the kidney*. *Bioessays*, 2006. **28**(2): p. 117-27.
14. Brophy, P.D., et al., *Regulation of ureteric bud outgrowth by Pax2-dependent activation of the glial derived neurotrophic factor gene*. *Development*, 2001. **128**(23): p. 4747-56.
15. Xu, P.X., et al., *Eya1-deficient mice lack ears and kidneys and show abnormal apoptosis of organ primordia*. *Nat Genet*, 1999. **23**(1): p. 113-7.
16. Nishinakamura, R., et al., *Murine homolog of SALL1 is essential for ureteric bud invasion in kidney development*. *Development*, 2001. **128**(16): p. 3105-15.
17. Kume, T., K. Deng, and B.L. Hogan, *Murine forkhead/winged helix genes Foxc1 (Mf1) and Foxc2 (Mfh1) are required for the early organogenesis of the kidney and urinary tract*. *Development*, 2000. **127**(7): p. 1387-95.
18. Sainio, K., et al., *Glial-cell-line-derived neurotrophic factor is required for bud initiation from ureteric epithelium*. *Development*, 1997. **124**(20): p. 4077-87.
19. Park, J.S., et al., *Six2 and Wnt regulate self-renewal and commitment of nephron progenitors through shared gene regulatory networks*. *Dev Cell*, 2012. **23**(3): p. 637-51.
20. Chi, X., et al., *Ret-dependent cell rearrangements in the Wolffian duct epithelium initiate ureteric bud morphogenesis*. *Dev Cell*, 2009. **17**(2): p. 199-209.
21. Costantini, F. and R. Kopan, *Patterning a complex organ: branching morphogenesis and nephron segmentation in kidney development*. *Dev Cell*, 2010. **18**(5): p. 698-712.
22. Pichel, J.G., et al., *Defects in enteric innervation and kidney development in mice lacking GDNF*. *Nature*, 1996. **382**(6586): p. 73-6.

23. Basson, M.A., et al., *Branching morphogenesis of the ureteric epithelium during kidney development is coordinated by the opposing functions of GDNF and Sprouty1*. Dev Biol, 2006. **299**(2): p. 466-77.
24. Pepicelli, C.V., et al., *GDNF induces branching and increased cell proliferation in the ureter of the mouse*. Dev Biol, 1997. **192**(1): p. 193-8.
25. Majumdar, A., et al., *Wnt11 and Ret/Gdnf pathways cooperate in regulating ureteric branching during metanephric kidney development*. Development, 2003. **130**(14): p. 3175-85.
26. Michos, O., et al., *Reduction of BMP4 activity by gremlin 1 enables ureteric bud outgrowth and GDNF/WNT11 feedback signalling during kidney branching morphogenesis*. Development, 2007. **134**(13): p. 2397-405.
27. Gordon, M.D. and R. Nusse, *Wnt signaling: multiple pathways, multiple receptors, and multiple transcription factors*. J Biol Chem, 2006. **281**(32): p. 22429-33.
28. Fuerer, C., R. Nusse, and D. Ten Berge, *Wnt signalling in development and disease*. Max Delbruck Center for Molecular Medicine meeting on Wnt signaling in Development and Disease. EMBO Rep, 2008. **9**(2): p. 134-8.
29. Carroll, T.J., et al., *Wnt9b plays a central role in the regulation of mesenchymal to epithelial transitions underlying organogenesis of the mammalian urogenital system*. Dev Cell, 2005. **9**(2): p. 283-92.
30. Itaranta, P., et al., *Wnt-6 is expressed in the ureter bud and induces kidney tubule development in vitro*. Genesis, 2002. **32**(4): p. 259-68.

31. Yu, J., et al., *A Wnt7b-dependent pathway regulates the orientation of epithelial cell division and establishes the cortico-medullary axis of the mammalian kidney.* Development, 2009. **136**(1): p. 161-71.
32. Park, J.S., M.T. Valerius, and A.P. McMahon, *Wnt/beta-catenin signaling regulates nephron induction during mouse kidney development.* Development, 2007. **134**(13): p. 2533-9.
33. Lin, Y., et al., *Induction of ureter branching as a response to Wnt-2b signaling during early kidney organogenesis.* Dev Dyn, 2001. **222**(1): p. 26-39.
34. Iglesias, D.M., et al., *Canonical WNT signaling during kidney development.* Am J Physiol Renal Physiol, 2007. **293**(2): p. F494-500.
35. MacDonald, B.T., K. Tamai, and X. He, *Wnt/beta-catenin signaling: components, mechanisms, and diseases.* Dev Cell, 2009. **17**(1): p. 9-26.
36. Zeng, X., et al., *Initiation of Wnt signaling: control of Wnt coreceptor Lrp6 phosphorylation/activation via frizzled, dishevelled and axin functions.* Development, 2008. **135**(2): p. 367-75.
37. Dreszer, T.R., et al., *The UCSC Genome Browser database: extensions and updates 2011.* Nucleic Acids Res, 2012. **40**(Database issue): p. D918-23.
38. Bridgewater, D., et al., *beta-catenin causes renal dysplasia via upregulation of Tgfbeta2 and Dkk1.* J Am Soc Nephrol, 2011. **22**(4): p. 718-31.
39. Karner, C.M., et al., *Canonical Wnt9b signaling balances progenitor cell expansion and differentiation during kidney development.* Development, 2011. **138**(7): p. 1247-57.

40. Brault, V., et al., *Inactivation of the beta-catenin gene by Wnt1-Cre-mediated deletion results in dramatic brain malformation and failure of craniofacial development.* Development, 2001. **128**(8): p. 1253-64.
41. Bridgewater, D., et al., *Canonical WNT/beta-catenin signaling is required for ureteric branching.* Dev Biol, 2008. **317**(1): p. 83-94.
42. Marose, T.D., et al., *Beta-catenin is necessary to keep cells of ureteric bud/Wolffian duct epithelium in a precursor state.* Dev Biol, 2008. **314**(1): p. 112-26.
43. Grote, D., et al., *Gata3 acts downstream of beta-catenin signaling to prevent ectopic metanephric kidney induction.* PLoS Genet, 2008. **4**(12): p. e1000316.
44. Grote, D., et al., *Pax 2/8-regulated Gata 3 expression is necessary for morphogenesis and guidance of the nephric duct in the developing kidney.* Development, 2006. **133**(1): p. 53-61.
45. Kobayashi, A., et al., *Distinct and sequential tissue-specific activities of the LIM-class homeobox gene *Lim1* for tubular morphogenesis during kidney development.* Development, 2005. **132**(12): p. 2809-23.
46. Davies, J.A. and D.R. Garrod, *Induction of early stages of kidney tubule differentiation by lithium ions.* Dev Biol, 1995. **167**(1): p. 50-60.
47. Kuure, S., et al., *Glycogen synthase kinase-3 inactivation and stabilization of beta-catenin induce nephron differentiation in isolated mouse and rat kidney mesenchymes.* J Am Soc Nephrol, 2007. **18**(4): p. 1130-9.
48. Pohl, M., et al., *Toward an etiological classification of developmental disorders of the kidney and upper urinary tract.* Kidney Int, 2002. **61**(1): p. 10-9.

49. Winyard, P. and L.S. Chitty, *Dysplastic kidneys*. *Semin Fetal Neonatal Med*, 2008. **13**(3): p. 142-51.
50. Neu, A.M., et al., *Chronic dialysis in children and adolescents. The 2001 NAPRTCS Annual Report*. *Pediatr Nephrol*, 2002. **17**(8): p. 656-63.
51. Goodyer, P., *Renal Dysplasia/Hypoplasia*, in *Pediatric Nephrology*, E. Avner, et al., Editors. 2009, Springer Berlin Heidelberg. p. 107-120.
52. Woolf, A.S., et al., *Evolving concepts in human renal dysplasia*. *J Am Soc Nephrol*, 2004. **15**(4): p. 998-1007.
53. Sanna-Cherchi, S., et al., *Genetic approaches to human renal agenesis/hypoplasia and dysplasia*. *Pediatr Nephrol*, 2007. **22**(10): p. 1675-84.
54. Piscione, T.D. and N.D. Rosenblum, *The malformed kidney: disruption of glomerular and tubular development*. *Clin Genet*, 1999. **56**(5): p. 341-56.
55. Rosenblum, N.D. (2012) *Overview of congenital anomalies of the kidney and urinary tract (CAKUT)*.
56. Trnka, P., et al., *Phenotypic transition of the collecting duct epithelium in congenital urinary tract obstruction*. *J Biomed Biotechnol*, 2010. **2010**: p. 696034.
57. Katabathina, V.S., et al., *Adult renal cystic disease: a genetic, biological, and developmental primer*. *Radiographics*, 2010. **30**(6): p. 1509-23.
58. Hu, M.C., T.D. Piscione, and N.D. Rosenblum, *Elevated SMAD1/beta-catenin molecular complexes and renal medullary cystic dysplasia in ALK3 transgenic mice*. *Development*, 2003. **130**(12): p. 2753-66.
59. McPherson, E., et al., *Dominantly inherited renal adysplasia*. *Am J Med Genet*, 1987. **26**(4): p. 863-72.

60. Thomas, R., et al., *HNF1B and PAX2 mutations are a common cause of renal hypodysplasia in the CKiD cohort*. *Pediatr Nephrol*, 2011. **26**(6): p. 897-903.
61. Jeanpierre, C., et al., *RET and GDNF mutations are rare in fetuses with renal agenesis or other severe kidney development defects*. *J Med Genet*, 2011. **48**(7): p. 497-504.
62. Jain, S., et al., *Expression profiles of congenital renal dysplasia reveal new insights into renal development and disease*. *Pediatr Nephrol*, 2007. **22**(7): p. 962-74.
63. El-Ghoneimi, A., et al., *Glial cell line derived neurotrophic factor is expressed by epithelia of human renal dysplasia*. *J Urol*, 2002. **168**(6): p. 2624-8.
64. Harada, N., et al., *Lack of tumorigenesis in the mouse liver after adenovirus-mediated expression of a dominant stable mutant of beta-catenin*. *Cancer Res*, 2002. **62**(7): p. 1971-7.
65. Cheon, S.S., et al., *beta-Catenin stabilization dysregulates mesenchymal cell proliferation, motility, and invasiveness and causes aggressive fibromatosis and hyperplastic cutaneous wounds*. *Proc Natl Acad Sci U S A*, 2002. **99**(10): p. 6973-8.
66. Soriano, P., *Generalized lacZ expression with the ROSA26 Cre reporter strain*. *Nature Genetics*, 1999. **21**(1): p. 70-71.
67. Di Giovanni, V., et al., *Alk3 controls nephron number and androgen production via lineage-specific effects in intermediate mesoderm*. *Development*, 2011. **138**(13): p. 2717-27.
68. Kobayashi, A., et al., *Six2 defines and regulates a multipotent self-renewing nephron progenitor population throughout mammalian kidney development*. *Cell Stem Cell*, 2008. **3**(2): p. 169-181.

69. Costantini, F., *Renal branching morphogenesis: concepts, questions, and recent advances*. Differentiation, 2006. **74**(7): p. 402-21.
70. Shakya, R., T. Watanabe, and F. Costantini, *The role of GDNF/Ret signaling in ureteric bud cell fate and branching morphogenesis*. Dev Cell, 2005. **8**(1): p. 65-74.
71. Costantini, F., *GDNF/Ret signaling and renal branching morphogenesis: From mesenchymal signals to epithelial cell behaviors*. Organogenesis, 2010. **6**(4): p. 252-62.
72. Burn, S.F., et al., *Calcium/NFAT signalling promotes early nephrogenesis*. Dev Biol, 2011. **352**(2): p. 288-98.
73. Hatini, V., et al., *Essential role of stromal mesenchyme in kidney morphogenesis revealed by targeted disruption of Winged Helix transcription factor BF-2*. Genes Dev, 1996. **10**(12): p. 1467-78.
74. Levinson, R.S., et al., *Foxd1-dependent signals control cellularity in the renal capsule, a structure required for normal renal development*. Development, 2005. **132**(3): p. 529-39.
75. Cullen-McEwen, L.A., G. Caruana, and J.F. Bertram, *The where, what and why of the developing renal stroma*. Nephron Exp Nephrol, 2005. **99**(1): p. e1-8.
76. Tanigawa, S., et al., *Wnt4 induces nephronic tubules in metanephric mesenchyme by a non-canonical mechanism*. Dev Biol, 2011. **352**(1): p. 58-69.
77. Kohn, A.D. and R.T. Moon, *Wnt and calcium signaling: beta-catenin-independent pathways*. Cell Calcium, 2005. **38**(3-4): p. 439-46.
78. Moon, R.T. and K. Shah, *Developmental biology: signalling polarity*. Nature, 2002. **417**(6886): p. 239-40.
79. Westfall, T.A., et al., *Wnt-5/pipetail functions in vertebrate axis formation as a negative regulator of Wnt/beta-catenin activity*. J Cell Biol, 2003. **162**(5): p. 889-98.

80. Tanwar, P.S., et al., *Constitutive WNT/beta-catenin signaling in murine Sertoli cells disrupts their differentiation and ability to support spermatogenesis*. Biol Reprod, 2010. **82**(2): p. 422-32.
81. Gong, K.Q., et al., *A Hox-Eya-Pax complex regulates early kidney developmental gene expression*. Mol Cell Biol, 2007. **27**(21): p. 7661-8.
82. Kiefer, S.M., et al., *Sall1-dependent signals affect Wnt signaling and ureter tip fate to initiate kidney development*. Development, 2010. **137**(18): p. 3099-106.
83. Basson, M.A., et al., *Sprouty1 is a critical regulator of GDNF/RET-mediated kidney induction*. Dev Cell, 2005. **8**(2): p. 229-39.
84. Qiao, J., et al., *Multiple fibroblast growth factors support growth of the ureteric bud but have different effects on branching morphogenesis*. Mech Dev, 2001. **109**(2): p. 123-35.
85. Michos, O., et al., *Kidney development in the absence of Gdnf and Spry1 requires Fgf10*. PLoS Genet, 2010. **6**(1): p. e1000809.
86. Cohen, E.D., et al., *Wnt/beta-catenin signaling promotes expansion of Isl-1-positive cardiac progenitor cells through regulation of FGF signaling*. J Clin Invest, 2007. **117**(7): p. 1794-804.
87. Sainio, K. and A. Raatikainen-Ahokas, *Mesonephric kidney--a stem cell factory?* Int J Dev Biol, 1999. **43**(5): p. 435-9.
88. Sainio, K., *6 - Development of the Mesonephric Kidney*, in *The Kidney*, D.V. Peter, et al., Editors. 2003, Academic Press: San Diego. p. 75-86.
89. Usongo, M. and R. Farookhi, *beta-catenin/Tcf-signaling appears to establish the murine ovarian surface epithelium (OSE) and remains active in selected postnatal OSE cells*. BMC Dev Biol, 2012. **12**(1): p. 17.

90. Nacher, V., et al., *beta-Catenin expression during vascular development and degeneration of avian mesonephros*. J Anat, 2005. **206**(2): p. 165-74.